Synthesis, characterization and coordination chemistry of indigo diimines

by

Simon Oakley
Honours B.Sc, McMaster University, 2006

A Thesis Submitted in Partial Fulfillment
of the Requirements for the Degree of

MASTER OF SCIENCE

in the Department of Chemistry

Supervisory Committee

Synthesis, characterization and coordination chemistry of indigo diimines

by

Simon Oakley
Honours B.Sc, McMaster University, 2006

Supervisory Committee

Dr. R. G. Hicks (Department of Chemistry)
Supervisor

Dr. D. J. Berg (Department of Chemistry)
Departmental Member

Dr. F. Hof (Department of Chemistry)
Departmental Member

Abstract

Supervisory Committee
Dr. R. G. Hicks (Department of Chemistry)
Supervisor
Dr. D. J. Berg (Department of Chemistry)
Departmental Member
Dr. F. Hof (Department of Chemistry)
Departmental Member

This work presents the synthesis and characterization of a new family of bridging ligands, indigo diimines (Nindigos). Nindigos are bis(bidentate) N-donor type ligands derived from the dye indigo. These Nindigos have been synthesized via reaction of indigo with primary amines, using $TiCl_4$ as a catalyst, in bromobenzene.

A family of Nindigo ligands was prepared with p-tolyl, p-methoxyphenyl, p-chlorophenyl, mesityl, and ^{t}Bu functional groups. The UV-Vis properties of the Nindigos were investigated. The λ_{max} for these ligands occurs in the range of 580-640nm, with extinction coefficients in the order of $1x10^4$ M^{-1} cm^{-1}. These absorptions are similar to that of indigo itself, which also shows a λ_{max} close to 600nm.

The reactions of selected Nindigo derivatives with $Pd(hfac)_2$ formed bimetallic complexes. Upon complexation with palladium, the major absorption of the Nindigo complexes was found to red-shift to ~ 910nm, while the extinction coefficient increased to approximately $2x10^4$ M^{-1} cm^{-1}. This demonstrates that both the Nindigos and their complexes are functional molecular dyes.

The electrochemistry of the p-tolyl, p-methoxyphenyl, and mesityl complexes show two reversible oxidations, with $E_{1/2}$ at approximately + 0.0V and + 0.50V. There is also a quasi-reverisble reduction at approximately -1.4V. The alkyl derivatized complex, ^{t}Bu Nindigo showed only one reversible oxidation at +0.32 V and one irreversible reduction at ~ -1.7 V. The Nindigo complexes now represent a new class of redox active bridging ligands, and thanks to the facile derivatization, they have more options for electronic and steric control around the metal center, which ultimately means greater control over redox activity.

Table of Contents

List of Tables

List of Figures

List of Schemes

List of Numbered Compounds

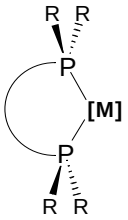

1.1

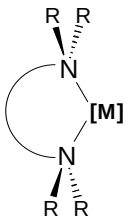

1.2

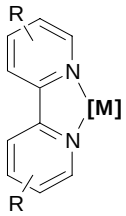

1.3

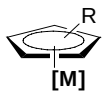

1.4

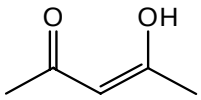

1.5

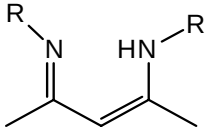

1.6

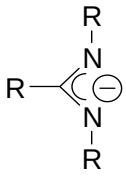

1.7

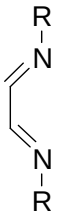

1.8

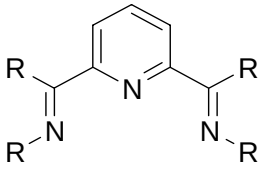

1.9

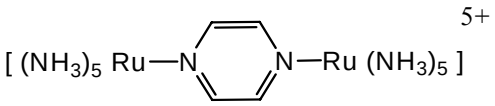

1.10

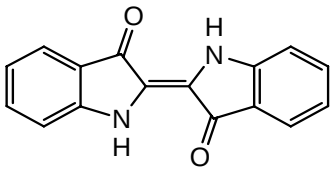

1.11

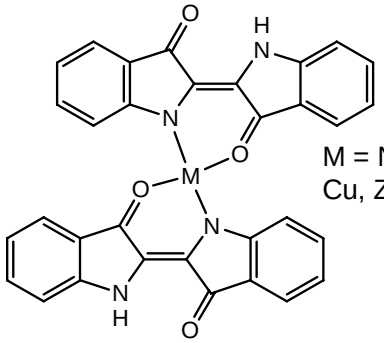

M = Ni, Co, Cu, Zn

1.12

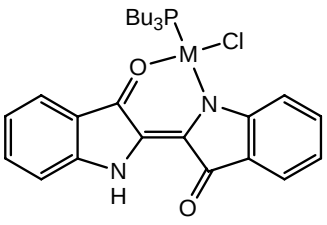

1.13 M = Pd, Pt

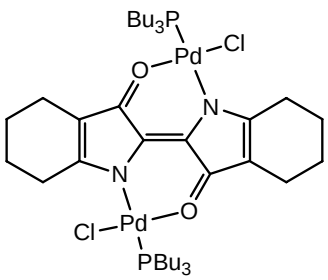

1.14

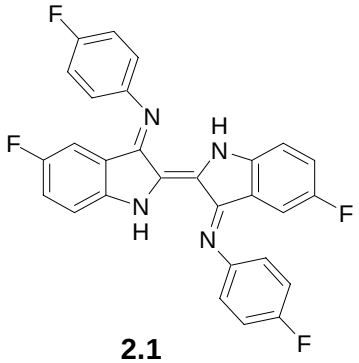

2.1

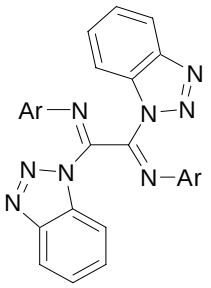

2.2

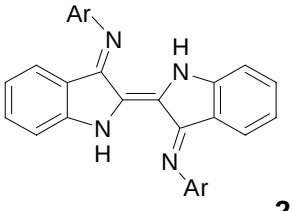

2.3

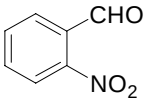

2.4

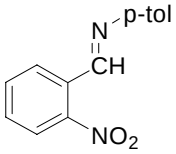

2.5

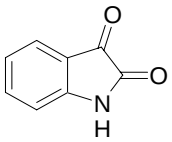

2.6

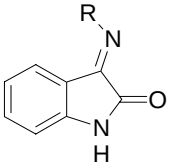

2.7

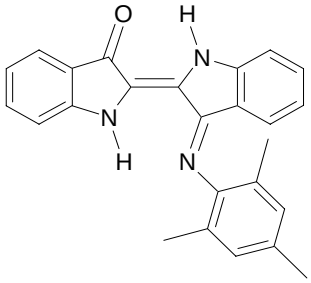

2.8

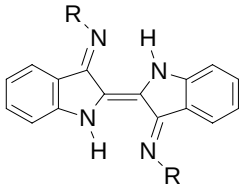

R = p-tolyl **2.9**
R = t-butyl **2.10**
R = mesityl **2.11**
R = p-methoxyphenyl **2.12**
R = p-chlorophenyl **2.13**
R = pentafluoro aniline **2.14**
R = p-CF_3 aniline **2.15**

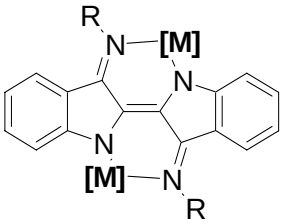

3.1

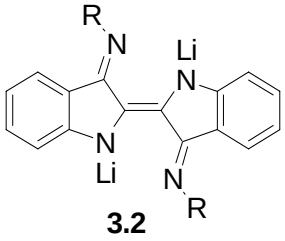

3.2

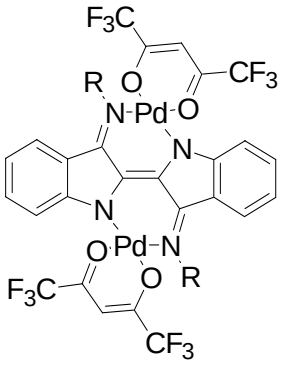

R = *p*-tolyl **3.3**

R = *p*-methyoxyphenyl **3.4**

R = ^{t}Butyl **3.5**

R = mesityl **3.6**

R = *p*-chlorophenyl **3.7**

List of Abbreviations

A	absorbance
Å	angstroms
acac	acetylacetonate
Ar	aryl substituent
Bu	butyl
^{o}C	degrees celcius
cm	centimetre
cm^{-1}	wavenumber
Cp	cyclopentadienyl
Cp*	pentamethylcyclopentadienyl
CV	cyclic voltammetry
d	doublet (NMR peak descriptor)
dd	double of doublets (NMR peak descriptor)
DCM	dichloromethane
d_6-acetone	deuterated acetone
E	energy
$E_{1/2}$	half cell potential
Et	ethyl
eV	electron volt
eq	equivalent
Fc	ferrocene
hrs	hours

hfac	1,1,1,5,5,5-hexafluoroacetylacetonate
Hz	hertz
IR	infrared
J	coupling constant (NMR)
kJ/mol	kilojoules per mole
L	litre
m	meta
M	molarity
M^{-1}	inverse molarity
Me	methyl
MHz	megahertz
Mes	mesityl
min	minutes
mL	millilitre
mmol	millimole
mV/s	millivolt per second
Nindigo	indigo diimine
nm	nanometre
NMR	nuclear magnetic resonance
o	ortho
OMe	methoxy
p	para
Ph	phenyl

ppm	parts per million
py	pyridine
R	generic functional group
R	least squares residual
RT	room temperature
s	singlet (NMR peak descriptor)
SCE	saturated calomel electrode
t	triplet (NMR peak descriptor)
^{t}Bu	tertiary butyl
TEA	triethylamine
THF	tetrahydrofuran
Tert	tertiary
Tol	tolyl
UV	ultraviolet
V	volts
δ	chemical shift in parts per million
ε	molar absorptivity (M^{-1} cm^{-1})
λ_{max}	wavelength at peak maximum

Acknowledgments

Firstly I would like to thank my boss, Dr. Robin Hicks, for his help and support over the last two and a half years, and for starting me on this Nindigo project, which turned out to be quite successful! Thanks!

Secondly I would like to thank Chris Greenwood for her assistance with all things NMR, and to Brian Patrick for solving all of my crystal structures – both of them provide invaluable services that are at the heart of any chemistry degree.

I would also like to thank Dr. David Emslie, who gave me the suggestion of using $TiCl_4$, the first Christmas I had back in Ontario, and to my old lab mate and friend, Carlos Cruz whose ear I have bent many a time, for a hell of a lot of reasons.

Finally I'd like to thank my friends and family wherever they are, for their support and encouragement. Also thanks to all the grad students in the department, but most notably Tyler Trefz, Eric Derrah, Mark Zsombor, Steve McKinnon, Joe Gilroy, and of course my brother Nick, whom made life much more interesting and enjoyable on the roller coaster of research. Hopefully Felicitas re-opens one more time before I graduate.

Dedication

As it was in the beginning and is in the end
for Mom and Dad

Chapter 1 : Introduction

1.1 Ligand Design

Ligand design plays a major role in the properties of inorganic complexes, because the properties of any metal complex are invariably linked to the ligands to which the metal is attached. Some of the best known ligands which have been successfully used to this purpose include multidentate phosphines[1] **1.1,** amines[2] **1.2**, bipyridines[3] **1.3**, and cyclopentadienides[4] **1.4** (Figure 1.1). These ligands can, and have, been functionalized in a variety of different ways, by choosing bulkier R-groups to provide steric bulk, or by altering the electronics via electron donating/removing substituents.

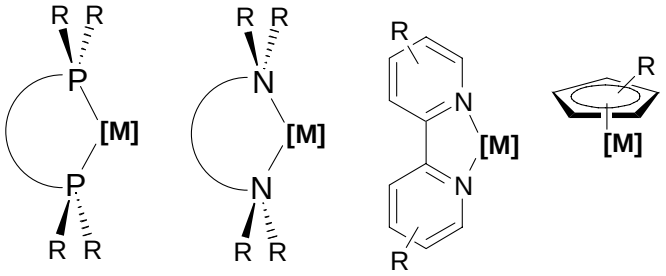

1.1 **1.2** **1.3** **1.4**

Figure 1.1: General structures of phosphines, amines, bipyridines and Cp rings, respectively.

More recently, β-diketiminates, also known as NacNacs **1.6**, have become a hugely popular and successful family of chelating ligands.[5] Most popularly derived from acetylacetonate, (or acac) **1.5**, they have found widespread success for their versatility as tunable spectator ligands. While there are a several procedures for the synthesis of NacNac, the most recent and popular synthesis of NacNac arises from the condensation of a β-diketone and an amine. R-groups such as mesityl and diisopropylphenyl have seen

much success in their ability to sterically hinder the resulting complex and limit interaction of other molecules with the coordination sphere of the metal.

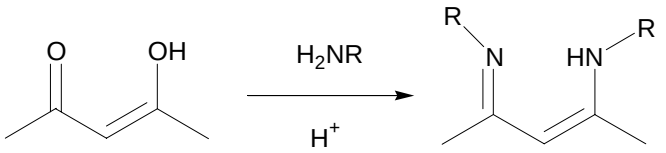

1.5 **1.6**

NacNacs are not the only type of ligand that can be tuned to suit the needs of the complex. Other popular π-conjugated polydentate N-donors include amidinates[6] **1.7**, α-diimines[7,8] **1.8**, and diimino pyridines[9,10] **1.9**. Similarly to NacNac, these ligands are multidentate chelates in which the imine R-group can be synthetically interchanged.

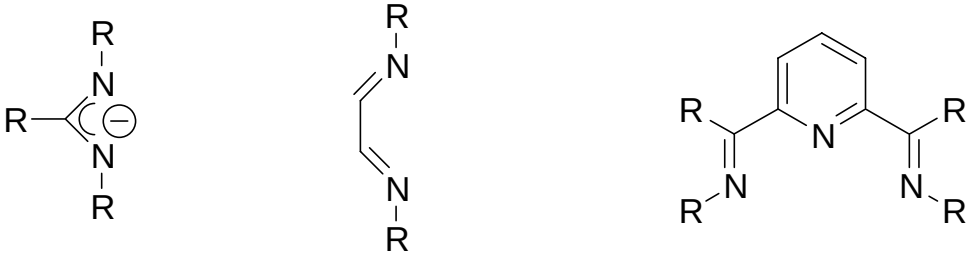

1.7 **1.8** **1.9**

1.2 Bridging Ligands

Tunable *bridging* ligands are not nearly as well known as the *ancillary* ligands described above. In the context of metal-metal communication, it is the ligand between the two metal centers - the bridging ligand - which plays the key role as it is responsible for mediating the interaction between the two metal centers. It is this interaction which gives rise to novel chemical, magnetic, and/or electron transfer properties that are associated with bi- or multimetallic complexes.

The simplest bridges are the single atom bridges such as ¯OR, ¯SR, and halides. Examples of common larger bridging ligands are shown in Figure 1.2. These bridging ligands allow the d-orbitals of both metals to overlap through the π-system of the ligand (Scheme 1.1), which is a key component in metal-metal communication.

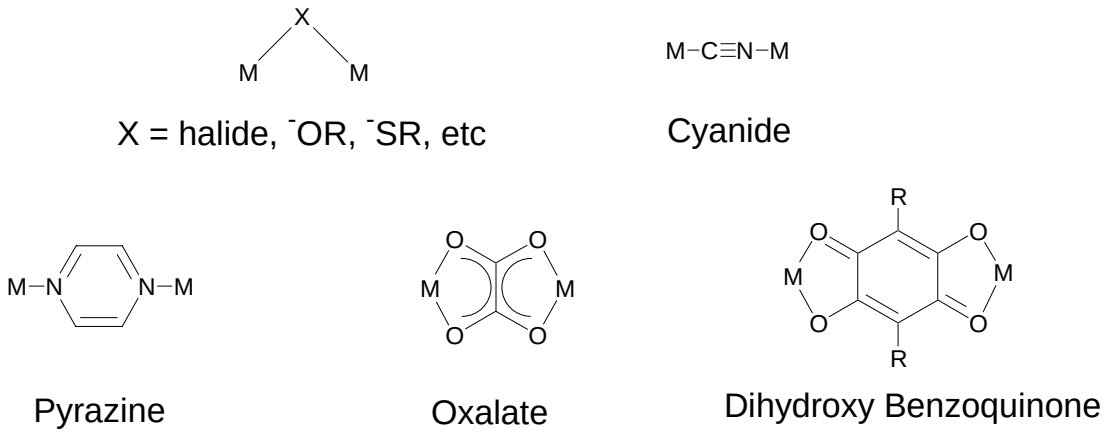

Figure 1.2: Representative bridging ligands

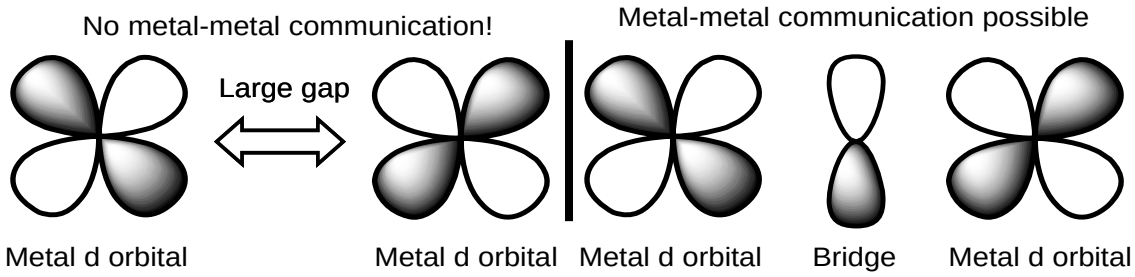

Scheme 1.1: Schematic use of bridging ligands to enhance metal-metal communication

Most bridging ligands which are able to facilitate any kind of metal-metal communication are very small, and/or have some degree of π-conjugation to serve as a conduit between the two metals. There are many studies of complexes based on these simple bridging ligands that delve into the spectroscopic, electronic, and magnetic properties[11-14].

One of the first complexes which exemplified the role played by the bridging ligand in metal-metal communication was the Creutz-Taube ion[15] **1.10**. Using UVVis spectroscopy it was discovered that rather that describing the ion as having discrete +3 and +2 charges on the two separate metal centers, the pyrazine bridge was found to delocalize the +5 charge such that each Ru atom effectively carries a charge of +2.5.

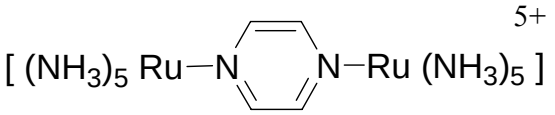

1.10

Magnetic properties are also affected by used of a bridging ligand. Since magnetic properties can arise when one or more paramagnetic metals are in a molecule, the interaction between multiple metals has been shown to increase the magnetic effects. Furthermore, as is the case with chloranilic acid, if the bridge can be oxidized or reduced to the radical form then this will have additional effects. Chloranilic acid has been used as a bridge between two cobalt centers (Figure 1.3), and it has been shown that radical form of the bridge enhances the spin coupling between the two metal centers due to direct spin exchange.[13]

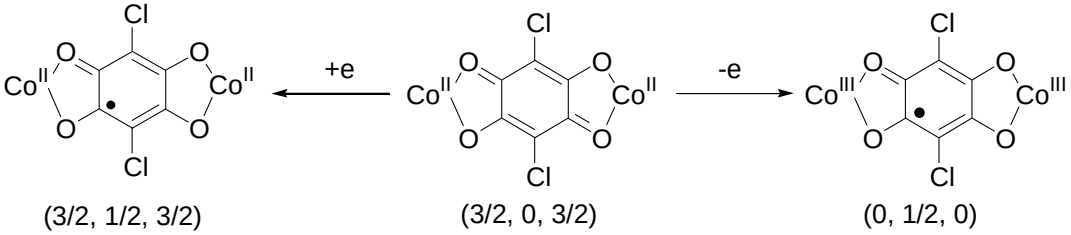

Figure 1.3: Exchange of electrons across chloranilic acid bridge enhances spin coupling. Numbers in parentheses indicate spin on metal centers and bridging ligand.[13]

It has also been found that the length of a π-conjugated bridging ligand has an effect on the properties of the complex. This has been shown using bridging Pt dimers with pyrazine, 4,4'-bipyridine, and trans-1,2-bis(4-pyridyl)ethylene as bridges (Figure 1.4).[16]

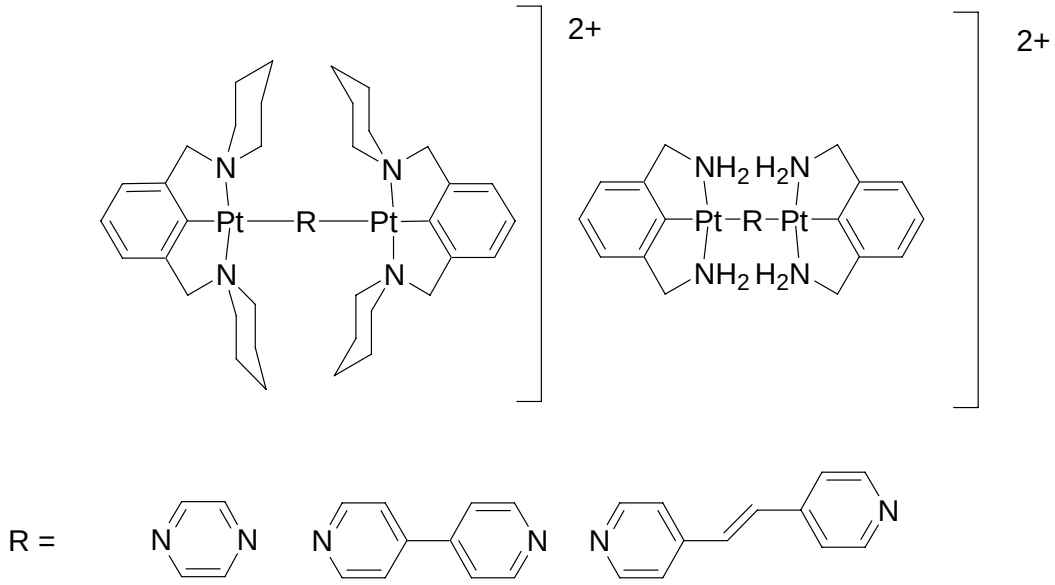

Figure 1.4: Systems used to test the effects of increasing the length of the π –conjugated bridge[16]

Since the transfer of electrons is mediated by the bridge, the degree to which the two metals interact, and therefore the properties that the complex displays, will be linked to how far the electrons must travel between the two metal centers. It was discovered that by increasing the length of the bridge increased the energies of the HOMO and LUMO, as well as the size of the gap between the two. Also, the HOMOs and LUMOs are located at different coordinated ligands, which means that the electronics of the molecule can be directly tuned by functionalizing the molecule with various electron donating or withdrawing groups.[16] They also found that the ionization potential decreased with

increasing bridge length, and could likewise be varied by adding to the electron donating ability of the phenyl ring.[16]

From the use of bridging ligands has sprung many different fields of research, as the interaction between two metal atoms through a bridge plays a key role in the properties of many important electronic, magnetic and optical inorganic compounds. Therefore, learning more about how two metals communicate across a bridge is of importance to the inorganic community[17-19], and so would be desirable to create a bridging ligand system that can be easily modified so that a variety of electronic properties can be obtained for the complex.

One challenge associated with these types of complexes is that there is currently little in the way of variation of design for bridging ligands (1) when compared to ancillary ligands such as NacNac, and (2) when restricted to π-conjugated systems. The single atom bridges either cannot be modified at all, as is the case with halides, or the R-group is so far removed from the metal center that all but the largest and most sterically hindering groups have an effect on the coordination sphere of the metal. While the current selection of bridges can be slightly derivatized, it cannot be done without adversely affecting the coordination sphere of the metal, and so there is little that can be done to tune the system at the bridge. For example, in Figure 1.5, even an R-group as small as a methyl on the pyrazine ring can obstruct the coordination sphere of a bound metal.

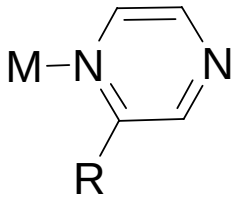

Figure 1.5: A substituted pyrazine bridge provides too much steric constraint to a coordinated metal

1.3 Indigo as Bridging Ligand?

The dye indigo (Figure 1.6) has been known for approximately 4000 years[20,21]. Originally isolated from the plant *indigofera tinctura*, indigo has been associated with power and royalty for many hundreds of years, in part due to the fact that indigo was so difficult to obtain in large quantities, but also because of the incredible insolubility of the dye itself, which made it rather difficult to work with. In order to dye cloth, the material had to literally be soaked in hot baths of urine for many days, in order to reduce indigo to its more soluble form such that the dye could adhere to the fabric[22]. Indigo was first chemically synthesized from isatin by Baeyer in 1870[23], and this method has been improved on such that it is now extremely cheap and commercially available, and it is most popularly found as the dye in blue jeans.

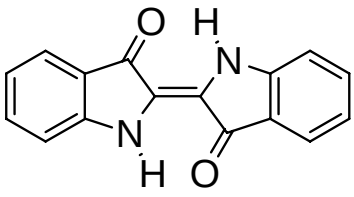

1.11

Figure 1.6: Left: indigo structure. Center: colour of the solid indigo dye. Right: 'solutions' of indigo in Et_2O and EtOH.

Despite the fact that the structure of indigo is well suited to function as a bridging ligand, there have been very few reports on the topic of indigo's coordination chemistry. Apart from a few papers dating back more than 80 years ago[24-26], there are only a handful of late-transition metal complexes made by Beck[27-30] (Figure 1.7), that explore the potential for indigo in a metal complex. The lack of activity in metal-indigo chemistry may in part be linked to the insolubility of indigo itself in most common organic solvents.

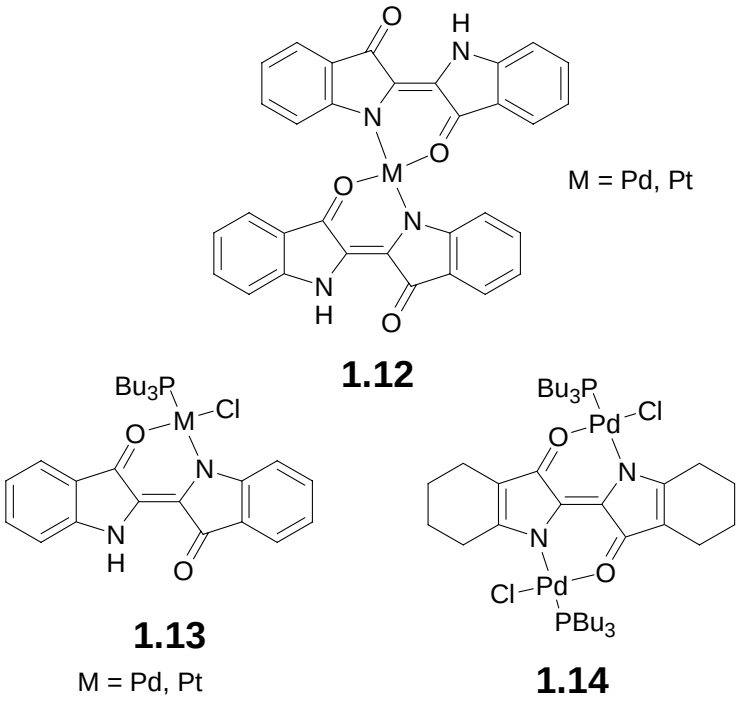

Figure 1.7: Beck's Palladium-indigo complexes[29].

Beck reported that complex **1.12** was too insoluble too be recrystallized to obtain X-ray quality crystals, and only the mono-substituted complex **1.13** could be made with indigo itself.[29] In order for a binuclear complex to be obtained, the indigo had to be converted to octahydroindigo[31] in order to disrupt the planarity of the bridge, thereby improving the solubility such that **1.14** could be isolated and characterized.

1.4 Thesis Objectives

Indigo could in theory be a useful bridging ligand. However, in order to have the same flexibility with indigo as exists with ancillary ligands, there would have to be some degree of derivatization available for indigo, as well as an improvement in its solubility. Referring to the conversion of acac to NacNac, theoretically a similar conversion of indigo to indigo diimine (Scheme 1.2), would lead to a new family of "Nindigo" bridging ligands which would hopefully alleviate both the solubility issue of indigo itself, as well as provide a practical way to modify indigo with a variety of different functional groups. In this context, the goals of this project are to synthesize these Nindigos derivatives and investigate their potential use as a new family of bridging ligands. Chapter 2 in this thesis will focus on the synthesis and characterization of a variety of Nindigo derivatives. Chapter 3 will focus on the synthesis of several palladium complexes isolated using Nindigo derivatives, and a discussion of their properties.

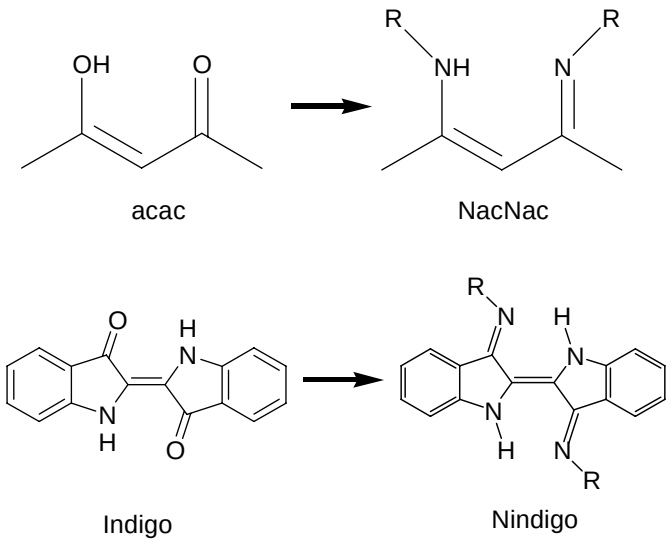

Scheme 1.2: Conceptual conversion of indigo to Nindigo

Chapter 2 : Synthesis and Characterization of Nindigo Derivatives

2.1 Introduction

As discussed in Chapter 1, the goals of this project are to create imine based derivatives of indigo, and to demonstrate their utility as bridging ligands. There have been three instances where Nindigo has been made, which will be briefly reviewed, along with both the unsuccessful and successful methods that were undertaken to synthesize Nindigo in this project. The characterization and properties of the Nindigo compounds synthesized during the course of this project will then be discussed.

2.2 Nindigo History

Indigo N,N'-diphenylimine was reported to have been prepared in 1910[32], from the reaction of indigo and aniline in the presence of boric acid. The latter acts as a drying agent to remove H_2O from the system as it is produced, thus preventing hydrolysis of the imine after it has formed.

Indigo diimines have been reported via the thermal oligomerization of aryl isonitriles[33,34] (Scheme 2.1). In the 1958 paper[33], phenyl isocyanides were reported to polymerize at room temperature in the presence of an acid, the yields recovered being in the 5-10% range. In the 2003 paper[34], 4-fluorophenyl isocyanide was heated at 135 ^{o}C for 3 hours whereupon it was cooled, forming a viscous orange-red gum. This was extracted with boiling benzene and the resulting solid was washed with benzene until the washings were colourless and then with hexanes, giving a 3.2% yield of black crystals **(2.1)**.

Although the synthesis is simple enough, the yields recovered are too low to be of any use in the area of synthetic ligand design.

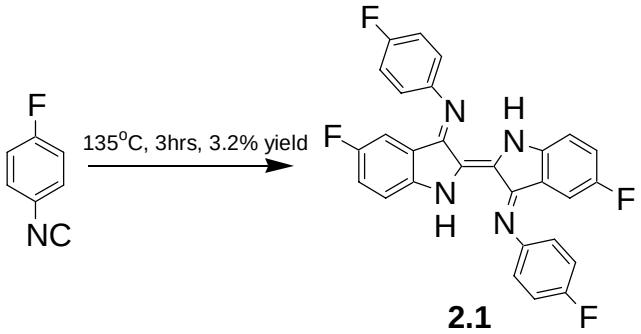

Scheme 2.1: Oligomerization of aryl isocyanides at high temperatures[34]

The crystal structure of **2.1** (Figure 2.1) confirmed the connectivity[34]. The phenyl rings in this compound are twisted at an angle of 79.4° to the plane of the backbone of the molecule, instead of perpendicular.

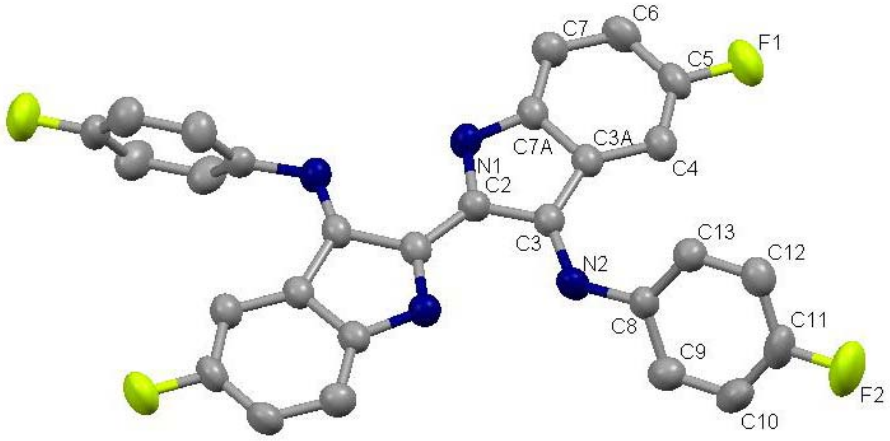

Figure 2.1: X-Ray crystal structure of 2.1 (50% thermal ellipsoids)[34]. All hydrogens have been removed for clarity. Molecule resides in a plane of symmetry.

Another method for the synthesis of Nindigos was also found via oximidoyl chloride derivatives (Method A)[35], in which solid magnesium was used to reduce the N,N' diaryl oximidoyl chloride to form **2.3**, through a proposed radical pathway

involving dimeric isocyanides (not shown). In the 2006 paper[36] (Method B), the oximidoylchloride was refluxed with benzotriazole in the presence of triethylamine, giving the imidobenzotriazole **2.2**. Subsequent additions of n-BuLi and lithium metal afforded **2.3** again via the same radical pathway as was proposed in 1999. Method A lacked the reaction with a benzotriazole and has one less step, but had yields in the 10% range. Method B was slightly better yielding, with the yields of the reduction steps in the 40-50% range, but this route required multiple steps in order to finally arrive at the desired Nindigo product. In both cases the oximidoylchloride precursor also had to be synthesized prior to use.

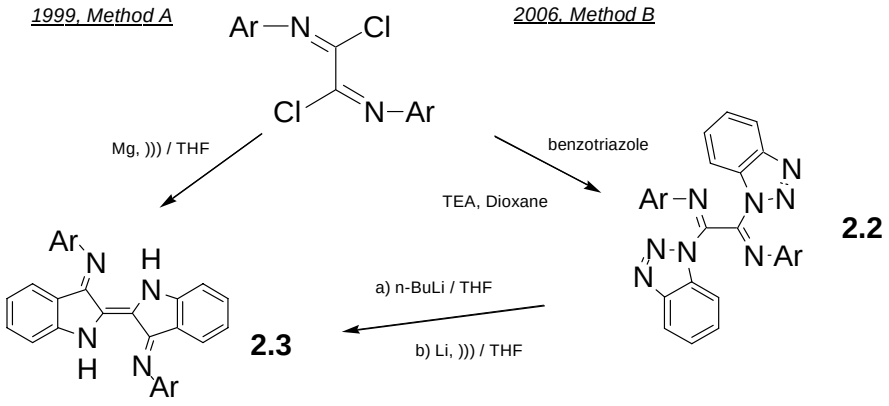

Scheme 2.2: The two different synthetic pathways using oximidoyl chlorides

2.3 Results and Discussion

2.3.1 Unsuccessful Attempts at Nindigo Synthesis

Our initial explorations in the synthesis of Nindigo derivatives were based on the well known one-pot synthesis of indigo[37]. This involves the reaction of *o*-nitrobenzaldehyde **2.4** with acetone in the presence of sodium hydroxide (Scheme 2.3A). By analogy, we reasoned that the corresponding *o*-nitrophenyl substituted imine **2.5**

could potentially also react in the same manner, thus forming Nindigo derivatives (Scheme 2.3B). However, it was found that Nindigos could not be synthesized via *o*-nitrophenyl imine **2.5**, as reactions with NaOH in acetone caused the decomposition of the imine and resulted in the reformation of *o*-nitrobenzaldehyde, which then continued to form indigo via route (A).

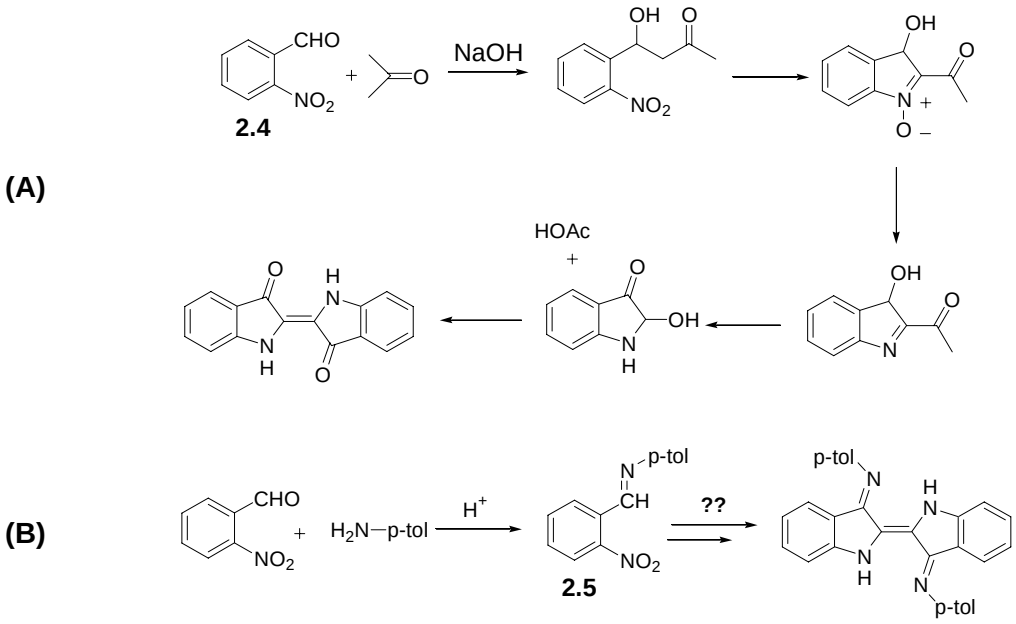

Scheme 2.3: (A) Synthetic route to Indigo via *o*-nitrobenzaldehyde (B) Proposed synthetic route to Nindigo via *o*-nitrophenyl imine

Another way to make indigo involves isatin **2.6**, a dione derivative of indole. The coupling of two carbonyls has been known for decades via a $TiCl_4$/Zn amalgam at high temperatures[38] (Scheme 2.4). Again, however, this route did not prove to be synthetically successful, as **2.7** could not be isolated.

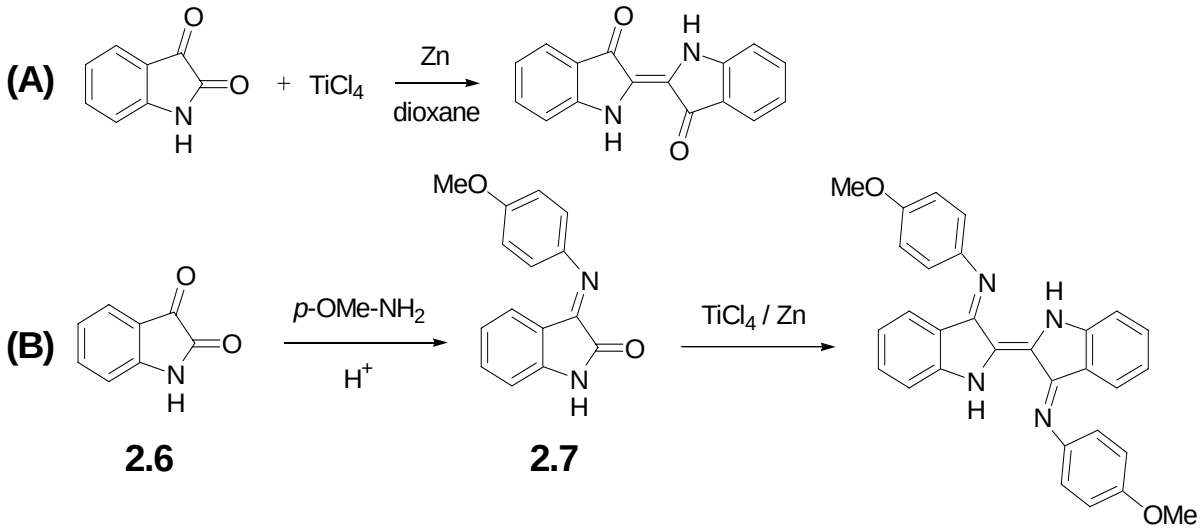

Scheme 2.4: (A) Theoretical Synthesis of Indigo via $TiCl_4$/Zn Amalgam
(B) Proposed reductive coupling of an imine derivative of Isatin to form Nindigo

2.3.2 Indigo as a Precursor to Nindigo

Subsequent forays into the synthesis of Nindigo were undertaken in an analogous manner to the synthesis of NacNac from acac (Chapter 1): ketone plus amine gives imine and water. In this manner, indigo was used in the hopes that the ketones could be converted to imines. In order to try to overcome the solubility barrier presented by indigo, reactions were attempted in several solvents ranging in boiling point from THF (66^{o}C), to toluene (111^{o}C) to mesitylene (163-166^{o}C), with trifluoroacetic acid as the catalyst. A Dean-Stark trap was used to collect the water which should form as the reaction progressed, however no water was collected after the reactions in these solvents. A purple solid was isolated that was mildly more soluble in organic solvents than indigo, but the ^{1}H-NMR spectrum of this material showed that this product was protonated indigo. This reaction was repeated with boric acid in solution to act as a drying agent[32], but still proved unsuccessful both in our lab and others[36].

$TiCl_4$ is a potent activating agent that has been found to give efficient and high yielding conversion of ketones to imines in the presence of an auxiliary amine and a base[39]. However, when a base with an unconstrained α-proton is used, such as triethylamine, then the $TiCl_4$ can react with the base instead of the amine, which renders both the base and the $TiCl_4$ unavailable for further reaction, thus limiting the yield. The reaction, shown below (Scheme 2.5), illustrates the fact that as the amine is oxidized to a radical cation by Ti^{4+}, followed by the loss of a α-hydrogen in order to stabilize the oxidized amine as the immonium ion, thus leading to decomposition[40]. Therefore if a bicyclic base was used, such as DABCO (1,4-diazabicyclo-[2.2.2] octane), then this oxidation/decomposition step would not occur as losing an α-hydrogen on DABCO would result in a violation of Bredt's rule[41].

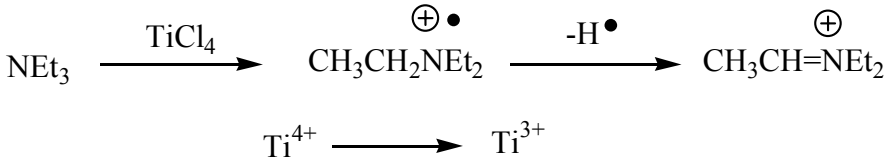

Scheme 2.5: Reaction of $TiCl_4$ with triethylamine

The first reactions using $TiCl_4$ to synthesize a Nindigo were done in refluxing THF over a period of 24-48 hrs. The initial amine used was 2, 4, 6-trimethylaniline. As per literature protocols, 0.6 equivalents of $TiCl_4$ was used per ketone, and 2 equivalents of aniline was used. Reflux periods were attempted for 24 -78 hrs, but the compound that was consistently obtained was the mono-substituted compound **2.8**.

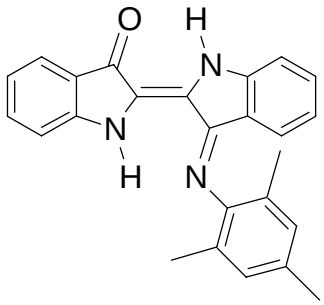

2.8

The structure of this compound was inferred from its ^{1}H NMR spectrum (Figure 2.2). There are two different sets of two doublets and two triplets, corresponding to the two different aromatic sets of signals in the 'core' of the indigo molecule. There are also two different NH protons, one adjacent to either an imine or a ketone. Both N-H protons are shifted well downfield of normal un-stabilized N-H protons, in the range of 9.0-10.0 ppm. Finally, the lone singlet from the *meta* protons on the mesitylene rings can be identified at 6.89 ppm and the methyl groups on the mesitylene ring can be identified at 2.26 and 1.95 ppm in a 1:2 ratio.

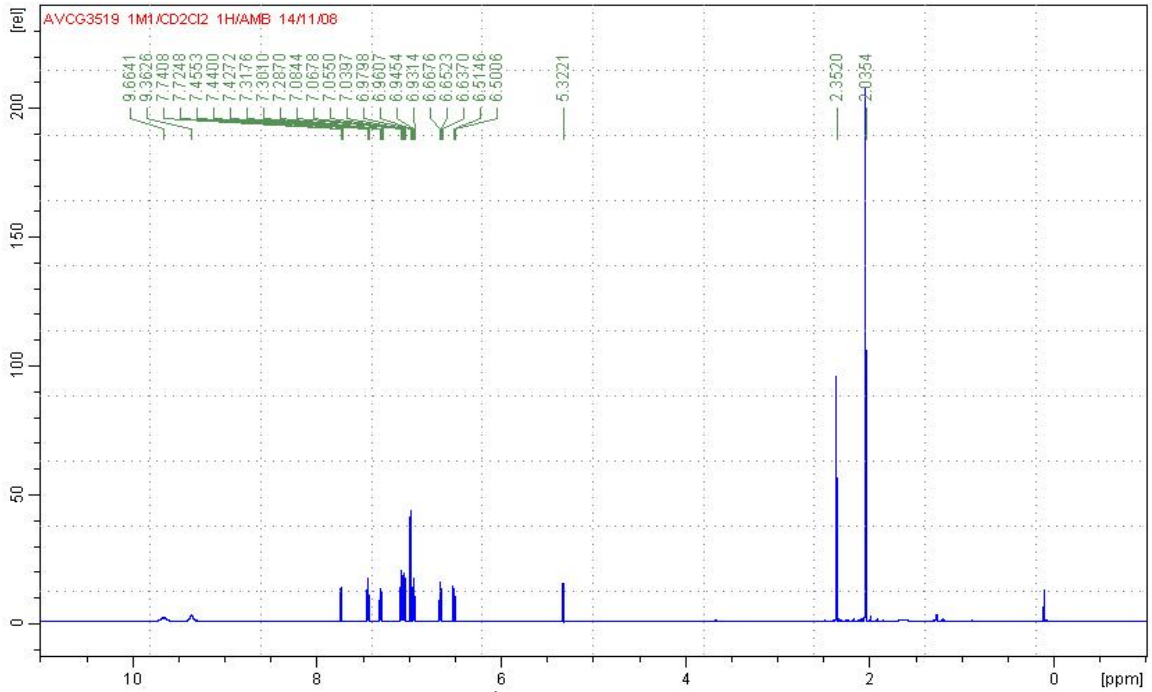

Figure 2.2: ^{1}H-NMR of 2.8 in CD_2Cl_2

With the addition of one mesityl substituent, **2.8** is much more soluble in organic solvents than indigo. The former is soluble in everything from hexanes to ether to dichloromethane. It is purple in more non polar solvents such as ether (λ_{max} = 588 nm, and $\varepsilon = 4.0 \times 10^4$ M^{-1} cm^{-1}), while being blue in more polar solvents, like ethanol (λ_{max} = 599 nm, and $\varepsilon = 4.2 \times 10^4$ M^{-1} cm^{-1}). However like indigo, **2.8** still does not dissolve well in water.

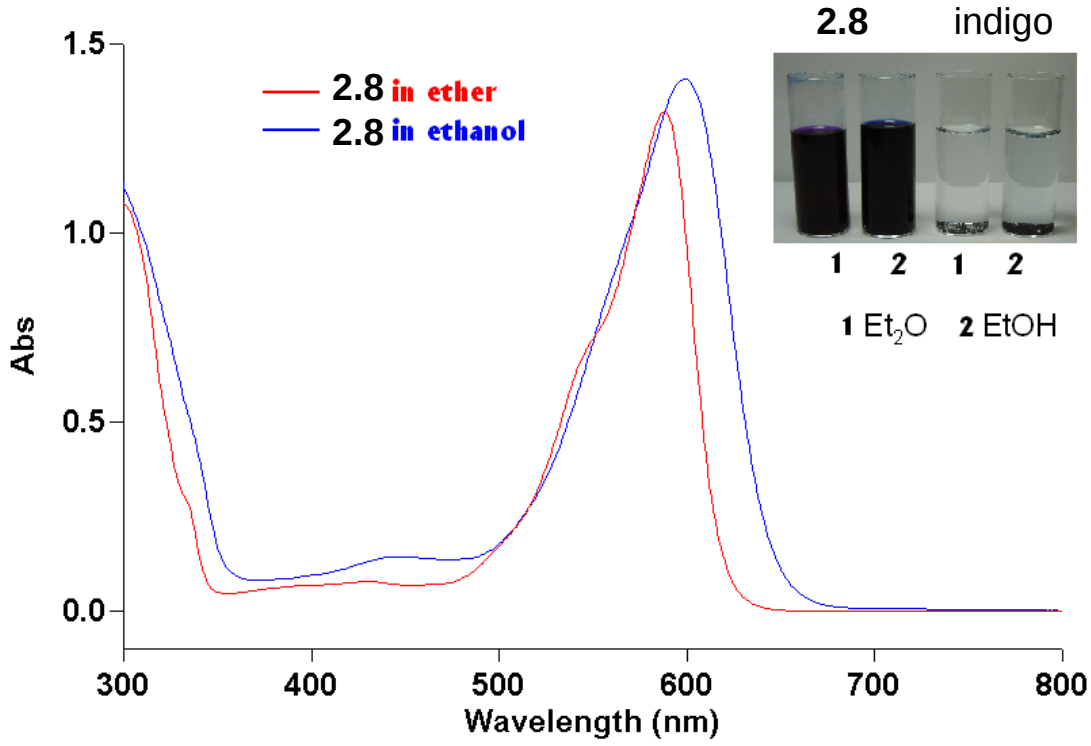

Figure 2.3: UV-Vis Spectraof 2.8 in ether (red) and ethanol (blue). Inset: solutions of 2.8 and of Indigo in ether and ethanol

A crystal structure of **2.8** was obtained (Figure 2.4), confirming the structure inferred from its ^{1}H-NMR spectra. As can be seen from Table 2.3.1, the bond lengths and angles in the molecule are unremarkable and similar to what would be expected based on simple indigo compounds[42,43].

Despite our efforts, it did not prove possible to isolate the desired diimine under these reaction conditions, and while it was good to confirm that it was indeed possible to replace the ketone with an imine using $TiCl_4$, the goal of the project was to substitute *both* locations on indigo to make a symmetrical bridging ligand.

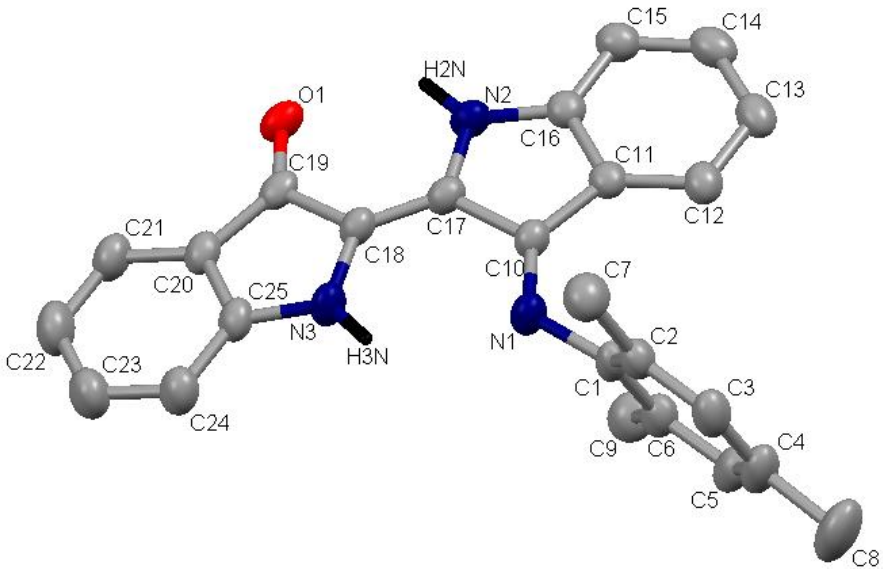

Figure 2.4: X-Ray crystal structure of 2.8 (50% thermal ellipsoids). All hydrogens other than N2H and N3H have been removed for clarity.

Table 2.3.1: Selected bond lengths and angles for 2.8

Bond Length (Å)		Angle (deg)	
C17-C18	1.355(3)	C1-N1-C10	120.74(16)
C18-C19	1.461(3)	C10-C17-C18	128.54(18)
C19-O1	1.256(2)	C17-C18-N3	126.51(18)
C18-N3	1.390(2)	C18-C19-O1	124.63(18)
C17-N2	1.377(2)	C-18-C17-N2	123.42(18)
C17-C10	1.474(3)	N1-C10-C17	120.19(18)
C10-N1	1.284(2)		

Since **2.8** was synthesized in a refluxing solution of THF, a higher boiling solvent would allow more indigo to be drawn into solution, and thus hopefully for more aniline to react over a shorter period of time. Bromobenzene was selected as a potential solvent as it

is high boiling (156^{o}C) and it dissolves indigo at room temperature to a greater extent than most other solvents. In addition to changing the solvent, the amine was switched to *para*-tolyl aniline instead of 2, 4, 6 trimethylaniline, as there was concern that the steric hindrance of the methyl groups at the 2 and 6 positions might be preventing the attachment of the second mesityl ring. As will be seen shortly, these concerns turned out to be unfounded.

The general scheme that was ultimately developed for the synthesis of Nindigos is shown in Scheme 2.7. The di-substituted product *p*-tolyl Nindigo **2.9** was the first to be synthesized, and was obtained in 61% yield as a shiny purple solid. A total of five different Nindigo derivatives were successfully synthesized using this method. In addition to the conditions shown in Scheme 2.7, it has also been found that for **2.9** and **2.11**, substituting DABCO with 4 extra equivalents of the desired aniline also produce the di-substituted product in approximately the same yield. However, one of the major problems that arose during the synthesis was the purification of the Nindigos. Since the aniline starting material often had similar solubility to the Nindigo product, they were often difficult to separate. The method of using DABCO as a base was more helpful in avoiding excessive purification steps.

The likelihood of this reaction to produce a di-substituted product seems to be related to the nucleophilicity of the aniline/amine chosen. Amines **2.9-2.13** are all sufficiently nucleophilic that the di-substituted product can be made via the reaction conditions shown in Scheme 2.7, and their yields are all in the range of 60-90%. However, as the substituents on the amine get progressively more electron withdrawing, the reaction becomes more unreliable. **2.13** has shown some inconsistency in the success

of synthesis despite repeating the same method, but it is however still isolable. Despite the fact that Nindigos are more soluble in most common organic solvents than the parent indigo, the are still often not soluble enough to obtain complete ^{13}C NMR data. Elemental analysis have been found to have low %C data, indicating that there may be incomplete combustion occurring.

The fact that such a potent activating agent like $TiCl_4$ is needed to ensure the completion of this reaction is likely because the carbonyl in indigo is a resonance stabilized vinylogous amide. This makes the carbonyl less susceptible to nucleophilic attack, which is why simple reactions in acid or with H_3BO_3 present were unsuccessful. Due to resonance stabilization, quinonoid carbonyls have also been found to be much less reactive to amine than aliphatic ketones, and anthraquinonoid diimines could only be obtained in very low yields using standard Lewis acid catalysts such as $AlCl_3$.[44] The reason $TiCl_4$ is needed may be due to the fact that $TiCl_4$ is not acting as a classical Lewis acid, as the reactive intermediate appears to be a titanium/aniline species (Scheme 2.6).[40] The authors reached this conclusion after running a battery of tests on their own conjugated ketone (anthraquinone), which determined that the lowest yields for their reaction occurred when the $TiCl_4$ was added to the carbonyl compound before the addition of the amine. They also found that the reactions were optimized in high boiling solvents such as chloro- and dichlorobenzene.[44]

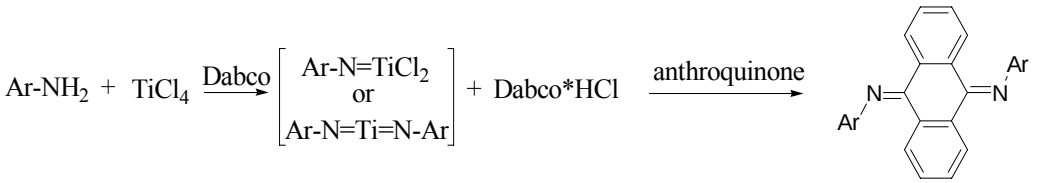

Scheme 2.6: The reaction of amines with $TiCl_4$ and resonance stabilized ketones.[40]

Nindigo derivatives **2.14** and **2.15** were meant to be synthesized from quite electron withdrawing aniline, namely pentafluoro and *para* CF_3 aniline, respectively. However, they are too electron withdrawing to allow for the compound to form. *Some* reaction does occur for **2.14** and **2.15**, as can be determined by the intense colour and solubility change, yet no amount of purification yields any di-substituted Nindigo with an electron withdrawing derivative. ^{1}H-NMR spectra for **2.14** and **2.15** were more complicated than a mono-substituted molecule would suggest, and so likely there is some more complicated reactions occurring.

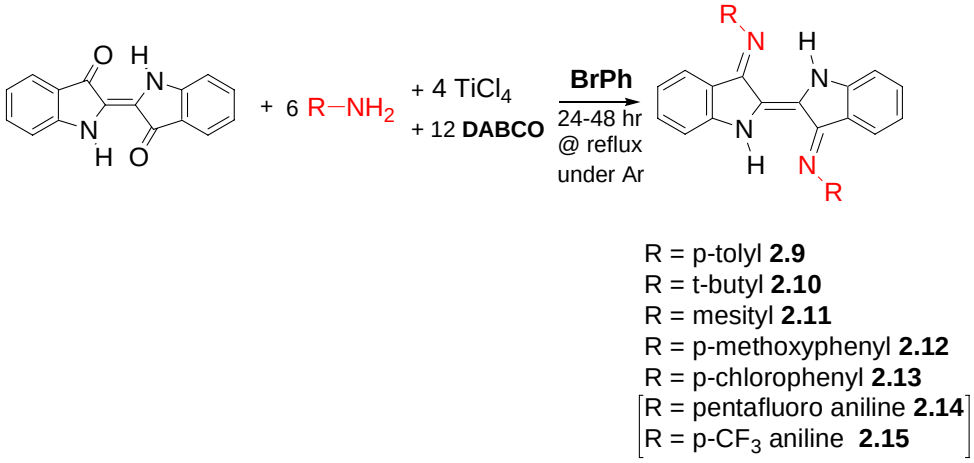

Scheme 2.7: $TiCl_4$ catalyzed reaction for the synthesis of Nindigo derivatives. Bracketed 2.14 and 2.15 were not isolated as pure compounds.

The ^{1}H-NMR of **2.9** (Figure 2.5) is shown as a representative of the new Nindigo derivatives. The acidic N-H proton which is again partially stabilized by the imine (as was the case with **2.8**), is shifted well downfield of a normal N-H proton to 10.27 ppm. The characteristic two doublets of a *para* substituted aromatic ring are partially masked by two doublets and two triplets of the backbone of the molecule. The protons of the remaining methyl group on the aniline are found at 2.38 ppm.

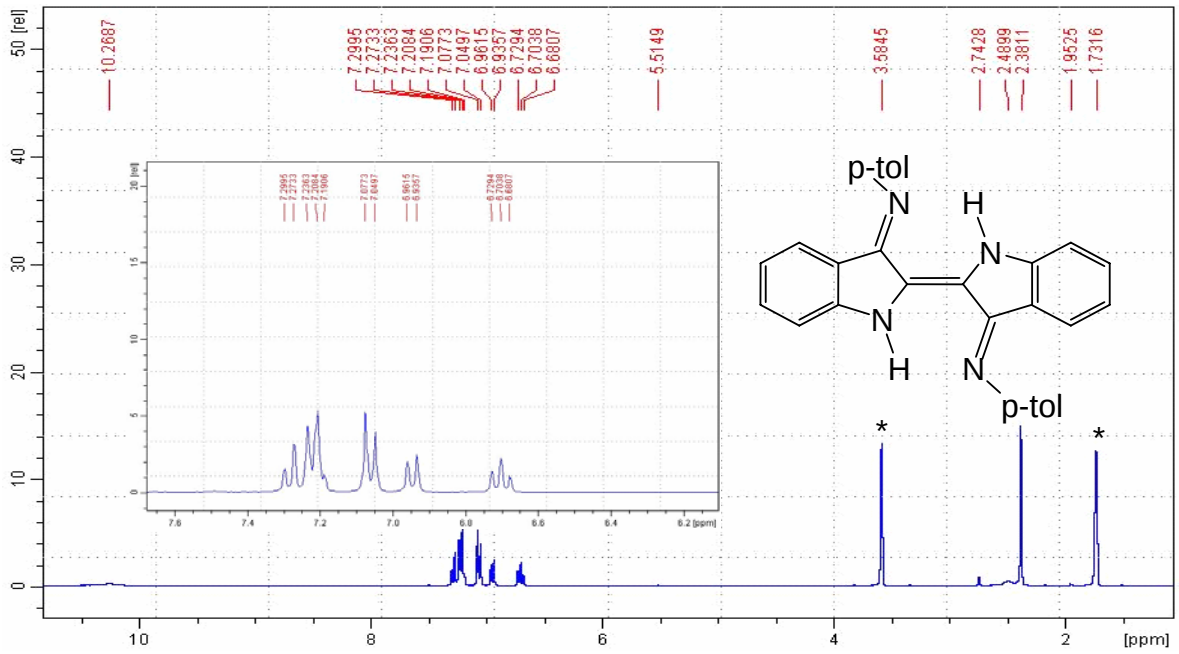

Figure 2.5: ^{1}H-NMR of p-tolyl Nindigo 2.9 in d_8THF. Peaks labeled with a asterisk correspond to the NMR solvent.

2.9 is highly soluble in solvents such as dichloromethane, acetone, and benzene (~0.1M or more), but is insoluble in solvents such as hexanes and ether. This insolubility made it very easy to purify **2.9** because all of the residual aniline starting material could be washed away in hexanes or ether. Nindigos **2.10** and **2.11** are soluble in a wide range of polar and non-polar solvents, from acetone and ethanol, to ether and hexanes. **2.12** and **2.13** are the least soluble of the series, where 5 mg of sample for an ^{1}H-NMR will only fully dissolve in either THF or dichloromethane.

2.3.3 UV-Vis Spectra of Nindigos

The UV-Vis spectrum of ^{t}butyl Nindigo **2.10** is shown in Figure 2.6. **2.10** has an absorption maximum at approximately 656 nm, with an extinction coefficient approaching $1x10^{4}$ L $cm^{-1}mol^{-1}$.

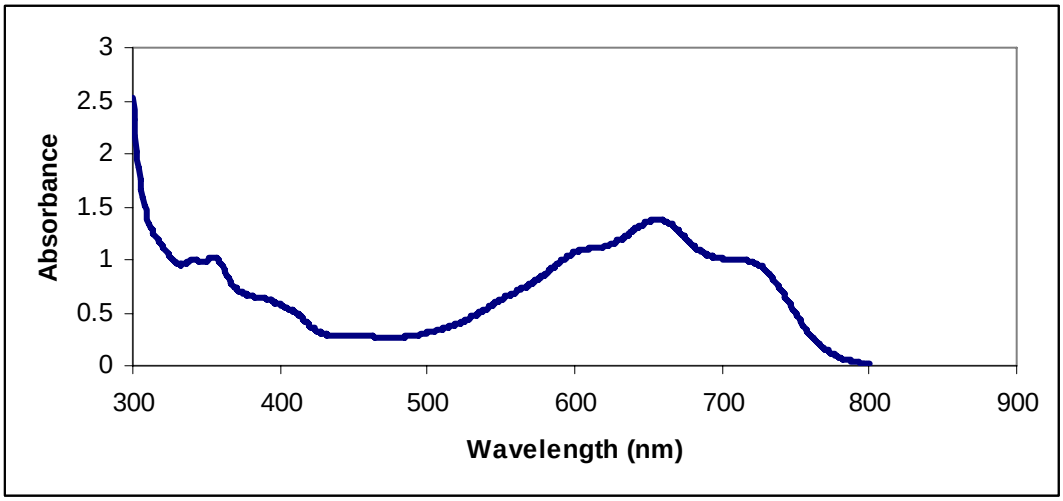

Figure 2.6: UV-Vis of ^{t}Bu Nindigo 2.10 in THF.

The UV-Vis spectra of **2.9**, **2.11-2.13** are qualitatively similar, each having a λ_{max} close to 600 nm (Figure 2.7). All derivatives also obey Beers law, in the 10^{-5} to 10^{-4} concentration range, indicating that solution aggregation is not occurring in this range. This is due to the more bulky derivatization of Nindigo relative to indigo preventing the stacking of dimers.

The spectra of **2.9-2.13** can be compared with the electronic spectrum of indigo itself, which also has an absorbance close to 600 nm, corresponding to a $\pi \rightarrow \pi^*$ transition.[45] It has also been found that the λ_{max} absorption for indigo increases with solvent polarity,[46] which is because the λ_{max} absorption is dependant on intermolecular hydrogen bonding between indigos, which are greatest in more polar solvents.[45] Therefore it stands to reason that the absorbances seen for the Nindigos are also due to $\pi \rightarrow \pi^*$ transitions, and that the λ_{max} absorption is varying in accordance with the ability of one Nindigo to form intermolecular hydrogen bonds with another. Therefore, the bathochromic shift of the λ_{max} absorption of ^{t}butyl Nindigo **2.10** relative to the other

Nindigos may be due to greater intermolecular hydrogen bonding in the case of ^{t}butyl Nindigo.[45]

Also, as the indigo concentration is increased, a second peak appears at 700 nm which continues to increase in absorbance with concentration until it eventually is of greater intensity than the original peak at 600 nm. This behavior was attributed to the aggregation of indigo in solution[47].

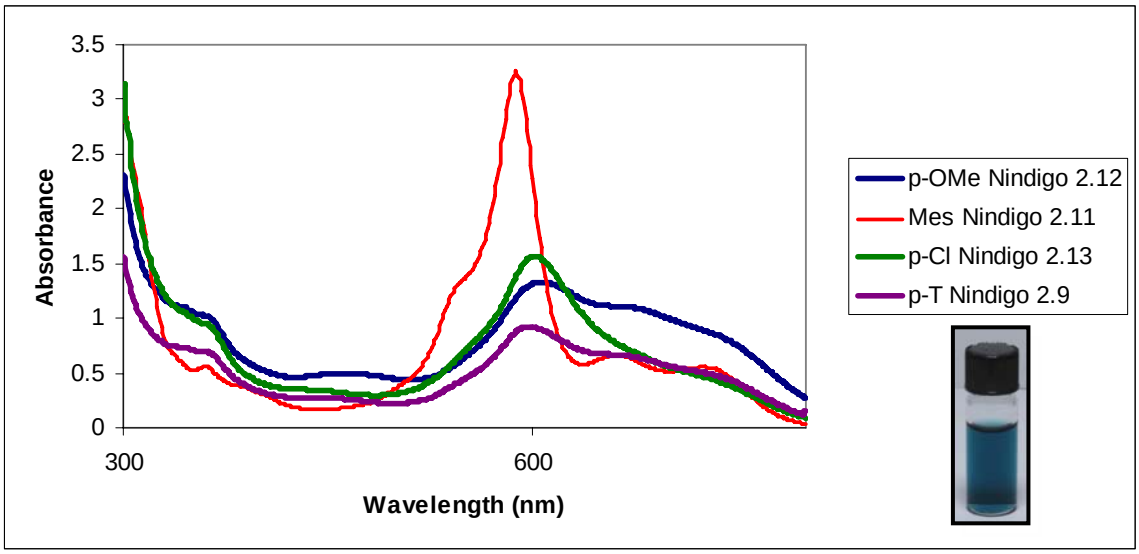

Figure 2.7: UV-Vis of 2.9, 2.11-2.13 in THF. Inset 0.1mM solution of 2.9 in THF.

2.3.4 Crystal Structures

Crystal structures of two Nindigo derivatives were also obtained. The X-ray crystal structure of mesityl-Nindigo **2.11** is shown in Figure 2.8. The aromatic substituents are twisted with respect to the plane of the backbone by an angle of 73.6^{o}. This is due to the steric interactions between the *ortho* methyl groups on the mesityl ring and the backbone of the molecule. However **2.1**, an aromatic Nindigo in which there are only *ortho* H atoms, the phenyl rings are twisted to an angle of 79.4^{o} to the plane of the molecule.

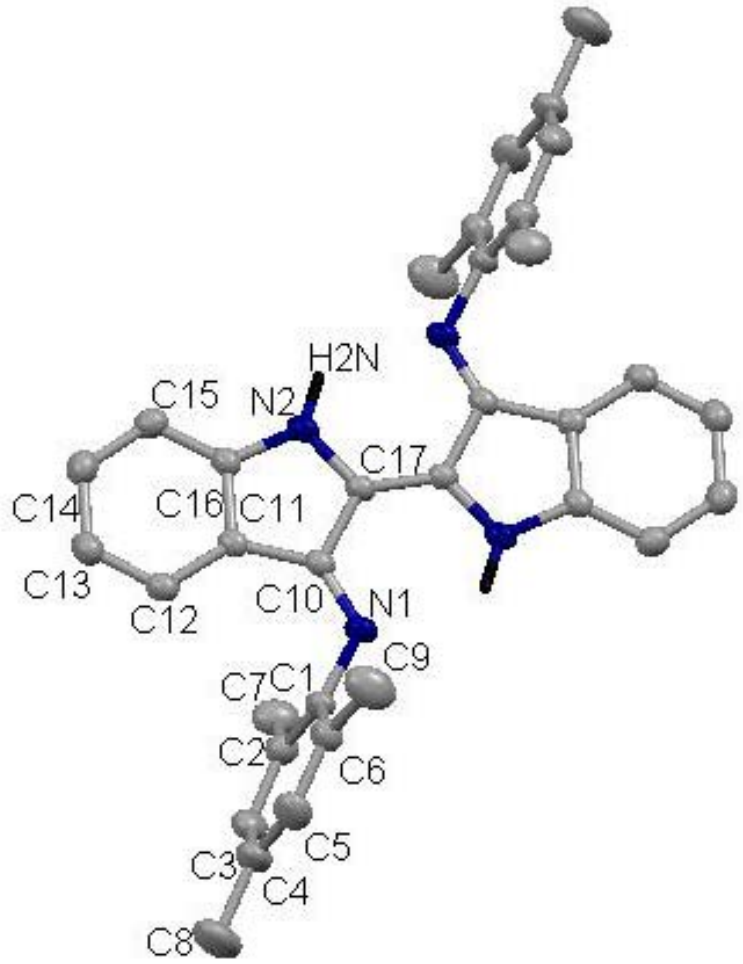

Figure 2.8: Crystal structure of 2.11 (50% thermal ellipsoids). All hydrogens other than H2N have been removed for clarity. Molecule resides in a plane of symmetry.

Table 2.3.2: Selected bond lengths and angles for 2.11

Bond Length (Å)		Angle (deg)	
C17-C17'	1.366(4)	C1-N1-C10	121.03(17)
C17-N2	1.378(3)	N1-C10-C17	121.41(18)
C17-C10	1.455(3)	C10-C17-C17	127.13(2)
C10-N1	1.301(3)	C17-C17-N2	124.20(2)
N1-C1	1.425(2)	C10-C17-N2	108.65(17)

The X-ray crystal structure of ^{t}Bu Nindigo **2.10** is presented in Figure 2.9. The central C=C bonds on the backbone of the molecule are 1.409 Å **2.10** and 1.366 Å **2.11**, are slightly longer than normal for alkenes, which however, is expected for donor-

acceptor substituted double bond. The fact that the central C=C bond of ^{t}Bu Nindigo is larger than that of mesityl Nindigo is likely due to the increased electron donating effects of the *tert*-butyl group vs. the mesityl group. Again as with **2.8**, the rest of the bonds and angles in the molecule are unremarkable and similar to what would be expected in simple indigo compounds[42,43]. The core of the molecule is planar in both structures.

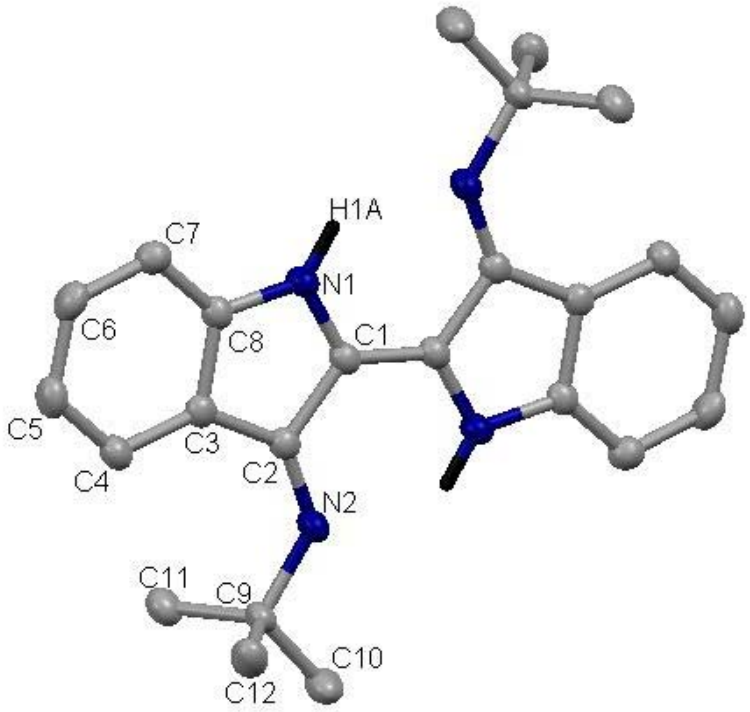

Figure 2.9: Crystal structure of 2.10 (50% thermal ellipsoids). All hydrogens other than H1A have been removed for clarity. Molecule resides in a plane of symmetry.

Table 2.3.3: Selected bond lengths and angles for 2.10

Bond Length (Å)		Angle (deg)	
C1-C1	1.409(3)	N1-C1-C1	123.0(2)
C1-C2	1.462(2)	C1-C1-C2	126.5(2)
C1-N1	1.355(2)	C1-C2-N2	119.57(14)
C2-N2	1.323(2)	C2-N2-C9	127.74(14)
N2-C9	1.474(2)	C2-C1-N1	110.50(14)

2.4 Summary

The conversion of the ketones on indigo to imines via the use of $TiCl_4$ has resulted in the successful synthesis of five Nindigo derivatives. These molecules are all highly coloured with extinction coefficients in the $1x10^4$ range and greater, and all show much greater solubility in organic solvents than that of indigo. The propensity of these molecules to act as bridging ligands can now be investigated to further understand their future role in the realm of inorganic coordination chemistry.

2.5 Experimental Section

Unless otherwise indicated, all reactions were carried out under an atmosphere of Argon using standard Shlenck techniques. Glassware was dried at 125^{o}C for 24h prior to each reaction. Bromobenzene, indigo, 1.0M $TiCl_4$ in toluene and 1,4-diazabicyclo-[2.2.2] octane (DABCO) were all purchased from Aldrich. 1, 1, 1, 5, 5, 5 – hexafluoroacetylacetonate was purchased from Alfa Aesar. All reagents were used as received, with the following exceptions: bromobenzene was dried with 4Å molecular sieves which had been dried in the oven for 125^{o}C for at least 24h. DABCO was dried by azeotropic distillation with benzene three times before use. THF was dried by refluxing over Na/Benzophenone for 2 hours prior to distillation, and then used immediately. All NMR spectra were recorded on a Bruker AC300 instrument (300 MHz for ^{1}H, 75.47 MHz for ^{13}C), unless otherwise noted. All spectra were referenced to the central solvent line, relative to tetramethylsilane. UV-Vis-NIR spectra were recorded on a Varian Cary 5 instrument in Dichloromethane or THF. IR samples were made into a KBR pellet and run using a Perkin-Elmer One FT-IR spectrometer. Elemental analyses were performed by Canadian Microanalytical Services, New Westminster, B.C.

See Appendix C for ^{1}H and ^{13}C NMR spectrum scans.

Indigo mono mesityl imine 2.8: 2, 4, 6 trimethylaniline (0.4 mL, 2.85 mmol) and DABCO (640 mg, 5.7 mmol) were added to 40 mL of dry THF. $TiCl_4$ (0.35 mL, 3.1 mmol) was then slowly added, forming a yellow suspension to which indigo (250 mg, 0.95 mmol) was added, at which point the solution turned purple. This mixture was heated at reflux for 20 hrs whereupon another 0.1 mL $TiCl_4$ was added and the solution was stirred at room temperature for another hour. The solution was filtered and the solvent was removed by rotary evaporation, then washed with hexanes and ether until the washings were colourless. The washings were then evaporated giving 324 mg (90% yield) of a purple solid, **2.8**. X-ray quality crystals were grown from the slow evaporation of Et_2O. UV-Vis (EtOH): λ_{max} 599nm, $\varepsilon = 4.2 \times 10^4\ M^{-1}\ cm^{-1}$. ^{1}H NMR (CD_2Cl_2): 9.66 ppm (s, 1H), 9.36 ppm (s, 1H), 7.73 ppm (d, 7.5 Hz, 1H), 7.44 ppm (t, 7.5 Hz, 1H), 7.30 ppm (t, 6.9 Hz, 1H), 7.07 ppm (d, 8 Hz, 1H), 7.04 ppm (d, 8 Hz, 1H), 6.97 ppm (s, 2H), 6.94 ppm (t, 7 Hz, 1H), 6.65 ppm (t, 7 Hz, 1H), 6.50 (d, 5Hz) 2.35 ppm (s, 3H), 2.03 ppm (s, 6H). ^{13}C NMR (CD_2Cl_2): 186.6, 162.4, 151.5, 149.1, 147.1, 135.1, 134.1, 133.7, 129.5, 127.8, 125.9, 125.7, 124.3, 121.32, 121.31, 120.4, 120.0, 118.8, 112.7, 111.9, 21.1, 18.2. Analysis Calcd. For $C_{25}H_{31}N_3O$: C: 79.13, H: 5.58, N: 11.07. Found C: 78.52, H: 5.51, N: 10.81.

Indigo-*N,N'*-bis(p-tolyl imine) 2.9: Indigo (250mg, 0.95 mmol) and p-toluidine (612mg, 5.72mmol were added to 40 mL of bromobenzene under argon in a 2-neck flask attached to a reflux condenser, giving a blue suspension. 3.8 mL of a 1.0M $TiCl_4$ solution in

toluene was then slowly added through the septum, turning the solution a deep red-brown colour. DABCO (1.280g, 11.44 mmol) was then added, which caused the solution to turn deep green. The mixture was heated at reflux gently for 40 hours. The resulting dark green solution was filtered while still warm, and washed with hexanes. The blue filtrate was then pumped to dryness on a rotary evaporator. The resulting dark blue-purple solid was thoroughly washed with ether and hexanes until the filtrate washings were colourless. The remaining solid was recrystallized from dichloromethane/ hexanes to give purple fibrous needles massing 258 mg (0.586 mmol, 61% yield). UV-Vis (THF): λ_{max} 598 nm, $\varepsilon = 9.2 \times 10^3$ M^{-1} cm^{-1}. ^1H NMR (d_8-THF) δ 10.26 (s, 2H), 7.27 (t, 7.9 Hz, 2H), 7.21 (m, 6H), 7.06 (d, 8.3 Hz, 4H), 6.95 (d, 7.8 Hz, 2H), 6.70 (t, 7.7 Hz, 2H), 2.38 (s, 6H) ppm. ^{13}C NMR δ 146.1, 134.3, 131.2, 130.5, 125.5, 121.3, 120.5, 119.7, 116.1, 21.1 ppm. Analysis Calcd. For $C_{30}H_{24}N_4$: C: 81.79, H: 5.49, N: 12.72. Found C: 81.21, H 5.44, N: 12.60.

Indigo-*N,N'*-di-*tert*-butylimine 2.10: This compound was prepared in an analogous manner to p-tolyl Nindigo: Starting with 0.6mL of *t*-butylamine. After removal of the bromobenzene the residue was washed with a minimal amount of ether to give as a shiny purple crystalline solid, yield 335mg (90% yield). X-Ray quality crystals were grown from a mixture of dichloromethane and hexanes. UV-Vis (THF): λ_{max} 656 nm, $\varepsilon = 9700$ M^{-1} cm^{-1}. ^1H NMR (CD_2Cl_2) δ 9.68 (s, 2H), 7.76 (d, J = 8.0 Hz, 2H), 7.18 (m, 4H), 6.92 (t, J = 6.6 Hz, 2H), 1.53 ppm (s, 18H). ^{13}C NMR (CD_2Cl_2): δ 129.9, 127.1, 121.3, 116.5, 102.6, 30.3, 2.0 ppm. Anal. Calcd For $C_{24}H_{28}N_4$: C: 77.38, H: 7.58, N: 15.04. Found C: 76.52, H: 7.66, N: 14.4.

Indigo-*N,N'*-bis(mesityl imine) 2.11: This compound was prepared in an analogous manner to p-tolyl Nindigo starting with 0.804 mL of 2, 4, 6 trimethylaniline. Upon removal of the bromobenzene after the filtration, 352mg of crude product were recovered. This was then columned on silica with acetone, and then with THF, which pushed through a dark purple band. This solution was pumped dry to give dark purple crystals, yield 310 mg (65%). X-ray quality crystals were grown from a mixture of DMSO and Et_2O. UV-Vis (THF): λ_{max} @ 588, ε = 30190 M^{-1} cm^{-1}. ^1H NMR (CD_2Cl_2) δ 9.89 (s, 2H), 7.23 (t, 7.7 Hz, 2H), 7.12 (d, 8.0 Hz, 2H), 7.01 (s, 4H), 6.63 (t, 7.4, 2H), 6.49 (d, 7.7 Hz, 2H), 2.37 (s, 6H), 2.14 (s, 12H) ppm. ^{13}C NMR (CD_2Cl_2): δ 157.6, 150.3, 144.1, 134.8, 131.8, 130.4, 129.4, 129.2, 124.6, 120.8, 119.5, 114.1, 21.2, 18.4 ppm. Analysis Calcd. For $C_{34}H_{32}N_4$: C: 82.22, H 6.49, N: 11.28. Found C: 79.70, H: 6.25, N: 10.81.

Indigo-*N,N'*-bis(p-methoxyphenyl imine) 2.12: This compound was prepared in an analogous manner to p-tolyl Nindigo with with following changes. 704 mg of p-OMe aniline was used instead of p-toluidine. Once the bromobenzene was removed from this solution, it was washed with ether and hexanes until the filtrate washings were colourless. 338 mg (75% yield) of shiny purple solid was recovered. UV-Vis (THF): λ_{max} = 607, ε = 1.2 x 10^4 M^{-1} cm^{-1}. ^1H NMR (d_8-THF): δ 10.71 ppm (2H, s), 7.15 ppm (2H, t, 7.6 Hz), 7.04 ppm (6H, m), 6.87 pm (6H, m), 6.58 ppm (2H, t, 7.4Hz), 3.72 ppm (6H, s). ^{13}C NMR(d_8-THF):δ 158.3, 141.4, 131.2, 125.3, 122.6, 121.1, 119.6, 116.1, 115.2, 55.7 ppm.

Analysis Calcd. For $C_{30}H_{24}N_4O_2$: C: 76.25, H: 5.12, N: 11.86. Found: C: 72.22, H: 5.01, N: 10.98.

Indigo-*N,N'*-bis(p-chlorophenyl imine) 2.13: This compound was prepared in an analogous manner to p-tolyl Nindigo with with following changes. 729 mg of p-Cl aniline was used instead of p-toluidine. Once the bromobenzene was removed from this solution, it was washed with ether and hexanes until the filtrate washings were colourless. 382 mg (83% yield) of shiny purple solid was recovered. UV-Vis (THF): λ_{max} @ 601, ε = 1.5 x 10^4 M^{-1} cm^{-1}. ^{1}H NMR (d_8-THF): δ 7.41 ppm (4H, d, 10 Hz), 7.32-7.22 ppm (4H, m), 7.14 ppm (4H, d, 10Hz), 6.92 ppm (2H, d, 7.5 Hz), 6.76 ppm (2H, t, 7.5 Hz). ^{13}C NMR: Insufficient solubility to obtain ^{13}C data. Analysis Calcd. For $C_{28}H_{18}N_4Cl_2$: C: 69.86, H: 3.77, N: 11.64. Found C: 69.86, H: 3.77, N: 10.59.

Chapter 3 : Synthesis and Characterization of Bridging Complexes of Nindigo Derivatives

3.1 Introduction

In Chapter 2 the synthesis of several Nindigo derivatives was described. The next step in the project was to see if Nindigo derivatives could be used as functional bridging ligands. As previously discussed (Chapter 1), there are only a handful of indigo based bridging complexes in the literature and, as far as the pre-existing Nindigo ligands made before this work are concerned, none of them have been tested for bridging potential.

3.2 Transition Metal Coordination Chemistry

The synthesis of binuclear Nindigo complexes could in principal be accessed by two routes (Scheme 3.1). Protonolysis can be achieved by the addition of two equivalents of a metal precursor, thus eliminating HX (X = hfac, acac, halide, etc) and resulting in the bimetallic species **3.1**. A base may be required to neutralize the HX byproduct, as the imine bond in the Nindigo is likely susceptible to hydrolysis in the presence of an acid and water. Another route involves the initial deprotonation of the Nindigo ligand with a strong base such as NaH or BuLi, followed by the subsequent reaction with the metal precursor and the elimination of a salt.

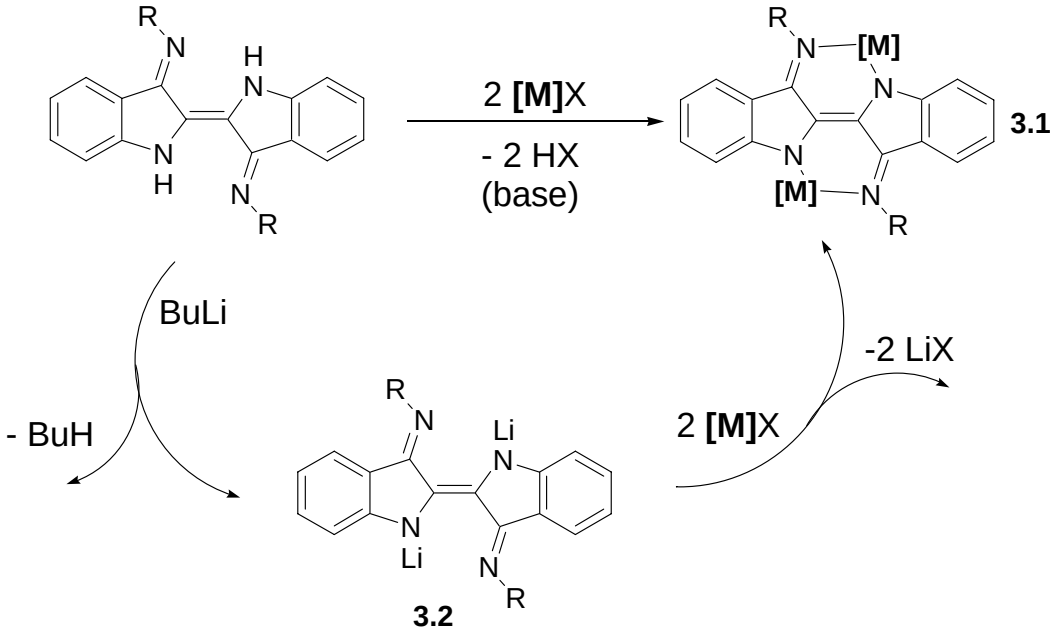

Scheme 3.1: General synthesis for binuclear Nindigo complexes

3.3 Results and Discussion

3.3.1 Synthesis of Nindigo Complexes

Initial explorations into the synthesis of Nindigo complexes were to be done with diamagnetic metals so that the resulting complexes made could be studied using NMR spectroscopy. With this in mind palladium bis (hexafluoroacetylacetonate) was chosen as an appropriate metal precursor to the complex. Palladium in its square planar form generally takes on the oxidation state of +2, and as such is diamagnetic and essentially redox-inert in the range in which we will be testing.[48-50] In addition, the hexafluoroacetylacetonate ancillary ligand offers two advantages. Firstly, the propensity of the second hfac group to come off the metal after the first has been removed is much lower. Ideally this will allow for the synthesis of a bimetallic palladium complex with each of the two metals being capped by a lone hfac ligand. Secondly, the CF_3 groups tend to render complexes more soluble. Another minor benefit is that hfac adds only one

additional proton and ^{19}F as an NMR active nucleus to the overall complex, and so the characterization by NMR will not be made overly complicated.

The first reactions were performed as shown in Scheme 3.2, with 2 equivalents of Pd per equivalent of Nindigo. The protonated hfac byproduct can be pumped away as it has a low boiling point. These reactions were also tried with $Pd(acac)_2$. However, relative to the reactions with $Pd(hfac)_2$, which changed colour to dark green instantaneously on mixing with the Nindigos, the reactions with $Pd(acac)_2$ showed no obvious colour change ever after several hours and so reactions involving $Pd(acac)_2$ were discontinued. The lack of reaction was later confirmed using ^1H-NMR spectroscopy.

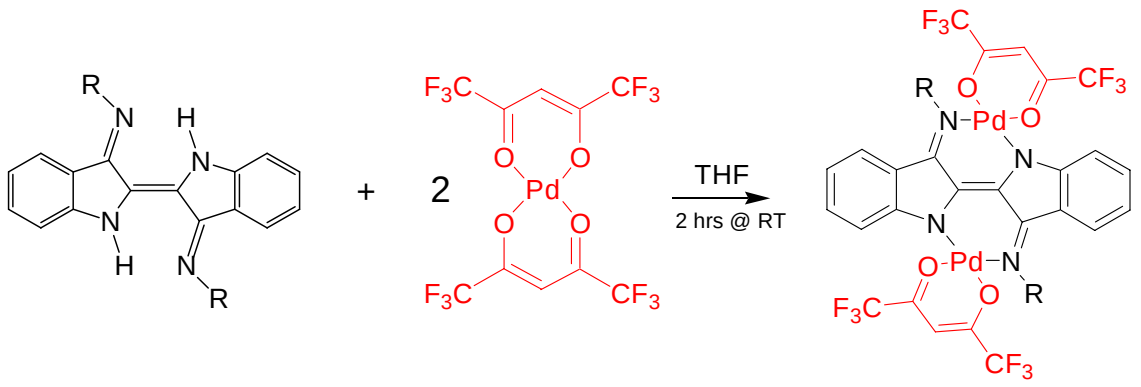

R = *p*-tolyl	**2.9**
R = *p*-methyoxyphenyl	**2.12**
R = ^{t}Butyl	**2.10**
R = mesityl	**2.11**
R = *p*-chlorophenyl	**2.13**

R = *p*-tolyl	**3.3**
R = *p*-methyoxyphenyl	**3.4**
R = ^{t}Butyl	**3.5**
R = mesityl	**3.6**
R = *p*-chlorophenyl	**3.7**

Scheme 3.2: Reaction conditions for the initial synthesis of Nindigo complexes with Palladium

Palladium-Nindigo complexes **3.3-3.7** were all isolated as green solids in 20-40% yields after purification by re-crystalization. The stability of these complexes in solution is somewhat limited if the reaction flask is not dried of solvent after 2 hours. Proteo hfac is a byproduct of the reaction, and Hhfac has a low enough boiling point that

it can be removed by vacuum at room temperature. The decomposition seen can likely be attributed to the Hhfac, which may be reacting with the imine of Nindigo. The obvious way around this was to add a base (such as DABCO or NEt_3), and while this prevented the formation of the brownish decomposition product, the green product that is isolated often appears as a mixture of compounds. The complexes do not survive column chromatography, and the desired product and the by-products have similar solubilities. A change in reaction solvent and conditions (ie. reflux, duration of reaction) has not yet shown to improve the reliability or yield. However, it was found that by increasing the amount of $Pd(hfac)_2$ used to 3 equivalents increased the purity such that multiple recrystalizations were not needed, and also increased the yield to near 60%. Despite the fact that Nindigo complexes are more soluble in most common organic solvents than the parent indigo, the are still often not soluble enough to obtain complete ^{13}C NMR data. Elemental analysis have also been found to have low %C data, indicating that there may be incomplete combustion occurring.

The proton NMR spectrum of **3.3** (Figure 3.1), is shown as a representative of the complexes. One of the doublets from a proton on the indigo backbone has been shifted significantly upfield to 5.80 ppm from its original aromatic chemical shift at ~7.2 ppm. The reason for this can be explained by referring to the crystal structure of **3.3** (Figure 3.4), where it can be seen that the proton attached to C4 is being heavily shielded by the aryl ring extending from N2. The remaining indigo backbone peaks as well as the two doublets from the *para* substituted are all also shifted upfield but to a much lesser degree. The singlet from the lone proton on hfac appears at 6.32 ppm, and the singlet for the *p*-tol methyl group has a chemical shift of 2.41 ppm.

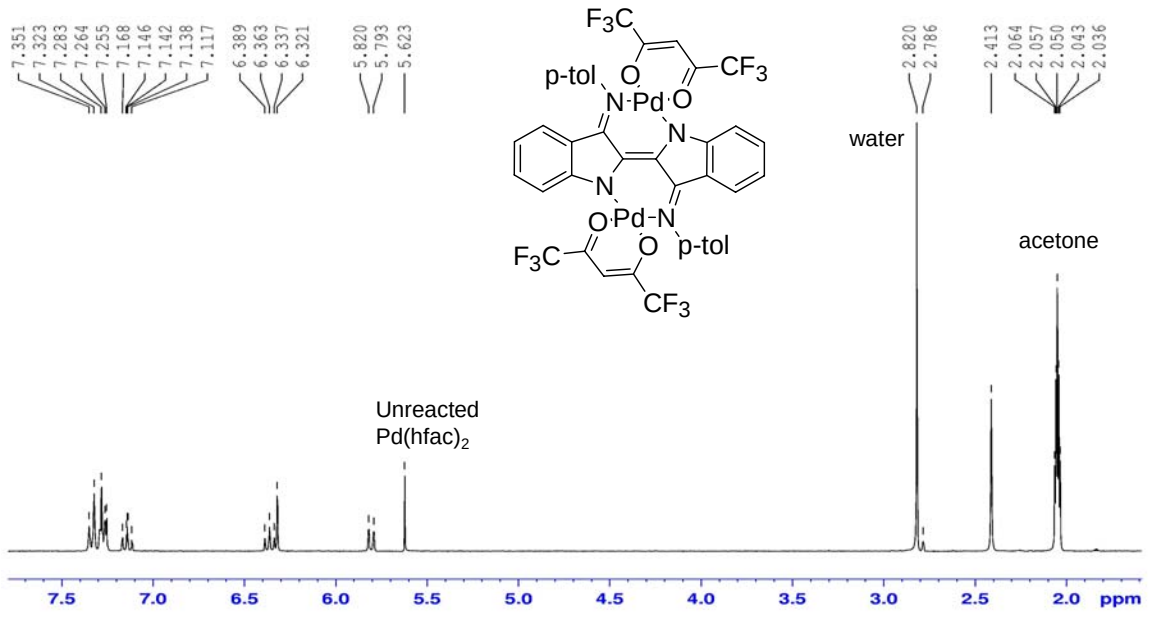

Figure 3.1: ^{1}H-NMR of 3.3 in d_6 acetone.

3.3 retains much of the solubility characteristics of its parent Nindigo, i.e. it is soluble in dichloromethane and acetone, but is still insoluble in hexanes and ether. In the case of **3.4** and **3.7**, the complexes are more soluble in solvents such as dichloromethane and acetone then their parent Nindigos, which is likely due to the solubility enhancing effects of the CF_3 groups on the hfac ligand. However, complexes **3.4** and **3.7** still remain the least soluble of the series.

3.3.2 UV-Vis spectra of Nindigo Complexes

The UV-Vis spectrum of **3.3** is shown in Figure 3.2. The spectrum of the free ligand **2.9** has an absorbance at approximately 600 nm with an extinction coefficient approaching $1x10^4$ M^{-1} cm^{-1}. However, the major absortion feature of complex **3.3** is shifted into the near infrared region (λ_{max} = 911 nm) with an extinction coefficient of $1.9x10^4$ M^{-1} cm^{-1}. The affect of this is most noticeable in solution, where the complex is a very pale green compared to the deep blue of the parent *para*-tolyl Nindigo compound.

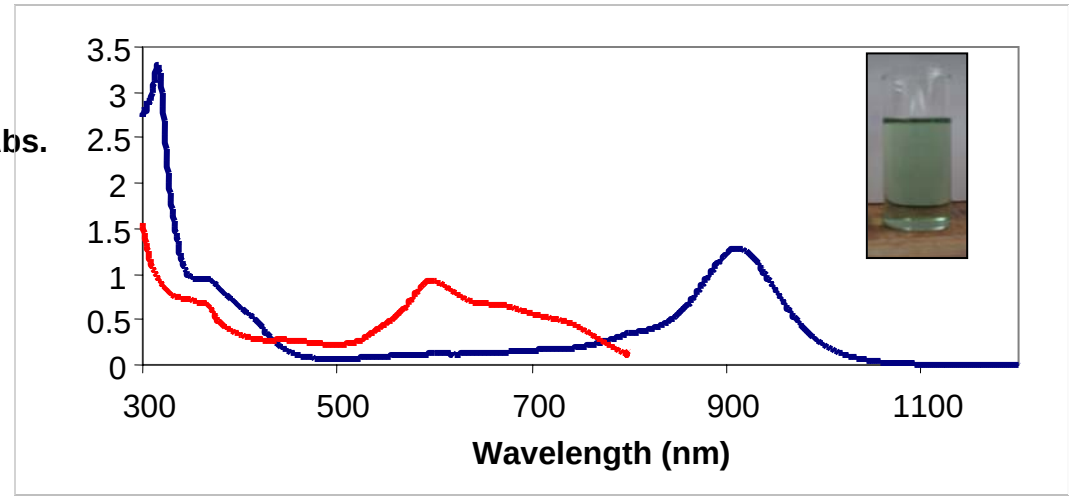

Figure 3.2: UV-Vis spectra of 3.3 in dichloromethane (blue), and that of p-tolyl Nindigo 2.9 in THF (red). Inset 0.1mM solution of 3.3 in dichloromethane

The UV-Vis spectrum of **3.4** is shown in Figure 3.3. The spectra of the free ligand **2.12** has an absorbance at approximately 600 nm with an extinction coefficient approaching $1x10^4$ M^{-1} cm^{-1}. Again, the major absortion feature of complex **3.4** is shifted into the infra-red region, now at 912 nm, with an extinction coefficient of $1.7x10^4$ M^{-1} cm^{-1}.

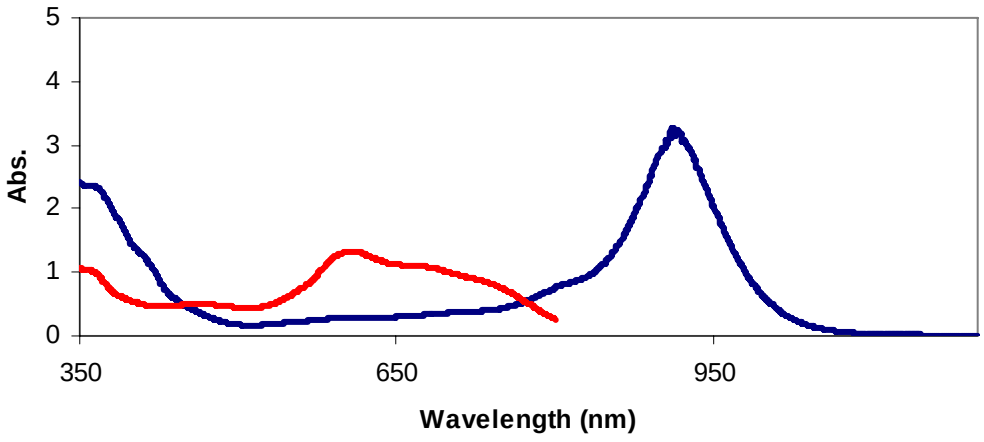

Figure 3.3: UV-Vis spectra of 3.4 in dichloromethane (blue), and that of p-methoxyphenyl Nindigo 2.12 in THF (red).

The significant red-shift observed can be attributed to the fact that there is a high degree of anionic character on the amine nitrogen in the covalent N-Pd bond, relative to that of the N-H bond on the free ligand. This is still a $\pi \rightarrow \pi^*$ transition, only the increased negative character on the nitrogen will raise the energy of the HOMO of the molecule, shortening the HOMO-LUMO gap and allowing transitions of a lower energy to occur.

3.3.3 Crystal Structures

Crystal structures of four complexes were obtained. The X-ray crystal structure of the complex of p-tolyl Nindigo **3.3** is shown in Figure 3.4. The Pd-Pd distance across the bridge is 6.04 Å, which is between the typical separation distance in oxalate-bridged binuclear complexes (5.4-5.7 Å)[51,52], and pyrazine-linked bridged binuclear complexes (6.8-7.2 Å)[53,54]. The core of the molecule is no longer planar as it was in the free ligand, with the core now being slightly saddle shaped. The two *para* tolyl rings are displaced in one direction and the Pd(hfac) rings in the other. As a result, the two Pd metal centers lie slightly above the planes defined by the NCCCN chelate at 0.512 Å and 0.56 Å for Pd1 and Pd2 respectively (Figure 3.5). Also, the NCCCN chelate of the bridge maintains a high degree of bond length alternation, which is not surprising given that the two nitrogens are fundamentally different from one another. This is unlike similar β-diktiminate complexes in which the NCCCN bond lengths are typically fully delocalized[5].

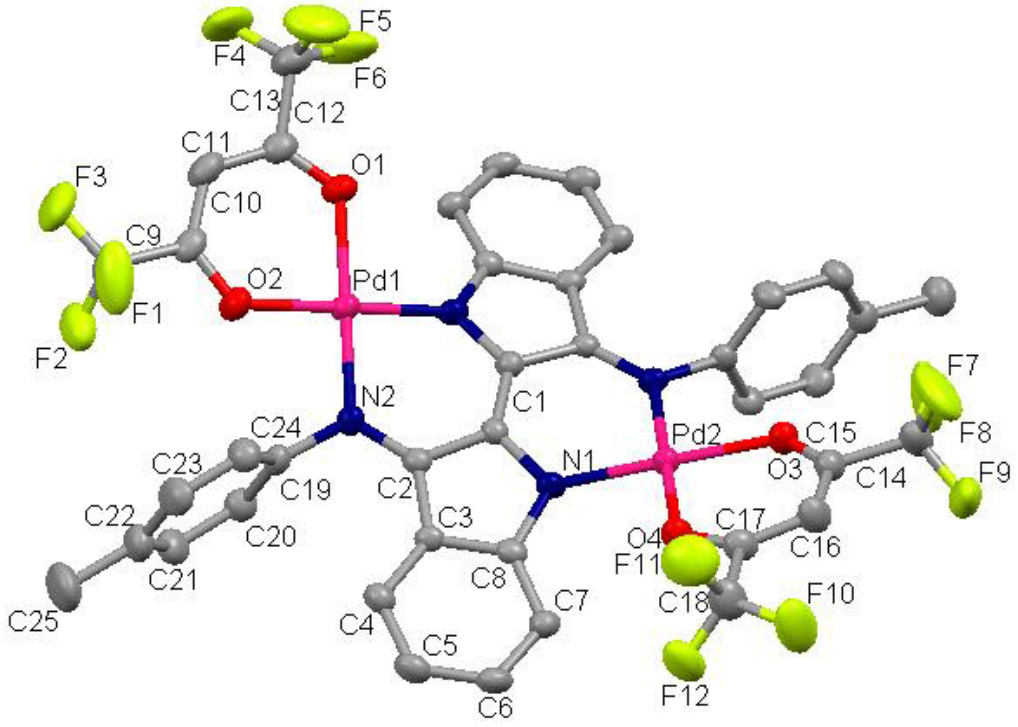

Figure 3.4: Crystal structure of 3.3 (50% thermal ellipsoids). All hydrogens have been removed for clarity.

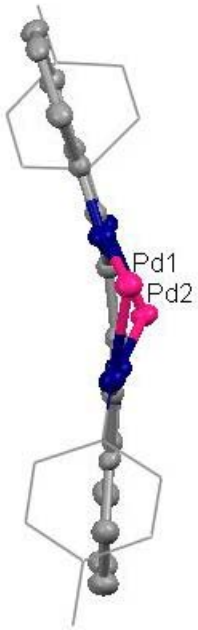

Figure 3.5: Side of view of the Nindigo core of 3.3. hfac ancillary ligands have been removed for clarity

Table 3.3.1: Selected bond lengths and angles for 3.3

Bond Length (Å)		Angle (deg)	
C1-C1’	1.368(5)	N1-C1-C1'	123.9(3)
C1-N1	1.362(4)	C2-N2-C19	117.1(3)
C2-N2	1.314(5)	C2-N2-Pd1	125.0(3)
N2-Pd1	1.986(3)	N1’-Pd1-N2	91.55(12)
N2-C19	1.439(5)		
Pd1-Pd2	6.04		

The X-ray crystal structure of Nindigo complex of **3.4**, is shown in Figure 3.6. The structure is similar to that of **3.3**, with the Pd-Pd distance being 6.161 Å, and the NCCCN chelate still shows bond length alternation. Unlike **3.3** however, the Pd centers are canted such that one is above the NCCCN plane by 0.477 Å and one is below the plane by 0.477 Å, yet the two *para* tolyl rings do not bend out of the plane of the molecule (Figure 3.7).

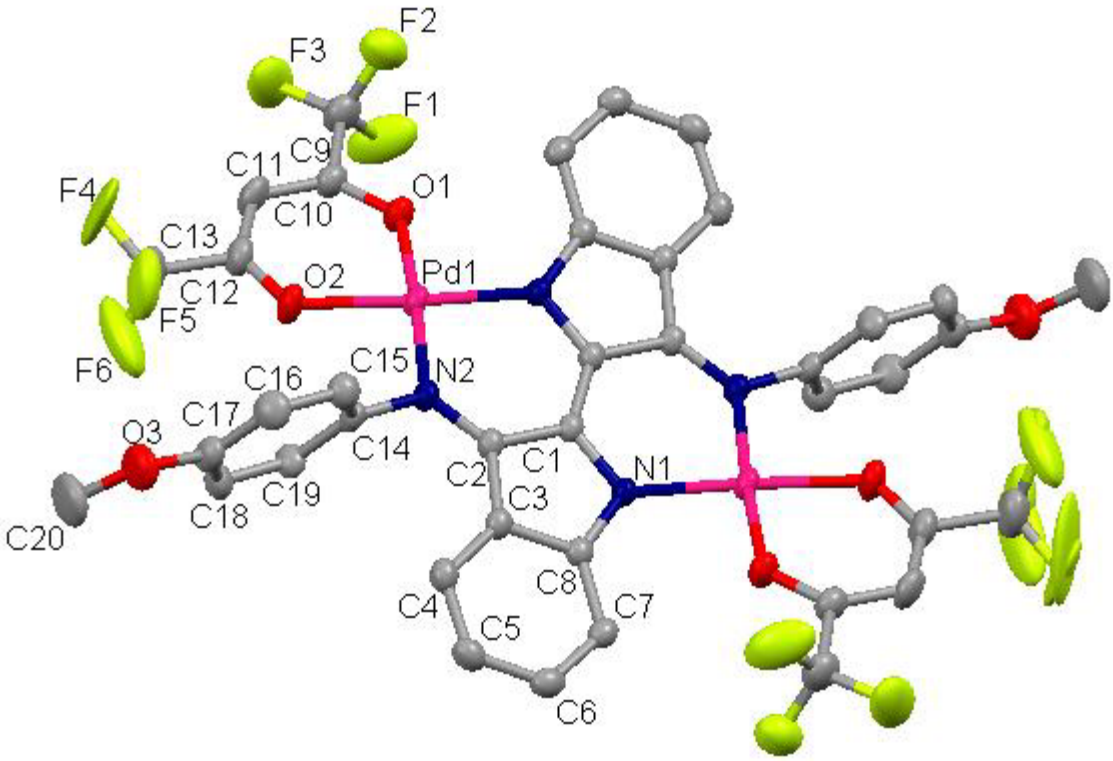

Figure 3.6: Crystal structure of 3.4 (50% thermal ellipsoids). All hydrogens have been removed for clarity.

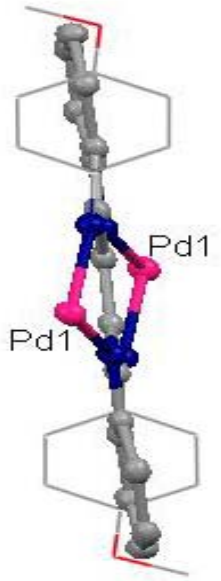

Figure 3.7: Side on view of the Nindigo core of 3.4. hfac ancillary ligands have been removed for clarity

Table 3.3.2: Selected bond lengths and angles for 3.4

Bond Length (Å)		Angle (deg)	
C1-C1’	1.379(7)	N1-C1-C1'	124.8(4)
C1-N1	1.370(4)	C2-N2-C14	117.5(3)
C2-N2	1.311(4)	C2-N2-Pd1	125.9(2)
N2-Pd1	1.989(3)	N1’-Pd1-N2	91.14(11)
N2-C14	1.444(4)		
Pd1-Pd1’	6.161		

In the attempt to obtain an X-ray crystal structure for **3.6,** the mesityl Nindigo complex, a mono-nuclear complex was obtained instead. A ChemDraw image showing the connectivity and bond order is shown in Figure 3.8. The X-ray crystal structure of the mono-nuclear mesityl complex is shown in Figure 3.9. It differs from what was expected in two important ways. Firstly, there is only one Pd in the complex, with an NH proton remaining for charge balance. The second unexpected feature is that the Pd is bound to

two indole N atoms, which means that the Nindigo core has isomerized from a *trans* to a *cis* alkene. Whether this formed in the initial reaction or is a decomposition product is not known. The Pd center is 0.235 Å above the NCCCN plane, and the NCCCN chelate still maintains bond length alternation, as was seen in **3.3** and **3.4**. Also, it is worth to note that while H4N is depicted on N4, the bond lengths of C10-N4, and C2-N3 are essentially equivalent and there is little desymmetrization of the bond lengths in the Nindigo core. Therefore it is likely that proton H4N is equally shared between N3 and N4.

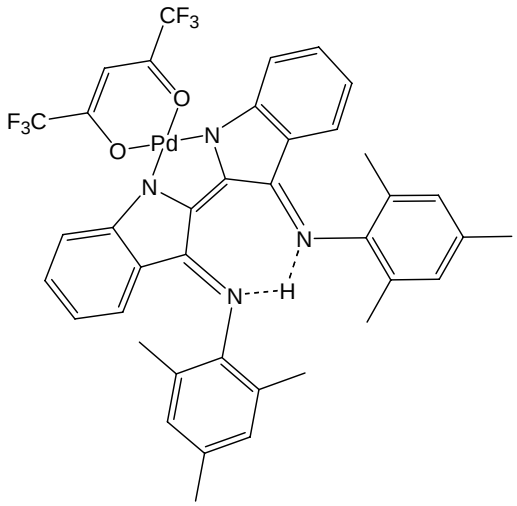

Figure 3.8: Bonding and connectivity of the mono-nuclear mesityl complex.

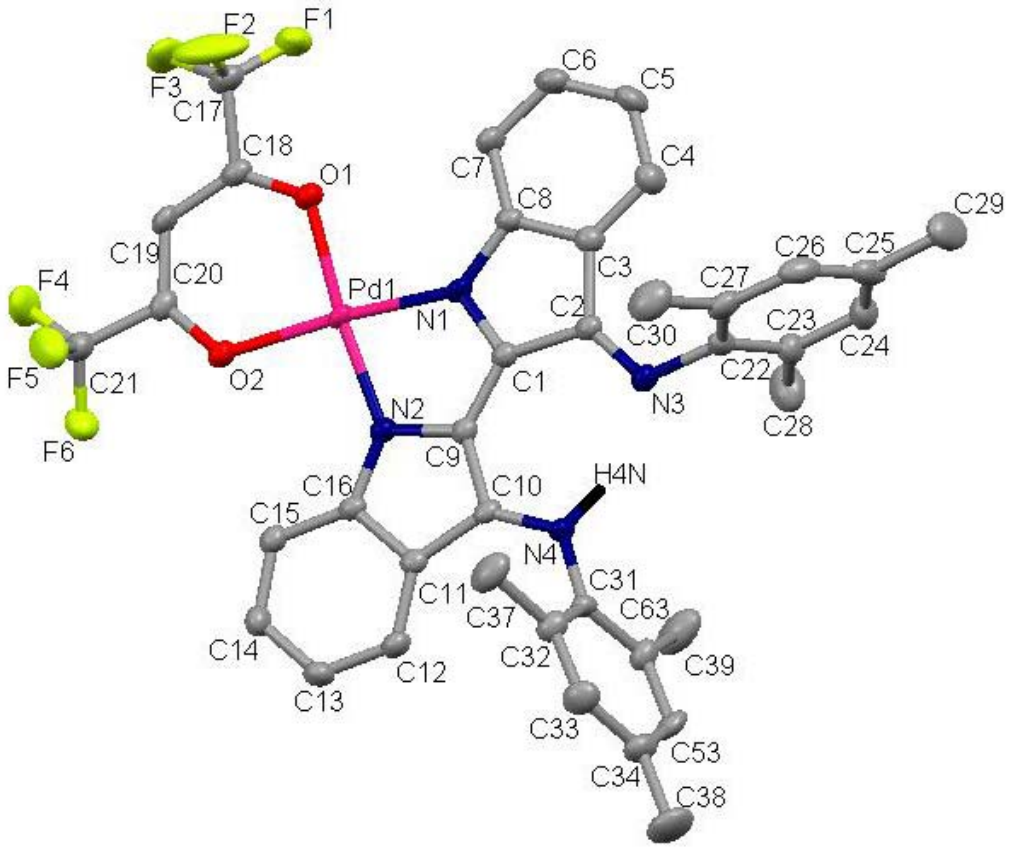

Figure 3.9: Crystal structure of the mono nuclear mesityl Nindigo complex (50% thermal ellipsoids). All hydrogens except H4N have been removed for clarity.

Table 3.3.3: Selected bond lengths and angles for the mono-nuclear mesityl Nindigo complex

Bond Length (Å)		Angle (deg)	
C1-N1	1.356(4)	N1-C1-C9	116.1(3)
C1-C9	1.387(4)	N1-C1-C2	110.2(3)
N1-Pd1	1.987(3)	N4-C10-C9	123.5(3)
C10-N4	1.333(4)	N1-Pd1-N2	80.88(10)
C2-N3	1.309(4)		
N4-C31	1.432(4)		

The structure of the ^{t}Bu Nindigo complex **3.5** is shown in Figure 3.10. The X-ray structural data was not of sufficient quality for publication or accurate bond length and angle measurement. Nonetheless the crude structure confirms the connectivity and

reveals some interesting features distinct from the other structures. The two *tert*-butyl groups both lie on the same side of the molecule i.e. the imine NC bond is nearly perpendicular to the square plane. As a result, to avoid steric interactions between the two *tert*-butyl groups the central C=C bond of the ligand is twisted by approximately 20^{o}, and this combined with steric repulsion between the two *tert*-butyl groups gives the molecule a considerable saddle shape.

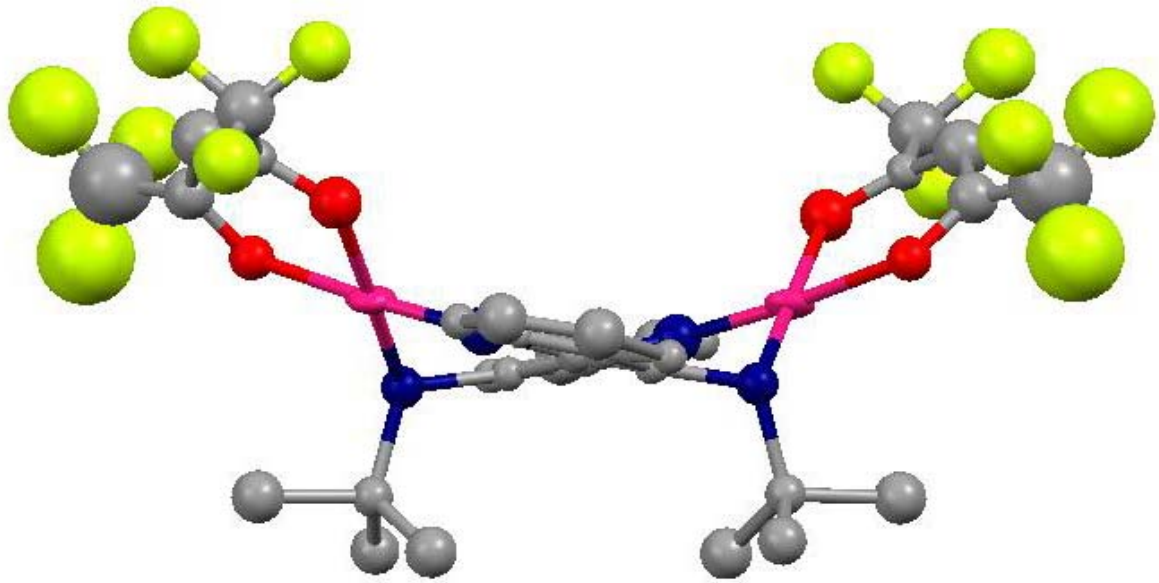

Figure 3.10: X-Ray Crystal structure of 3.5 (50% thermal ellipsoids). All hydrogens have been removed for clarity.

3.3.4 Cyclic Voltammetry of Nindigo Complexes

The cyclic voltammogram of **3.3** is shown in Figure 3.11. Since palladium in its square planar form generally takes on the oxidation state of +2, it is essentially redox-inert over the range in which these compounds are tested.[48-50] Therefore the processes

which occur can be attributed to ligand based electron transfers and not metal based redox processes. It shows two reversible one electron oxidations at $E_{1/2}$ = +0.05 V and $E_{1/2}$ = +0.51 V vs. Fc/Fc^{+}. There is also a quasi-reversible reduction at -1.33 V. The two oxidation waves correspond to the oxidation of the coordinated ligand from its dianionic form to the anionic radical and then to the neutral species, dehydronindigo. The reduction occurring at -1.33 V is the reduction of the coordinated dianion to a radical trianion.

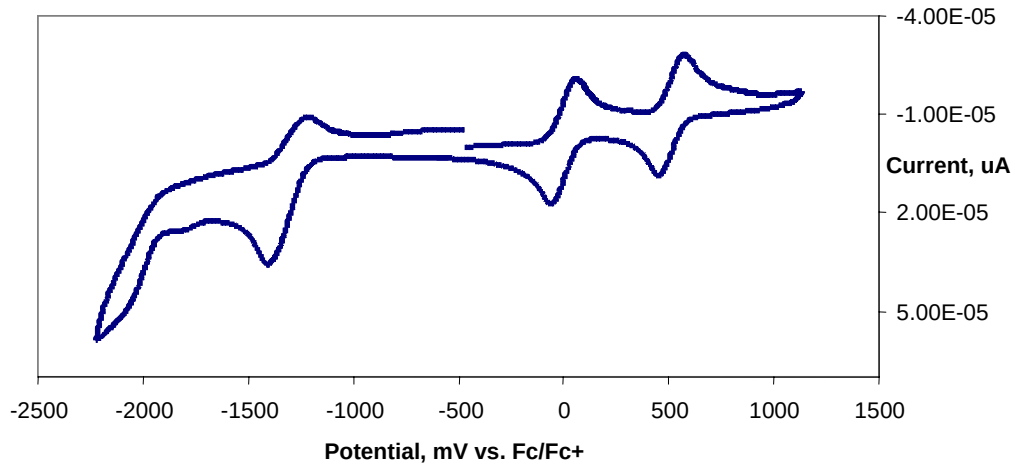

Figure 3.11: Cyclic Voltammogram of 3.3 (CH_2Cl_2 solution, 0.1M Bu_4NBF_4 electrolyte, scan rate 100 mV/s).

The cyclic voltammograms of complexes **3.4-3.6** are shown in Figure 3.12-Figure 3.14 respectively. **3.4** and **3.6** have $E_{1/2}$ values for the oxidation of the dianion to the radical anion, and from the radical anion to the neutral species, at similar values as the p-tolyl complex. The ^{t}Bu Nindigo complex **3.5** has only one reversible oxidation, occurring at +0.32 V. This is likely due to the fact that the increased electron donating ability of the *tert*-butyl group relative to the other funcational groups makes compound **3.5** more difficult to oxidize in the range being tested. All the redox processes both reversible and otherwise for all the complexes are summarized in Table 3.3.4. It should be noted that

when the cyclic voltammogram was run it was not known whether the Mesityl Nindigo complex is actually of the form shown in Figure 3.8, or of the more general Nindigo complex form as per Scheme 3.2.

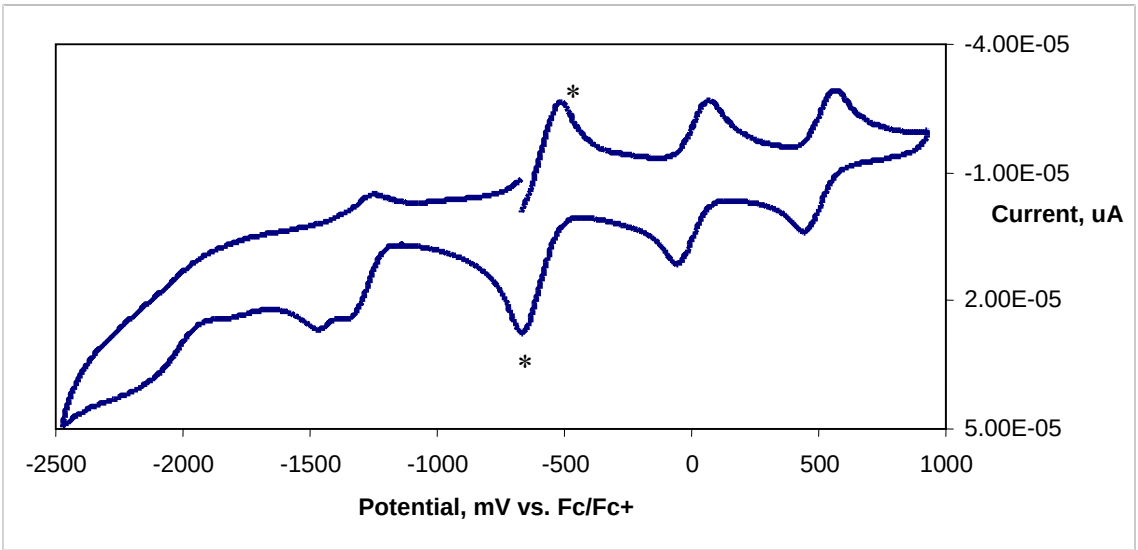

Figure 3.12: p-OMe Nindigo Complex 3.4. (CH_2Cl_2 solution, 0.1M Bu_4NBF_4 electrolyte, scan rate 100 mV/s). Starred waves correspond to decamethylferrocene added as a quasi-reference.

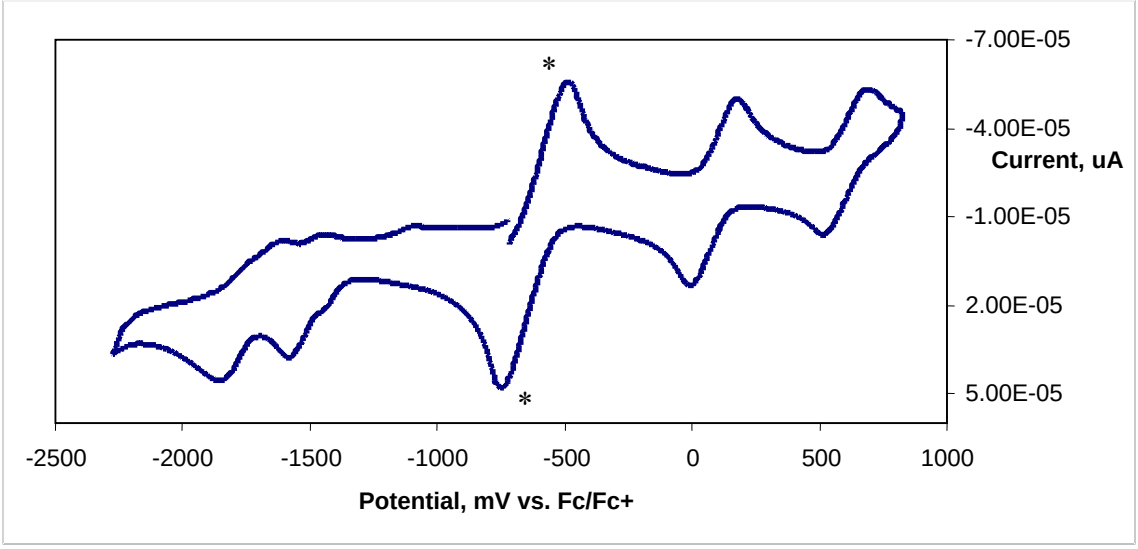

Figure 3.13: Mesityl Nindigo complex 3.6. (CH_2Cl_2 solution, 0.1M Bu_4NBF_4 electrolyte, scan rate 100 mV/s). Starred waves correspond to decamethylferrocene added as a quasi-reference.

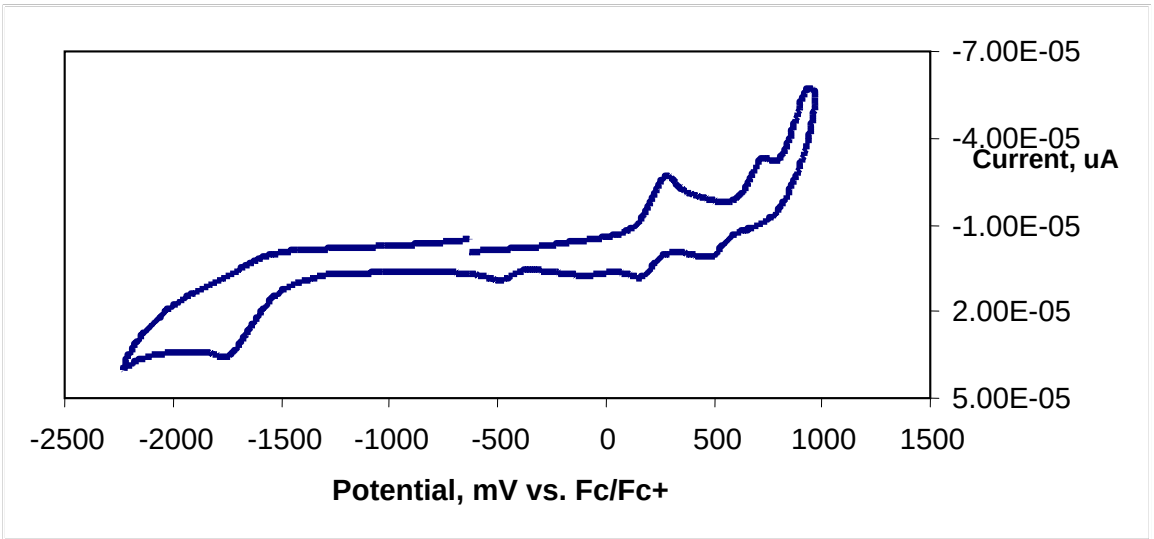

Figure 3.14: ^{t}Bu Nindigo complex 3.5. (CH_2Cl_2 solution, 0.1M Bu_4NBF_4 electrolyte, scan rate 250 mV/s).

Table 3.3.4: Half cell potentials for the redox processes of the Nindigo complexes. Potentials are given vs. Fc/Fc^+ in CH_2Cl_2.

Complex	$E_{1/2}$ (-1/0)	$E_{1/2}$ (0/+1)	$E_{1/2}$ (+1/+2)
3.4 p-OMe Nindigo	-1.37 V	+0 V	+0.50 V
3.3 p-Tolyl Nindigo	-1.33 V	+0.01 V	+0.52 V
3.6 Mesityl Nindigo	-1.52 V	+0.09 V	+0.60 V
3.5 ^{t}Butyl Nindigo	-1.67 V (Irreversible)	+0.32 V	+0.81 V (Irreversible)

As mentioned earlier, since square planar Pd(II) is essentially redox inert in the range over which these compounds are being tested,[48-50] these redox processes are therefore ligand based and correspond to electron transfer processes (Figure 3.15). The first oxidation corresponds to the oxidation of the coordinated ligand in its dianionic form to its anionic radical form. Further oxidation converts the anionic radical to neutral dehydronindigo. In the negative direction, reduction of the complex results in the formation of the trianion. Further reductions are sometimes observable but are rarely reversible once higher reduction potentials are reached.

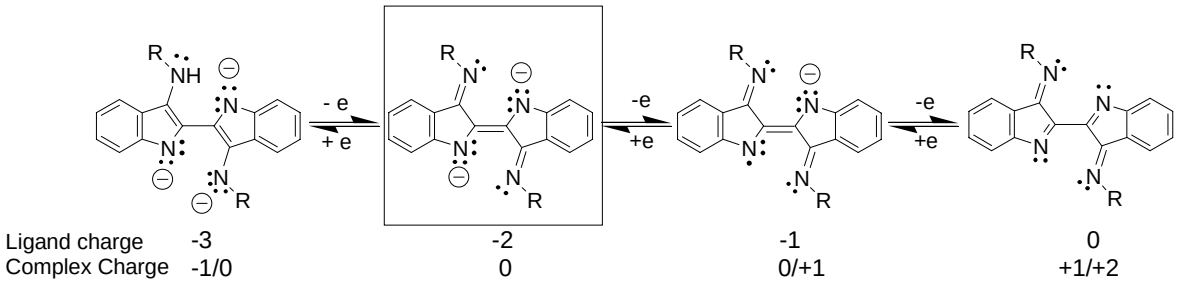

Figure 3.15: Various ligand oxidation states based on redox potentials found for the complexes.

The electrochemistry of the complexes indicates that Nindigo is a new class of redox active bridging ligands, where previously this was limited to the dioxolene unit[13], azo compounds[55], and polynitriles[56,57]. The Nindigo synthesis offers a facile way to introduce a variety of different functional groups to a bridging ligand, which is an option that is not available in any of the aforementioned classes. This means that bridging complexes using Nindigo derivatives have more options for electronic and steric control around the metal center, which ultimately means greater control over redox activity.

3.4 Summary

Despite the fact that the cooperation between the bridging ligand and the metals is so vastly important[13,15,16,19,58], no family of ligands exists such that the properties of their complexes can be easily tuned by a chemically straightforward modification to the structure of the ligand. The Nindigo derivatives now represent a new family of ligands for which modification is a relatively simple process, and which also showing promise in the area of bimetallic bridging metal complexes. The Nindigo complexes are found to be near-infrared dyes, which is quite different from the uncomplexed ligands which are visible range dyes. When complexed to a redox inert metal such as Pd(II), the Nindigo

ligands show a number of interesting electron transfer processes, both reversible and irreversible.

Future directions with this project could involve the synthesis of dehydroindigo[59,60] (Figure 3.16), such that the cyclic voltammetry of dehydroindigo can be compared to that of the Nindigo complexes.

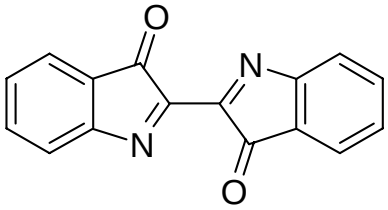

Figure 3.16: Dehydroindigo

Additionally, since it has been found that several different oxidation states exist for the Nindigo complexes in the cyclic voltammetry solution cell, then it would be interesting to find out whether these oxidation states can be isolated in the solid state via the use of chemical reagents.

Finally, since the Nindigo family of ligands have been found to successfully bind to Palladium, then there are many other potential complexes that can be made with other transition metals and/or main group elements. For example, since binuclear ruthenium complexes have seen a great deal of study in the area of metal-metal communication via bridging ligands[12,61,62], then complexes of the form shown in Figure 3.17 will be of some interest to study. Due to the natural redox activity of the Nindigo ligand, it is expected that a binuclear ruthenium Nindigo complex should have some interesting mixed valence properties.

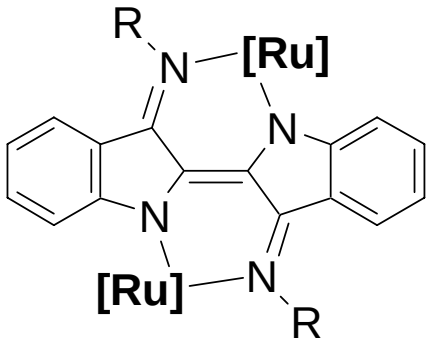

Figure 3.17: Binuclear Ruthenium Nindigo Complexes

3.5 Experimental Section

See Chapter 2 for general experimental details.

Cyclic voltammetry experiments were run on a Bioanalytical Systems CV50 voltammetric analyzer using an electrochemical cell containing the analyte (1mM), $Bu_4N^+BF_4^-$ (0.1M) as the electrolyte, a silver wire as the reference electrode and decamethylferrocene / decamethylferrocinium as an internal reference.

See Appendix C for ^1H and ^{13}C NMR spectrum scans.

Indigo-*N,N'*-bis(p-tolyl imine) bis (palladium hexafluoroacetylacetonate) 3.3: 100 mg of p-tolyl Nindigo (0.22mmol) and 360 mg $Pd(hfac)_2$ (0.66 mmol) were individually dissolved in THF giving a deep blue and a clear yellow solution, respectively. On mixing the solution immediately turned dark green. This mixture was stirred vigorously for 30 min at room temperature at which point the solution was pumped dry on a rotary evapourator. The solid was then washed with hexanes to remove impurities. The remaining dark green solid was dissolved in minimal dichloromethane and layered with hexanes for recrystalization, ultimately resulting in 159 mg of dark green crystals (68% yield). UV-Vis (CH_2Cl_2): λ_{max} 911 nm, $\varepsilon = 1.9 \times 10^4$ M^{-1} cm^{-1}. ^1H NMR (acetone d_6) δ

7.32 (d, 8.2 Hz, 2H), 7.28 - 7.66 (m, 8H), 7.14 (t, 7.4 Hz, 2H), 6.36 (t, 7.7 Hz, 2H), 6.32 (s, 2H), 5.81 (d, 8.1 Hz, 2H), 2.41 ppm (s, 6H). Anal. Calcd For $C_{40}H_{25}F_{12}N_4O_4Pd_2$: C: 45.09, H: 2.27, N: 5.26. Found C: 44.59, H: 2.25, N: 5.26.

Indigo-*N,N'*-bis(p-methoxyphenyl imine) bis (palladium hexafluoroacetylacetonate) 3.4: This compound was prepared in an analogous manner to **3.3**, with the following changes: 100 mg of p-methoxy Nindigo were used to 330 mg of $Pd(hfac)_2$. Once the solvent had been removed on the rotary evapourator, the solid was washed with methanol. This gave 111 mg of dark green solid (47% yield). UV-Vis (CH_2Cl_2): λ_{max} 912 nm, $\varepsilon = 1.7 \times 10^4\ M^{-1}\ cm^{-1}$. ^1H NMR (CD_2Cl_2): δ 7.12-6.99 (m, 8H), 6.88 (d, 9.3 Hz, 4H), 6.28 (t, 7.5 Hz, 2H), 6.10 (s, 2H), 5.77 (d, 7.8 Hz, 2H), 3.79 ppm (s, 6H). ^{13}C NMR (CD_2Cl_2): δ 159.6, 115.0, 92.8, 68.3, 56.2, 26.2 ppm

Indigo-*N,N'*-di-*tert*-butylimine bis (palladium hexafluoroacetylacetonate) 3.5: This compound was prepared in an analogous manner to **3.3**, with the following changes: 50 mg of ^{t}Bu Nindigo was used to 140 mg of $Pd(hfac)_2$. After removing the solvent, the dark green solid was washed in acetone and air dried, giving 85 mg of dark green solid. This solid was then recrystalized from an acetone/EtOH/hexanes mixture, giving 20 mg of red crystals (15% yield). ^1H NMR (CD_2Cl_2): δ 7.39 (m, 2H), 7.26 (m, 2H), 6.92 (m, 4H), 6.22 (s, 2H), 1.34 ppm (s, 18H). ^{13}C NMR (CD_2Cl_2): δ 126.1, 120.7, 119.3, 117.2, 115.5, 92.7, 67.0, 29.2 ppm

Indigo-*N,N'*-bis(mesityl imine) bis (palladium hexafluoroacetylacetonate) 3.6: This compound was prepared in an analogous manner to **3.3**, with the following changes: 100 mg of mesityl Nindigo were used to 315 mg of $Pd(hfac)_2$, and the solution was allowed to stir for 1 hour. The solvent was removed on the rotary evapourator, giving 46 mg (21% yield) of dark green, crude product. The solid was left to recrystalize from a dichloromethane/hexanes mixture, yielding crystals of the structure shown in (Figure 3.9). ^{1}H NMR (CD_2Cl_2): δ 7.53 (m, 2H), 7.22 (t, 2H, 9Hz), 6.98 (s, 4H), 6.55 (m, 2H), 6.40 (s, 2H), 6.34 (d, 2H, 8Hz), 2.33 (s, 6H), 2.07 ppm (s, 12H).

Indigo-*N,N'*-bis(p-chlorophenyl imine) bis (palladium hexafluoroacetylacetonate) 3.7: This compound was prepared in an analogous manner to **3.3**, with the following changes: 50 mg of p-methoxy Nindigo were used to 108 mg of $Pd(hfac)_2$, and the solution was stirred for two hours. The solvent was removed on the rotary evapourator, giving 87 mg (39% yield) of dark green, crude product. The solid was left to recrystalize from a dichloromethane/hexanes mixture. ^{1}H NMR (CD_2Cl_2): δ 7.60 (d, 2H, 9Hz), 7.37 (d, 4H, 12 Hz), 7.28-7.22 (t, 2H, 9 Hz), 7.14 (d, 2H, 9 Hz), 7.04 (d, 2H, 12 Hz), 6.69 (t, 2H, 9 Hz), 6.34 ppm (s, 2H). ^{13}C NMR: Insufficient solubility to obtain ^{13}C data.

Bibliography

1. Tolman, C. A. *Chem. Rev.* **1977**, *77*, 313.

2. Gavrilova, A. L.; Bosnich, B. *Chem. Rev.* **2004**, *104*, 349.

3. Kaes, C.; Katz, A.; Hosseini, M. W. *Chem. Rev.* **2000**, *100*, 3553.

4. Barlow, S.; O'Hare, D. *Chem. Rev.* **1997**, *97*, 637.

5. Bourget-Merle, L.; Lappert, M. F.; Severn, J. R. *Chem. Rev.* **2002**, *102*, 3031.

6. Shriner, R. L.; Neumann, F. W. *Chem. Rev.* **1944**, *35*, 351.

7. Johnson, L. K.; M., K. C.; Brookhart, M. *J. Am. Chem. Soc* **1995**, *117*.

8. vanKoten, G.; Vrieze, K. *Adv. Organomet. Chem* **1982**, *21*, 151.

9. Britovsek, G. J. P.; Bruce, M.; Gibson, V. C.; Kimberley, B. S.; Maddox, P. J.; Mastroianni, S.; McTavish, S. J.; Redshaw, C.; Solan, G. A.; Stromberg, S.; White, A. J. P.; Williams, D. J. *J. Am. Chem. Soc.* **1999**, *121*, 8728.

10. Vedernikov, A. N.; Wu, P.; Huffman, J. C.; Caulton, K. G. *Inorg. Chim. Acta* **2002**, *330*, 103.

11. Steel, P. J. *Coord. Chem. Rev.* **1990**, *106*, 227.

12. Kaim, W.; Lahiri, G. K. *Angew. Chem. Int. Ed* **2007**, *46*, 1778.

13. Min, K. S.; DiPasquale, A. G.; Golen, J. A.; Rheingold, A. L.; Miller, J. S. *J. Am. Chem. Soc* **2007**, *129*, 2360.

14. Steel, P. J. *Acc. Chem. Res.* **2005**, *38*, 243.

15. Cruetz, C.; Taube, H. *J. Am. Chem. Soc* **1969**, *91*, 3988.

16. Shi, L.-L.; Liao, Y.; Yang, G.-C.; Zhong-Min, S.; Zhao, S.-S. *Inorg. Chem.* **2008**, *47*, 2347.

17. Demadis, K. D.; Hartshorn, C. M.; Meyer, T. J. *Chem. Rev.* **2001**, *101*, 2655.

18. Richardson, D. E.; Taube, H. *Coord. Chem. Rev.* **1984**, *60*, 107.

19. McCleverty, J. A.; Ward, M. D. *Acc. Chem. Res.* **1998**, *31*, 842.

20. Clark, R. J. H.; Cooksey, C. J.; Daniels, M. A. M.; Withnall, R. *Endeavour* **1993**, *17*, 191.

21. Ferreira, E. S. B.; Hulme, A. N.; McNab, H.; Quye, A. *Chem. Soc. Rev.* **2004**, *33*, 329.

22. Sandberg, G. *Indigo Textiles: Technique and History* **1989**, *A&C Black, London*.
23. Baeyer, A. *Ber. Deutsch. Chem. Ges* **1870**, *3*, 514.

24. Kunz, K.; Gunther, O. *Ber. Deutsch. Chem. Ges* **1923**, *58B*, 2027.

25. Kunz, K.; Stuhlinger, W. *Ber. Deutsch. Chem. Ges* **1925**, *58B*, 1860.

26. Machemer, H. *J. Prakt. Chem.* **1930**, *127*, 109.

27. Andreas, L.; Schmidt, C.; Lehmann, A.; Wagner, B.; Beck, W. *Z. Naturforsch* **1997**, *52B*, 474.

28. Andreas, L.; Suenkel, K.; Beck, W. *Z. Naturforsch* **1996**, *51B*.

29. Beck, W.; Schmidt, S.; Wienold, R.; Steimann, M.; Wagner, B. *Angew. Chem. Int. Ed* **1989**, *28*, 1529.

30. Schmidt, C.; Wagner, H. U.; Beck, W. *Chem. Ber.* **1992**, *125*, 2347.

31. Pfeiffer, G.; Bauer, H. *Leibigs. Ann. Chem.* **1976**, *383*, 564.

32. Grandmougin, E.; Dessonlavy, E. *Berichte.* **1910**, *42*, 4401.

33. Grundmann, C. J. *Chem. Ber.* **1958**, *91*, 1380.

34. Boeyens, J. C. A.; Cook, L. M.; Ding, Y. X.; Friedrich, M.; Reid, D. H. *Org. Biomol. Chem.* **2003**, *1*, 2168.

35. Wenzel, M.; Lehmann, F.; Beckert, R.; Gunther, W.; Gorls, H. *Monatsh. Chem.* **1999**, *130*, 1373.

36. Kuhn, C.; Beckert, R.; Friedrich, M.; Gorls, H. *J. Heterocyclic Chem.* **2006**, *43*, 1569.

37. McKee, J. R.; Zanger, M. *J. Chem. Ed* **1991**, *68*, A242.

38. Mukaiyama, T.; Sato, T.; Hanna, J. *Chem. Lett.* **1973**, 1041.

39. Ram, R. N.; Khan, A. A. *Synth. Comm.* **2001**, *3*, 841.

40. Hall, H. K.; Park, D. K.; Williams, P. A.; Gosau, J. M.; Boone, H. W.; Park, D. K. *Macromolecules* **1995**, *28*, 1.

41. Bredt, J. *Liebigs Ann. Chem.* **1924**, *437*, 1.

42. Larson, S.; Watjen, F. *Acta Chem. Scand.* **1980**, *A34*, 171.

43. Susse, P.; Steins, M.; Kupcik, V. *Z. Krist.* **1988**, *184*, 269.

44. Hall, H. K.; Padias, A. B.; Yahagi, I.; Williams, P. A.; Bruck, M. A.; Drujon, X. *Macromolecules* **1995**, *28*, 9.

45. Monahan, A., R.; Kuder, J. E. *J. Org. Chem.* **1972**, *37*, 4182.

46. Christie, R. M. *Biotech. Histochem.* **2007**, *82*, 51.

47. Miliani, C.; Romani, A.; Favaro, G. *Spectrochimica Acta Part A* **1998**, *54*, 581.

48. Herebian, D.; Bothe, E.; Neese, F.; Weyhermuller, T.; Wieghardt, K. *J. Am. Chem. Soc.* **2003**, *125*, 9116.

49. Kotatam, S. L.; Chaudhuri, P.; Weyhermuller, T.; Wieghardt, K. *Dalton Trans.* **2007**, 373.

50. Cotton, F. A.; Matusz, M.; Poli, R. *Inorg. Chem.* **1987**, *26*, 1472.

51. Yuan-Zhu, Z.; Zhe-Ming, W.; Gao, S. *Inorg. Chem.* **2006**, *45*, 5447.

52. Clemente-Leon, M.; Coronado, E.; Dias, J. C.; Soriano-Portillo, A.; Willett, R. D. *Inorg. Chem.* **2008**, *47*, 6458.

53. Maggard, P. A.; Boyle, P. D. *Inorg. Chem.* **2003**, *42*, 4250.

54. Podgajny, R.; Pinkowicz, D.; Korzeniak, T.; Nitek, W.; Rams, M.; Sieklucka, B. *Inorg. Chem.* **2007**, *46*, 10416.

55. Kaim, W. *Coord. Chem. Rev.* **2001**, *219*, 463.

56. Hunig, S.; Herberth, E. *Chem. Rev.* **2004**, *104*, 5535.

57. Kaim, W.; Moscherosch, M. *Coord. Chem. Rev.* **1994**, *129*, 157.

58. Ward, M. D. *Chem. Soc. Rev.* **1995**, *24*, 121.

59. Hein, M.; Nguyen, T. B. P.; Dirk, M.; Gorls, H.; Lalk, M.; Langer, P. *Tetrahedron Lett.* **2006**, *47*, 5741.

60. Russell, G. A.; Konoka, R. *J. Org. Chem* **1967**, *32*, 234.

61. Kaim, W.; Klein, A.; Glockle, M. *Acc. Chem. Res.* **2000**, *33*, 755.

62. Sauvage, J. P.; Collin, J. P.; Chambron, J. C.; Guillerez, S.; Coudret, C.; Balzani, V.; Barigelletti, F.; Decola, L.; Flamigni, L. *Chem. Rev.* **1994**, *94*.

Appendix A: Crystallographic Parameters

Table A-1 – Crystallographic parameters for **2.8**

A. Crystal Data	
Empirical Formula	$C_{25}H_{21}N_3O$
Formula Weight	379.45
Crystal Color, Habit	purple, needle
Crystal Dimensions	0.10 X 0.20 X 0.50 mm
Crystal System	primitive
Lattice Type	triclinic
Lattice Parameters	a = 11.768(1) Å b = 12.2045(7) Å c = 15.970(1) Å α = 74.637(2) ^{o} β = 89.109(2) ^{o} γ = 65.132(2) ^{o} V = 1994.6(3) Å^3
Space Group	*P* -1 (#2)
Z value	4
D_{calc}	1.264 g/cm^3
F_{000}	800.00
μ(MoKα)	0.79 cm^{-1}
B. Intensity Measurements	
Diffractometer	Bruker X8 APEX II
Radiation	MoKα (λ = 0.71073 Å) graphite monochromated
Data Images	1293 exposures @ 15.0 seconds
Detector Position	36.00 mm
$2\theta_{max}$	50.0^o
No. of Reflections Measured	Total: 17456 Unique: 6835 (R_{int} = 0.035)
Corrections	Absorption (T_{min} = 0.849, T_{max}= 0.992) Lorentz-polarization
C. Structure Solution and Refinement	
Structure Solution	Direct Methods (SIR97)
Refinement	Full-matrix least-squares on F^2
Function Minimized	Σ w (Fo^2 - Fc^2)^2

Least Squares Weights	$w=1/(\sigma^2(Fo^2)+(0.0581P)^2+0.0208P)$
Anomalous Dispersion	All non-hydrogen atoms
No. Observations (I>0.00σ(I))	6835
No. Variables	545
Reflection/Parameter Ratio	12.54
Residuals (refined on F^2, all data): R1; wR2	0.081; 0.120
Goodness of Fit Indicator	1.03
No. Observations (I>2.00σ(I))	4512
Residuals (refined on F): R1; wR2	0.046; 0.104
Max Shift/Error in Final Cycle	0.00
Maximum peak in Final Diff. Map	0.16 $e^-/Å^3$
Minimum peak in Final Diff. Map	-0.24 $e^-/Å^3$

Table A-2 – Crystallographic parameters for **2.11**

A. Crystal Data	
Empirical Formula	$C_{34}H_{32}N_4$
Formula Weight	496.64
Crystal Color, Habit	dark-blue, plate
Crystal Dimensions	0.03 X 0.15 X 0.35 mm
Crystal System	primitive
Lattice Type	monoclinic
Lattice Parameters	a = 14.555(3) Å b = 7.0908(12) Å c = 13.413(3) Å α = 90.0 ° β = 102.241(8) ° γ = 90.0 ° V = 1352.8(5) $Å^3$
Space Group	*P* $2_1/c$ (#14)
Z value	2
D_{calc}	1.219 g/cm^3
F_{000}	528.00
μ(MoKα)	0.72 cm^{-1}

B. Intensity Measurements	
Diffractometer	Bruker X8 APEX II
Radiation	MoKα (λ = 0.71073 Å) graphite monochromated
Data Images	871 exposures @ 45.0 seconds
Detector Position	36.00 mm

$2\theta_{max}$	50.3^{o}
No. of Reflections Measured	Total: 11246 Unique: 2393 (R_{int} = 0.069)
Corrections	Absorption (T_{min} = 0.815, T_{max}= 0.998) Lorentz-polarization

C. Structure Solution and Refinement

Structure Solution	Direct Methods (SIR97)
Refinement	Full-matrix least-squares on F^2
Function Minimized	Σ w $(Fo^2 - Fc^2)^2$
Least Squares Weights	$w=1/(\sigma^2(Fo^2)+(0.0497P)^2+0.0319P)$
Anomalous Dispersion	All non-hydrogen atoms
No. Observations (I>0.00σ(I))	2393
No. Variables	179
Reflection/Parameter Ratio	13.37
Residuals (refined on F^2, all data): R1; wR2	0.120; 0.116
Goodness of Fit Indicator	1.03
No. Observations (I>2.00σ(I))	1376
Residuals (refined on F): R1; wR2	0.050; 0.094
Max Shift/Error in Final Cycle	0.00
Maximum peak in Final Diff. Map	0.20 $e^-/Å^3$
Minimum peak in Final Diff. Map	-0.18 $e^-/Å^3$

Table A-3 – Crystallographic parameters for **2.10**

A. Crystal Data

Empirical Formula	$C_{24}H_{28}N_4$
Formula Weight	372.50
Crystal Color, Habit	green, needle
Crystal Dimensions	0.05 X 0.12 X 0.30 mm
Crystal System	triclinic
Lattice Type	primitive
Lattice Parameters	a = 6.6748(9) Å b = 8.7859(11) Å c = 17.067(3) Å $\alpha = 90.0^{o}$ $\beta = 100.662(5)^{o}$ $\gamma = 90.0^{o}$ V = 983.6(2) $Å^3$
Space Group	*P* $2_1/n$ (#14)
Z value	2
D_{calc}	1.258 g/cm^3

F_{000}	400.00
μ(MoKα)	0.76 cm^{-1}

B. Intensity Measurements

Diffractometer	Bruker X8 APEX II
Radiation	MoKα (λ = 0.71073 Å) graphite monochromated
Data Images	705 exposures @ 30.0 seconds
Detector Position	36.00 mm
$2\theta_{max}$	50.0°
No. of Reflections Measured	Total: 5101 Unique: 1659 (R_{int} = 0.032)
Corrections	Absorption (T_{min} = 0.837, T_{max}= 0.996) Lorentz-polarization

C. Structure Solution and Refinement

Structure Solution	Direct Methods (SIR97)
Refinement	Full-matrix least-squares on F^2
Function Minimized	Σ w (Fo^2 - Fc^2)^2
Least Squares Weights	w=1/($\sigma^2(Fo^2)$+(0.0384P) ^{2}+ 0.2519P)
Anomalous Dispersion	All non-hydrogen atoms
No. Observations (I>0.00σ(I))	1659
No. Variables	138
Reflection/Parameter Ratio	12.02
Residuals (refined on F^2, all data): R1; wR2	0.063; 0.094
Goodness of Fit Indicator	1.06
No. Observations (I>2.00σ(I))	1220
Residuals (refined on F): R1; wR2	0.039; 0.082
Max Shift/Error in Final Cycle	0.00
Maximum peak in Final Diff. Map	0.18 e^-/Å^3
Minimum peak in Final Diff. Map	-0.16 e^-/Å^3

Table A-4 - Crystallographic parameters for **3.3**

A. Crystal Data

Empirical Formula	$C_{43}H_{31}N_4O_4F_{12}Pd_2$
Formula Weight	1108.52
Crystal Color, Habit	green, plate
Crystal Dimensions	0.01 X 0.10 X 0.25 mm
Crystal System	triclinic
Lattice Type	primitive
Lattice Parameters	a = 11.2026(10) Å

	b = 13.2615(12) Å
	c = 13.8826(12) Å
	α = 90.508(5) o
	β = 92.453(5) o
	γ = 92.795(5) o
	V = 2058.0(3) Å^3
Space Group	*P* -1 (#2)
Z value	2
D_{calc}	1.789 g/cm^3
F_{000}	1098.00
μ(MoKα)	9.78 cm^{-1}

B. Intensity Measurements

Diffractometer	Bruker X8 APEX II
Radiation	MoKα (λ = 0.71073 Å) graphite monochromated
Data Images	2313 exposures @ 20.0 seconds
Detector Position	36.00 mm
$2\theta_{max}$	56.0o
No. of Reflections Measured	Total: 43171 Unique: 9794(R_{int} = 0.039)
Corrections	Absorption (T_{min} = 0.883, T_{max}= 0.990)
	Lorentz-polarization

C. Structure Solution and Refinement

Structure Solution	Direct Methods (SIR97)
Refinement	Full-matrix least-squares on F^2
Function Minimized	Σ w (Fo^2 - Fc^2)^2
Least Squares Weights	w=1/(σ^2(Fo^2)+(0.0386P) ^{2}+ 3.5952P)
Anomalous Dispersion	All non-hydrogen atoms
No. Observations (I>0.00σ(I))	9794
No. Variables	589
Reflection/Parameter Ratio	16.63
Residuals (refined on F^2, all data): R1; wR2	0.073; 0.101
Goodness of Fit Indicator	1.06
No. Observations (I>2.00σ(I))	6880
Residuals (refined on F): R1; wR2	0.039; 0.085
Max Shift/Error in Final Cycle	0.00
Maximum peak in Final Diff. Map	1.57 e$^-$/Å^3
Minimum peak in Final Diff. Map	-0.97 e$^-$/Å^3

Table A-5 – Crystalographic parameters for **3.4**

A. Crystal Data	
Empirical Formula	$C_{40}H_{24}N_4O_6Pd_2$
Formula Weight	1097.43
Crystal Color, Habit	green, needle
Crystal Dimensions	0.02 X 0.10 X 0.50 mm
Crystal System	triclinic
Lattice Type	primitive
Lattice Parameters	a = 5.5243(4) Å b = 11.0622(8) Å c = 16.4452(12) Å α = 97.128(4) ^{o} β = 96.593(4) ^{o} γ = 102.633(4) ^{o} V = 6848.2(2) Å^3
Space Group	*P* -1 (#2)
Z value	1
D_{calc}	1.893 g/cm^3
F_{000}	540.00
μ(MoKα)	10.48 cm^{-1}
B. Intensity Measurements	
Diffractometer	Bruker X8 APEX II
Radiation	MoKα (λ = 0.71073 Å) graphite monochromated
Data Images	3751 exposures @ 15.0 seconds
Detector Position	36.00 mm
$2\theta_{max}$	55.8^o
No. of Reflections Measured	Total: 28933 Unique: 4506 (R_{int} = 0.048)
Corrections	Absorption (T_{min} = 0.882, T_{max}= 0.979) Lorentz-polarization
C. Structure Solution and Refinement	
Structure Solution	Direct Methods (SIR97)
Refinement	Full-matrix least-squares on F^2
Function Minimized	Σ w (Fo^2 - Fc^2)^2
Least Squares Weights	w=1/(σ^2(Fo^2)+(0.0269P) ^{2}+ 2.2959P)
Anomalous Dispersion	All non-hydrogen atoms
No. Observations (I>0.00σ(I))	4506
No. Variables	318

Reflection/Parameter Ratio	14.17
Residuals (refined on F^2, all data): R1; wR2	0.066; 0.091
Goodness of Fit Indicator	1.10
No. Observations ($I>2.00\sigma(I)$)	3603
Residuals (refined on F): R1; wR2	0.041; 0.078
Max Shift/Error in Final Cycle	0.00
Maximum peak in Final Diff. Map	1.08 $e^-/Å^3$
Minimum peak in Final Diff. Map	-1.01 $e^-/Å^3$

Table A-6 – Crystallographic parameters for **3.6**

A. Crystal Data

Empirical Formula	$C_{40.5}H_{35}N_4O_{2.5}F_6Pd$
Formula Weight	838.13
Crystal Color, Habit	black, plate
Crystal Dimensions	0.05 X 0.20 X 0.20 mm
Crystal System	triclinic
Lattice Type	primitive
Lattice Parameters	a = 12.0116(5) Å b = 12.8180(4) Å c = 13.9589(6) Å α = 112.866(1) ^{o} β = 98.231(1) ^{o} γ = 107.377(1) ^{o} V = 1805.93(12) $Å^3$
Space Group	*P* -1 (#2)
Z value	2
D_{calc}	1.541 g/cm^3
F_{000}	852.00
μ(MoKα)	5.89 cm^{-1}

B. Intensity Measurements

Diffractometer	Bruker X8 APEX II
Radiation	MoKα (λ = 0.71073 Å) graphite monochromated
Data Images	798 exposures @ 20.0 seconds
Detector Position	36.00 mm
$2\theta_{max}$	50.0^o
No. of Reflections Measured	Total: 13761 Unique: 6184 (R_{int} = 0.031)
Corrections	Absorption (T_{min} = 0.903, T_{max}= 0.971) Lorentz-polarization

C. Structure Solution and Refinement

Structure Solution	Direct Methods (SIR97)
Refinement	Full-matrix least-squares on F^2
Function Minimized	Σ w $(Fo^2 - Fc^2)^2$
Least Squares Weights	$w=1/(\sigma^2(Fo^2)+(0.0337P)^2+1.9972P)$
Anomalous Dispersion	All non-hydrogen atoms
No. Observations (I>0.00σ(I))	6184
No. Variables	508
Reflection/Parameter Ratio	12.17
Residuals (refined on F^2, all data): R1; wR2	0.052; 0.085
Goodness of Fit Indicator	1.01
No. Observations (I>2.00σ(I))	5099
Residuals (refined on F): R1; wR2	0.036; 0.077
Max Shift/Error in Final Cycle	0.00
Maximum peak in Final Diff. Map	0.46 $e^-/Å^3$
Minimum peak in Final Diff. Map	-0.69 $e^-/Å^3$

Appendix B: Complete listings of bond lengths and angles

Table B-1 – Bond lengths [Å], angles [deg] and atomic coordinates for **2.8**

Atom1-Atom2	Distance
C(1)-C(6)	1.395(3)
C(1)-C(2)	1.399(3)
C(1)-N(1)	1.423(2)
C(2)-C(3)	1.381(3)
C(2)-C(7)	1.507(3)
C(3)-C(4)	1.376(3)
C(3)-H(3)	0.9500
C(4)-C(5)	1.389(3)
C(4)-C(8)	1.512(3)
C(5)-C(6)	1.387(3)
C(5)-H(5)	0.9500
C(6)-C(9)	1.507(3)
C(7)-H(7A)	0.9800
C(7)-H(7B)	0.9800
C(7)-H(7C)	0.9800
C(8)-H(8A)	0.9800
C(8)-H(8B)	0.9800
C(8)-H(8C)	0.9800
C(9)-H(9A)	0.9800
C(9)-H(9B)	0.9800
C(9)-H(9C)	0.9800
C(10)-N(1)	1.284(2)
C(10)-C(11)	1.469(3)
C(10)-C(17)	1.474(3)
C(11)-C(12)	1.386(3)
C(11)-C(16)	1.403(3)
C(12)-C(13)	1.391(3)
C(12)-H(12)	0.9500
C(13)-C(14)	1.387(3)
C(13)-H(13)	0.9500
C(14)-C(15)	1.380(3)
C(14)-H(14)	0.9500
C(15)-C(16)	1.384(3)
C(15)-H(15)	0.9500
C(16)-N(2)	1.387(3)
C(17)-C(18)	1.355(3)
C(17)-N(2)	1.377(2)
C(18)-N(3)	1.390(2)
C(18)-C(19)	1.461(3)

C(19)-O(1)	1.256(2)
C(19)-C(20)	1.446(3)
C(20)-C(21)	1.392(3)
C(20)-C(25)	1.400(3)
C(21)-C(22)	1.371(3)
C(21)-H(21)	0.9500
C(22)-C(23)	1.405(3)
C(22)-H(22)	0.9500
C(23)-C(24)	1.378(3)
C(23)-H(23)	0.9500
C(24)-C(25)	1.388(3)
C(24)-H(24)	0.9500
C(25)-N(3)	1.379(2)
N(2)-H(2N)	0.93(2)
N(3)-H(3N)	0.91(2)
C(26)-C(31)	1.399(3)
C(26)-C(27)	1.399(3)
C(26)-N(4)	1.417(2)
C(27)-C(28)	1.384(3)
C(27)-C(32)	1.507(3)
C(28)-C(29)	1.376(3)
C(28)-H(28)	0.9500
C(29)-C(30)	1.390(3)
C(29)-C(33)	1.509(3)
C(30)-C(31)	1.386(3)
C(30)-H(30)	0.9500
C(31)-C(34)	1.510(3)
C(32)-H(32A)	0.9800
C(32)-H(32B)	0.9800
C(32)-H(32C)	0.9800
C(33)-H(33A)	0.9800
C(33)-H(33B)	0.9800
C(33)-H(33C)	0.9800
C(34)-H(34A)	0.9800
C(34)-H(34B)	0.9800
C(34)-H(34C)	0.9800
C(35)-N(4)	1.287(2)
C(35)-C(36)	1.470(2)
C(35)-C(42)	1.470(3)
C(36)-C(37)	1.391(3)
C(36)-C(41)	1.397(3)
C(37)-C(38)	1.387(3)
C(37)-H(37)	0.9500
C(38)-C(39)	1.388(3)
C(38)-H(38)	0.9500
C(39)-C(40)	1.376(3)

C(39)-H(39)	0.9500
C(40)-C(41)	1.383(3)
C(40)-H(40)	0.9500
C(41)-N(5)	1.385(2)
C(42)-C(43)	1.360(3)
C(42)-N(5)	1.377(2)
C(43)-N(6)	1.382(2)
C(43)-C(44)	1.466(3)
C(44)-O(2)	1.248(2)
C(44)-C(45)	1.453(3)
C(45)-C(46)	1.394(3)
C(45)-C(50)	1.399(3)
C(46)-C(47)	1.378(3)
C(46)-H(46)	0.9500
C(47)-C(48)	1.395(3)
C(47)-H(47)	0.9500
C(48)-C(49)	1.380(3)
C(48)-H(48)	0.9500
C(49)-C(50)	1.390(3)
C(49)-H(49)	0.9500
C(50)-N(6)	1.379(2)
N(5)-H(5N)	0.88(2)
N(6)-H(6N)	0.91(2)

Atom1-Atom2-Atom3	Angle
C(6)-C(1)-C(2)	121.22(18)
C(6)-C(1)-N(1)	120.66(17)
C(2)-C(1)-N(1)	117.84(17)
C(3)-C(2)-C(1)	118.18(19)
C(3)-C(2)-C(7)	121.72(19)
C(1)-C(2)-C(7)	120.09(18)
C(4)-C(3)-C(2)	122.3(2)
C(4)-C(3)-H(3)	118.8
C(2)-C(3)-H(3)	118.8
C(3)-C(4)-C(5)	118.2(2)
C(3)-C(4)-C(8)	121.1(2)
C(5)-C(4)-C(8)	120.7(2)
C(6)-C(5)-C(4)	122.0(2)
C(6)-C(5)-H(5)	119.0
C(4)-C(5)-H(5)	119.0
C(5)-C(6)-C(1)	118.04(19)
C(5)-C(6)-C(9)	120.72(19)
C(1)-C(6)-C(9)	121.24(18)
C(2)-C(7)-H(7A)	109.5
C(2)-C(7)-H(7B)	109.5

H(7A)-C(7)-H(7B)	109.5
C(2)-C(7)-H(7C)	109.5
H(7A)-C(7)-H(7C)	109.5
H(7B)-C(7)-H(7C)	109.5
C(4)-C(8)-H(8A)	109.5
C(4)-C(8)-H(8B)	109.5
H(8A)-C(8)-H(8B)	109.5
C(4)-C(8)-H(8C)	109.5
H(8A)-C(8)-H(8C)	109.5
H(8B)-C(8)-H(8C)	109.5
C(6)-C(9)-H(9A)	109.5
C(6)-C(9)-H(9B)	109.5
H(9A)-C(9)-H(9B)	109.5
C(6)-C(9)-H(9C)	109.5
H(9A)-C(9)-H(9C)	109.5
H(9B)-C(9)-H(9C)	109.5
N(1)-C(10)-C(11)	134.28(18)
N(1)-C(10)-C(17)	120.19(18)
C(11)-C(10)-C(17)	105.47(16)
C(12)-C(11)-C(16)	119.96(18)
C(12)-C(11)-C(10)	133.51(18)
C(16)-C(11)-C(10)	106.53(17)
C(11)-C(12)-C(13)	118.4(2)
C(11)-C(12)-H(12)	120.8
C(13)-C(12)-H(12)	120.8
C(14)-C(13)-C(12)	120.5(2)
C(14)-C(13)-H(13)	119.8
C(12)-C(13)-H(13)	119.8
C(15)-C(14)-C(13)	122.1(2)
C(15)-C(14)-H(14)	118.9
C(13)-C(14)-H(14)	118.9
C(14)-C(15)-C(16)	117.1(2)
C(14)-C(15)-H(15)	121.4
C(16)-C(15)-H(15)	121.4
C(15)-C(16)-N(2)	127.84(19)
C(15)-C(16)-C(11)	121.90(19)
N(2)-C(16)-C(11)	110.26(17)
C(18)-C(17)-N(2)	123.42(18)
C(18)-C(17)-C(10)	128.55(18)
N(2)-C(17)-C(10)	107.79(17)
C(17)-C(18)-N(3)	126.51(18)
C(17)-C(18)-C(19)	124.71(18)
N(3)-C(18)-C(19)	108.36(17)
O(1)-C(19)-C(20)	129.96(18)
O(1)-C(19)-C(18)	124.63(18)
C(20)-C(19)-C(18)	105.31(17)

C(21)-C(20)-C(25)	120.5(2)
C(21)-C(20)-C(19)	132.22(19)
C(25)-C(20)-C(19)	107.26(17)
C(22)-C(21)-C(20)	118.6(2)
C(22)-C(21)-H(21)	120.7
C(20)-C(21)-H(21)	120.7
C(21)-C(22)-C(23)	120.2(2)
C(21)-C(22)-H(22)	119.9
C(23)-C(22)-H(22)	119.9
C(24)-C(23)-C(22)	122.1(2)
C(24)-C(23)-H(23)	118.9
C(22)-C(23)-H(23)	118.9
C(23)-C(24)-C(25)	117.2(2)
C(23)-C(24)-H(24)	121.4
C(25)-C(24)-H(24)	121.4
N(3)-C(25)-C(24)	128.26(19)
N(3)-C(25)-C(20)	110.40(18)
C(24)-C(25)-C(20)	121.31(19)
C(10)-N(1)-C(1)	120.74(16)
C(17)-N(2)-C(16)	109.93(17)
C(17)-N(2)-H(2N)	120.7(14)
C(16)-N(2)-H(2N)	129.2(14)
C(25)-N(3)-C(18)	108.64(17)
C(25)-N(3)-H(3N)	127.5(15)
C(18)-N(3)-H(3N)	123.9(15)
C(31)-C(26)-C(27)	120.01(18)
C(31)-C(26)-N(4)	117.91(17)
C(27)-C(26)-N(4)	121.70(18)
C(28)-C(27)-C(26)	118.43(19)
C(28)-C(27)-C(32)	120.65(19)
C(26)-C(27)-C(32)	120.90(19)
C(29)-C(28)-C(27)	123.0(2)
C(29)-C(28)-H(28)	118.5
C(27)-C(28)-H(28)	118.5
C(28)-C(29)-C(30)	117.5(2)
C(28)-C(29)-C(33)	121.5(2)
C(30)-C(29)-C(33)	121.0(2)
C(31)-C(30)-C(29)	121.9(2)
C(31)-C(30)-H(30)	119.1
C(29)-C(30)-H(30)	119.1
C(30)-C(31)-C(26)	119.13(18)
C(30)-C(31)-C(34)	121.15(19)
C(26)-C(31)-C(34)	119.72(19)
C(27)-C(32)-H(32A)	109.5
C(27)-C(32)-H(32B)	109.5
H(32A)-C(32)-H(32B)	109.5

C(27)-C(32)-H(32C)	109.5
H(32A)-C(32)-H(32C)	109.5
H(32B)-C(32)-H(32C)	109.5
C(29)-C(33)-H(33A)	109.5
C(29)-C(33)-H(33B)	109.5
H(33A)-C(33)-H(33B)	109.5
C(29)-C(33)-H(33C)	109.5
H(33A)-C(33)-H(33C)	109.5
H(33B)-C(33)-H(33C)	109.5
C(31)-C(34)-H(34A)	109.5
C(31)-C(34)-H(34B)	109.5
H(34A)-C(34)-H(34B)	109.5
C(31)-C(34)-H(34C)	109.5
H(34A)-C(34)-H(34C)	109.5
H(34B)-C(34)-H(34C)	109.5
N(4)-C(35)-C(36)	134.98(18)
N(4)-C(35)-C(42)	120.10(16)
C(36)-C(35)-C(42)	104.83(16)
C(37)-C(36)-C(41)	119.62(18)
C(37)-C(36)-C(35)	133.33(19)
C(41)-C(36)-C(35)	107.03(17)
C(38)-C(37)-C(36)	118.5(2)
C(38)-C(37)-H(37)	120.7
C(36)-C(37)-H(37)	120.7
C(37)-C(38)-C(39)	120.6(2)
C(37)-C(38)-H(38)	119.7
C(39)-C(38)-H(38)	119.7
C(40)-C(39)-C(38)	121.8(2)
C(40)-C(39)-H(39)	119.1
C(38)-C(39)-H(39)	119.1
C(39)-C(40)-C(41)	117.4(2)
C(39)-C(40)-H(40)	121.3
C(41)-C(40)-H(40)	121.3
C(40)-C(41)-N(5)	127.70(19)
C(40)-C(41)-C(36)	122.10(19)
N(5)-C(41)-C(36)	110.20(16)
C(43)-C(42)-N(5)	123.58(18)
C(43)-C(42)-C(35)	128.16(17)
N(5)-C(42)-C(35)	108.25(16)
C(42)-C(43)-N(6)	125.80(17)
C(42)-C(43)-C(44)	125.72(17)
N(6)-C(43)-C(44)	108.48(15)
O(2)-C(44)-C(45)	129.81(18)
O(2)-C(44)-C(43)	125.21(17)
C(45)-C(44)-C(43)	104.98(15)
C(46)-C(45)-C(50)	120.37(18)

C(46)-C(45)-C(44)	132.37(18)
C(50)-C(45)-C(44)	107.19(16)
C(47)-C(46)-C(45)	118.46(19)
C(47)-C(46)-H(46)	120.8
C(45)-C(46)-H(46)	120.8
C(46)-C(47)-C(48)	120.30(19)
C(46)-C(47)-H(47)	119.9
C(48)-C(47)-H(47)	119.9
C(49)-C(48)-C(47)	122.4(2)
C(49)-C(48)-H(48)	118.8
C(47)-C(48)-H(48)	118.8
C(48)-C(49)-C(50)	116.9(2)
C(48)-C(49)-H(49)	121.5
C(50)-C(49)-H(49)	121.5
N(6)-C(50)-C(49)	128.10(18)
N(6)-C(50)-C(45)	110.38(16)
C(49)-C(50)-C(45)	121.52(18)
C(35)-N(4)-C(26)	123.44(16)
C(42)-N(5)-C(41)	109.68(17)
C(42)-N(5)-H(5N)	118.3(14)
C(41)-N(5)-H(5N)	131.9(14)
C(50)-N(6)-C(43)	108.93(16)
C(50)-N(6)-H(6N)	125.3(14)
C(43)-N(6)-H(6N)	125.1(14)

Table B-2 - Bond lengths [Å], angles [deg] and atomic coordinates for **2.11**

Atom1-Atom2	Distance
C(1)-C(6)	1.388(3)
C(1)-C(2)	1.400(3)
C(1)-N(1)	1.425(2)
C(2)-C(3)	1.387(3)
C(2)-C(7)	1.494(3)
C(3)-C(4)	1.382(3)
C(3)-H(3)	0.9500
C(4)-C(5)	1.375(3)
C(4)-C(8)	1.506(3)
C(5)-C(6)	1.386(3)
C(5)-H(5)	0.9500
C(6)-C(9)	1.510(3)
C(7)-H(7A)	0.9800
C(7)-H(7B)	0.9800
C(7)-H(7C)	0.9800
C(8)-H(8A)	0.9800
C(8)-H(8B)	0.9800
C(8)-H(8C)	0.9800

C(9)-H(9A)	0.9800
C(9)-H(9B)	0.9800
C(9)-H(9C)	0.9800
C(10)-N(1)	1.301(3)
C(10)-C(17)	1.455(3)
C(10)-C(11)	1.464(3)
C(11)-C(16)	1.396(3)
C(11)-C(12)	1.399(3)
C(12)-C(13)	1.374(3)
C(12)-H(12)	0.9500
C(13)-C(14)	1.388(3)
C(13)-H(13)	0.9500
C(14)-C(15)	1.374(3)
C(14)-H(14)	0.9500
C(15)-C(16)	1.383(3)
C(15)-H(15)	0.9500
C(16)-N(2)	1.384(3)
C(17)-C(17)#1	1.366(4)
C(17)-N(2)	1.378(3)
N(2)-H(2N)	0.94(3)

Atom1-Atom2-Atom3	Angle
C(6)-C(1)-C(2)	120.8(2)
C(6)-C(1)-N(1)	118.1(2)
C(2)-C(1)-N(1)	120.8(2)
C(3)-C(2)-C(1)	118.2(2)
C(3)-C(2)-C(7)	120.0(2)
C(1)-C(2)-C(7)	121.8(2)
C(4)-C(3)-C(2)	122.3(2)
C(4)-C(3)-H(3)	118.8
C(2)-C(3)-H(3)	118.8
C(5)-C(4)-C(3)	117.6(2)
C(5)-C(4)-C(8)	121.5(2)
C(3)-C(4)-C(8)	120.9(2)
C(4)-C(5)-C(6)	122.7(2)
C(4)-C(5)-H(5)	118.6
C(6)-C(5)-H(5)	118.6
C(5)-C(6)-C(1)	118.3(2)
C(5)-C(6)-C(9)	121.1(2)
C(1)-C(6)-C(9)	120.6(2)
C(2)-C(7)-H(7A)	109.5
C(2)-C(7)-H(7B)	109.5
H(7A)-C(7)-H(7B)	109.5
C(2)-C(7)-H(7C)	109.5
H(7A)-C(7)-H(7C)	109.5
H(7B)-C(7)-H(7C)	109.5

C(4)-C(8)-H(8A)	109.5
C(4)-C(8)-H(8B)	109.5
H(8A)-C(8)-H(8B)	109.5
C(4)-C(8)-H(8C)	109.5
H(8A)-C(8)-H(8C)	109.5
H(8B)-C(8)-H(8C)	109.5
C(6)-C(9)-H(9A)	109.5
C(6)-C(9)-H(9B)	109.5
H(9A)-C(9)-H(9B)	109.5
C(6)-C(9)-H(9C)	109.5
H(9A)-C(9)-H(9C)	109.5
H(9B)-C(9)-H(9C)	109.5
N(1)-C(10)-C(17)	121.42(18)
N(1)-C(10)-C(11)	133.42(19)
C(17)-C(10)-C(11)	105.16(18)
C(16)-C(11)-C(12)	119.2(2)
C(16)-C(11)-C(10)	106.84(18)
C(12)-C(11)-C(10)	133.9(2)
C(13)-C(12)-C(11)	118.9(2)
C(13)-C(12)-H(12)	120.5
C(11)-C(12)-H(12)	120.5
C(12)-C(13)-C(14)	120.7(2)
C(12)-C(13)-H(13)	119.6
C(14)-C(13)-H(13)	119.6
C(15)-C(14)-C(13)	121.5(2)
C(15)-C(14)-H(14)	119.2
C(13)-C(14)-H(14)	119.2
C(14)-C(15)-C(16)	117.9(2)
C(14)-C(15)-H(15)	121.1
C(16)-C(15)-H(15)	121.1
C(15)-C(16)-N(2)	128.0(2)
C(15)-C(16)-C(11)	121.71(19)
N(2)-C(16)-C(11)	110.25(19)
C(17)#1-C(17)-N(2)	124.2(2)
C(17)#1-C(17)-C(10)	127.1(2)
N(2)-C(17)-C(10)	108.66(17)
C(10)-N(1)-C(1)	121.04(17)
C(17)-N(2)-C(16)	109.09(18)
C(17)-N(2)-H(2N)	119.5(16)
C(16)-N(2)-H(2N)	131.3(17)

Table B-3 - Bond lengths [Å], angles [deg] and atomic coordinates for **2.10**

Atom1-Atom2	Distance
C(1)-N(1)	1.355(2)

C(1)-C(1)#1	1.409(3)
C(1)-C(2)	1.462(2)
C(2)-N(2)	1.323(2)
C(2)-C(3)	1.469(2)
C(3)-C(4)	1.405(2)
C(3)-C(8)	1.416(2)
C(4)-C(5)	1.379(2)
C(4)-H(4)	0.9500
C(5)-C(6)	1.394(3)
C(5)-H(5)	0.9500
C(6)-C(7)	1.376(2)
C(6)-H(6)	0.9500
C(7)-C(8)	1.389(2)
C(7)-H(7)	0.9500
C(8)-N(1)	1.384(2)
C(9)-N(2)	1.474(2)
C(9)-C(10)	1.528(2)
C(9)-C(12)	1.530(3)
C(9)-C(11)	1.534(2)
C(10)-H(10A)	0.9800
C(10)-H(10B)	0.9800
C(10)-H(10C)	0.9800
C(11)-H(11A)	0.9800
C(11)-H(11B)	0.9800
C(11)-H(11C)	0.9800
C(12)-H(12A)	0.9800
C(12)-H(12B)	0.9800
C(12)-H(12C)	0.9800
N(1)-H(1A)	0.87(4)
N(2)-H(1B)	0.96(4)

Atom1-Atom2-Atom3	Angle
N(1)-C(1)-C(1)#1	123.0(2)
N(1)-C(1)-C(2)	110.49(14)
C(1)#1-C(1)-C(2)	126.5(2)
N(2)-C(2)-C(1)	119.57(14)
N(2)-C(2)-C(3)	135.76(15)
C(1)-C(2)-C(3)	104.67(14)
C(4)-C(3)-C(8)	118.03(15)
C(4)-C(3)-C(2)	136.53(16)
C(8)-C(3)-C(2)	105.44(14)
C(5)-C(4)-C(3)	119.89(17)
C(5)-C(4)-H(4)	120.1
C(3)-C(4)-H(4)	120.1
C(4)-C(5)-C(6)	120.75(17)
C(4)-C(5)-H(5)	119.6

C(6)-C(5)-H(5)	119.6
C(7)-C(6)-C(5)	121.03(17)
C(7)-C(6)-H(6)	119.5
C(5)-C(6)-H(6)	119.5
C(6)-C(7)-C(8)	118.52(17)
C(6)-C(7)-H(7)	120.7
C(8)-C(7)-H(7)	120.7
N(1)-C(8)-C(7)	126.84(16)
N(1)-C(8)-C(3)	111.38(14)
C(7)-C(8)-C(3)	121.78(15)
N(2)-C(9)-C(10)	105.69(14)
N(2)-C(9)-C(12)	110.48(15)
C(10)-C(9)-C(12)	108.58(16)
N(2)-C(9)-C(11)	111.03(14)
C(10)-C(9)-C(11)	108.26(16)
C(12)-C(9)-C(11)	112.52(14)
C(9)-C(10)-H(10A)	109.5
C(9)-C(10)-H(10B)	109.5
H(10A)-C(10)-H(10B)	109.5
C(9)-C(10)-H(10C)	109.5
H(10A)-C(10)-H(10C)	109.5
H(10B)-C(10)-H(10C)	109.5
C(9)-C(11)-H(11A)	109.5
C(9)-C(11)-H(11B)	109.5
H(11A)-C(11)-H(11B)	109.5
C(9)-C(11)-H(11C)	109.5
H(11A)-C(11)-H(11C)	109.5
H(11B)-C(11)-H(11C)	109.5
C(9)-C(12)-H(12A)	109.5
C(9)-C(12)-H(12B)	109.5
H(12A)-C(12)-H(12B)	109.5
C(9)-C(12)-H(12C)	109.5
H(12A)-C(12)-H(12C)	109.5
H(12B)-C(12)-H(12C)	109.5
C(1)-N(1)-C(8)	108.01(14)
C(1)-N(1)-H(1A)	120(2)
C(8)-N(1)-H(1A)	132(2)
C(2)-N(2)-C(9)	127.74(14)
C(2)-N(2)-H(1B)	118.2(19)
C(9)-N(2)-H(1B)	113.7(19)

Table B-4 - Bond lengths [Å], angles [deg] and atomic coordinates for **3.3**

Atom1-Atom2	Distance
C(1)-N(1)	1.362(4)

C(1)-C(1')	1.368(5)
C(1)-C(2)	1.445(5)
C(1')-N(1')	1.366(4)
C(1')-C(2')	1.453(5)
C(2)-N(2)	1.314(5)
C(2)-C(3)	1.444(5)
C(2')-N(2')	1.315(4)
C(2')-C(3')	1.446(5)
C(3')-C(4')	1.396(5)
C(3')-C(8')	1.409(5)
C(3)-C(8)	1.402(5)
C(3)-C(4)	1.404(5)
C(4)-C(5)	1.378(5)
C(4)-H(4)	0.9500
C(4')-C(5')	1.370(5)
C(4')-H(4')	0.9500
C(5')-C(6')	1.386(6)
C(5')-H(5')	0.9500
C(5)-C(6)	1.393(6)
C(5)-H(5)	0.9500
C(6')-C(7')	1.372(5)
C(6')-H(6')	0.9500
C(6)-C(7)	1.374(5)
C(6)-H(6)	0.9500
C(7')-C(8')	1.397(5)
C(7')-H(7')	0.9500
C(7)-C(8)	1.388(5)
C(7)-H(7)	0.9500
C(8')-N(1')	1.392(5)
C(8)-N(1)	1.395(5)
C(9)-F(2)	1.302(6)
C(9)-F(1)	1.308(5)
C(9)-F(3)	1.323(5)
C(9)-C(10)	1.525(6)
C(10)-O(2)	1.249(5)
C(10)-C(11)	1.375(6)
C(11)-C(12)	1.383(6)
C(11)-H(11)	0.9500
C(12)-O(1)	1.246(5)
C(12)-C(13)	1.518(6)
C(13)-F(6)	1.299(6)
C(13)-F(4)	1.305(6)
C(13)-F(5)	1.312(6)
C(14)-F(7)	1.283(5)
C(14)-F(9)	1.297(5)
C(14)-F(8)	1.321(6)

C(14)-C(15)	1.525(6)
C(15)-O(3)	1.245(5)
C(15)-C(16)	1.385(6)
C(16)-C(17)	1.365(6)
C(16)-H(16)	0.9500
C(17)-O(4)	1.255(5)
C(17)-C(18)	1.531(6)
C(18)-F(12)	1.310(5)
C(18)-F(11)	1.324(6)
C(18)-F(10)	1.335(5)
C(19')-C(24')	1.370(5)
C(19')-C(20')	1.379(5)
C(19')-N(2')	1.438(5)
C(19)-C(20)	1.376(6)
C(19)-C(24)	1.384(6)
C(19)-N(2)	1.439(5)
C(20')-C(21')	1.375(5)
C(20')-H(20')	0.9500
C(20)-C(21)	1.381(6)
C(20)-H(20)	0.9500
C(21)-C(22)	1.385(7)
C(21)-H(21)	0.9500
C(21')-C(22')	1.384(6)
C(21')-H(21')	0.9500
C(22)-C(23)	1.388(7)
C(22)-C(25)	1.503(6)
C(22')-C(23')	1.374(6)
C(22')-C(25')	1.509(6)
C(23)-C(24)	1.377(6)
C(23)-H(23)	0.9500
C(23')-C(24')	1.377(6)
C(23')-H(23')	0.9500
C(24')-H(24')	0.9500
C(24)-H(24)	0.9500
C(25')-H(25A)	0.9800
C(25')-H(25B)	0.9800
C(25')-H(25C)	0.9800
C(25)-H(25D)	0.9800
C(25)-H(25E)	0.9800
C(25)-H(25F)	0.9800
C(26)-C(27)	1.493(9)
C(26)-C(26)#1	1.703(14)
C(26)-H(26A)	0.9900
C(26)-H(26B)	0.9900
C(27)-C(28)	1.514(9)
C(27)-H(27A)	0.9900

C(27)-H(27B)	0.9900
C(28)-H(28A)	0.9800
C(28)-H(28B)	0.9800
C(28)-H(28C)	0.9800
N(1)-Pd(2)	1.970(3)
N(1')-Pd(1)	1.976(3)
N(2')-Pd(2)	1.994(3)
N(2)-Pd(1)	1.986(3)
O(1)-Pd(1)	2.028(3)
O(2)-Pd(1)	2.012(3)
O(3)-Pd(2)	2.023(3)
O(4)-Pd(2)	2.018(3)

Atom1-Atom2-Atom3	Angle
N(1)-C(1)-C(1')	123.9(3)
N(1)-C(1)-C(2)	110.2(3)
C(1')-C(1)-C(2)	125.4(3)
N(1')-C(1')-C(1)	124.9(3)
N(1')-C(1')-C(2')	109.9(3)
C(1)-C(1')-C(2')	124.7(3)
N(2)-C(2)-C(3)	130.6(3)
N(2)-C(2)-C(1)	123.8(3)
C(3)-C(2)-C(1)	105.5(3)
N(2')-C(2')-C(3')	130.4(3)
N(2')-C(2')-C(1')	123.9(3)
C(3')-C(2')-C(1')	105.6(3)
C(4')-C(3')-C(8')	120.3(3)
C(4')-C(3')-C(2')	134.1(3)
C(8')-C(3')-C(2')	105.6(3)
C(8)-C(3)-C(4)	119.6(3)
C(8)-C(3)-C(2)	106.0(3)
C(4)-C(3)-C(2)	134.4(3)
C(5)-C(4)-C(3)	118.8(4)
C(5)-C(4)-H(4)	120.6
C(3)-C(4)-H(4)	120.6
C(5')-C(4')-C(3')	119.0(4)
C(5')-C(4')-H(4')	120.5
C(3')-C(4')-H(4')	120.5
C(4')-C(5')-C(6')	120.4(4)
C(4')-C(5')-H(5')	119.8
C(6')-C(5')-H(5')	119.8
C(4)-C(5)-C(6)	120.3(4)
C(4)-C(5)-H(5)	119.9
C(6)-C(5)-H(5)	119.9
C(7')-C(6')-C(5')	122.1(3)
C(7')-C(6')-H(6')	118.9

C(5')-C(6')-H(6')	118.9
C(7)-C(6)-C(5)	122.1(4)
C(7)-C(6)-H(6)	119.0
C(5)-C(6)-H(6)	119.0
C(6')-C(7')-C(8')	118.3(4)
C(6')-C(7')-H(7')	120.9
C(8')-C(7')-H(7')	120.9
C(6)-C(7)-C(8)	117.7(4)
C(6)-C(7)-H(7)	121.1
C(8)-C(7)-H(7)	121.1
N(1')-C(8')-C(7')	128.7(4)
N(1')-C(8')-C(3')	111.4(3)
C(7')-C(8')-C(3')	119.9(3)
C(7)-C(8)-N(1)	127.7(3)
C(7)-C(8)-C(3)	121.3(3)
N(1)-C(8)-C(3)	110.9(3)
F(2)-C(9)-F(1)	108.6(5)
F(2)-C(9)-F(3)	105.9(4)
F(1)-C(9)-F(3)	107.3(4)
F(2)-C(9)-C(10)	111.4(4)
F(1)-C(9)-C(10)	111.0(4)
F(3)-C(9)-C(10)	112.4(4)
O(2)-C(10)-C(11)	128.3(4)
O(2)-C(10)-C(9)	111.7(4)
C(11)-C(10)-C(9)	120.0(4)
C(10)-C(11)-C(12)	122.4(4)
C(10)-C(11)-H(11)	118.8
C(12)-C(11)-H(11)	118.8
O(1)-C(12)-C(11)	129.3(4)
O(1)-C(12)-C(13)	114.0(4)
C(11)-C(12)-C(13)	116.6(4)
F(6)-C(13)-F(4)	107.5(4)
F(6)-C(13)-F(5)	106.7(5)
F(4)-C(13)-F(5)	105.9(5)
F(6)-C(13)-C(12)	110.7(4)
F(4)-C(13)-C(12)	113.3(4)
F(5)-C(13)-C(12)	112.3(4)
F(7)-C(14)-F(9)	109.7(5)
F(7)-C(14)-F(8)	105.6(4)
F(9)-C(14)-F(8)	105.8(4)
F(7)-C(14)-C(15)	113.2(4)
F(9)-C(14)-C(15)	112.2(4)
F(8)-C(14)-C(15)	110.0(4)
O(3)-C(15)-C(16)	128.9(4)
O(3)-C(15)-C(14)	114.6(4)
C(16)-C(15)-C(14)	116.5(4)

C(17)-C(16)-C(15)	122.6(4)
C(17)-C(16)-H(16)	118.7
C(15)-C(16)-H(16)	118.7
O(4)-C(17)-C(16)	129.1(4)
O(4)-C(17)-C(18)	111.5(4)
C(16)-C(17)-C(18)	119.4(4)
F(12)-C(18)-F(11)	107.0(4)
F(12)-C(18)-F(10)	107.8(4)
F(11)-C(18)-F(10)	107.2(4)
F(12)-C(18)-C(17)	112.1(4)
F(11)-C(18)-C(17)	110.1(4)
F(10)-C(18)-C(17)	112.4(4)
C(24')-C(19')-C(20')	119.7(3)
C(24')-C(19')-N(2')	119.8(3)
C(20')-C(19')-N(2')	120.5(3)
C(20)-C(19)-C(24)	119.8(4)
C(20)-C(19)-N(2)	119.7(4)
C(24)-C(19)-N(2)	120.5(4)
C(21')-C(20')-C(19')	119.6(4)
C(21')-C(20')-H(20')	120.2
C(19')-C(20')-H(20')	120.2
C(19)-C(20)-C(21)	119.6(4)
C(19)-C(20)-H(20)	120.2
C(21)-C(20)-H(20)	120.2
C(20)-C(21)-C(22)	121.8(4)
C(20)-C(21)-H(21)	119.1
C(22)-C(21)-H(21)	119.1
C(20')-C(21')-C(22')	121.5(4)
C(20')-C(21')-H(21')	119.2
C(22')-C(21')-H(21')	119.2
C(21)-C(22)-C(23)	117.5(4)
C(21)-C(22)-C(25)	121.5(5)
C(23)-C(22)-C(25)	121.0(5)
C(23')-C(22')-C(21')	117.6(4)
C(23')-C(22')-C(25')	120.6(4)
C(21')-C(22')-C(25')	121.9(4)
C(24)-C(23)-C(22)	121.4(4)
C(24)-C(23)-H(23)	119.3
C(22)-C(23)-H(23)	119.3
C(22')-C(23')-C(24')	121.7(4)
C(22')-C(23')-H(23')	119.2
C(24')-C(23')-H(23')	119.2
C(19')-C(24')-C(23')	119.9(4)
C(19')-C(24')-H(24')	120.1
C(23')-C(24')-H(24')	120.1
C(23)-C(24)-C(19)	119.9(4)

C(23)-C(24)-H(24)	120.1
C(19)-C(24)-H(24)	120.1
C(22')-C(25')-H(25A)	109.5
C(22')-C(25')-H(25B)	109.5
H(25A)-C(25')-H(25B)	109.5
C(22')-C(25')-H(25C)	109.5
H(25A)-C(25')-H(25C)	109.5
H(25B)-C(25')-H(25C)	109.5
C(22)-C(25)-H(25D)	109.5
C(22)-C(25)-H(25E)	109.5
H(25D)-C(25)-H(25E)	109.5
C(22)-C(25)-H(25F)	109.5
H(25D)-C(25)-H(25F)	109.5
H(25E)-C(25)-H(25F)	109.5
C(27)-C(26)-C(26)#1	110.2(7)
C(27)-C(26)-H(26A)	109.6
C(26)#1-C(26)-H(26A)	109.6
C(27)-C(26)-H(26B)	109.6
C(26)#1-C(26)-H(26B)	109.6
H(26A)-C(26)-H(26B)	108.1
C(26)-C(27)-C(28)	108.6(6)
C(26)-C(27)-H(27A)	110.0
C(28)-C(27)-H(27A)	110.0
C(26)-C(27)-H(27B)	110.0
C(28)-C(27)-H(27B)	110.0
H(27A)-C(27)-H(27B)	108.3
C(27)-C(28)-H(28A)	109.5
C(27)-C(28)-H(28B)	109.5
H(28A)-C(28)-H(28B)	109.5
C(27)-C(28)-H(28C)	109.5
H(28A)-C(28)-H(28C)	109.5
H(28B)-C(28)-H(28C)	109.5
C(1)-N(1)-C(8)	107.2(3)
C(1)-N(1)-Pd(2)	123.7(2)
C(8)-N(1)-Pd(2)	128.0(2)
C(1')-N(1')-C(8')	107.2(3)
C(1')-N(1')-Pd(1)	122.9(2)
C(8')-N(1')-Pd(1)	129.7(2)
C(2')-N(2')-C(19')	118.4(3)
C(2')-N(2')-Pd(2)	125.0(2)
C(19')-N(2')-Pd(2)	116.6(2)
C(2)-N(2)-C(19)	117.1(3)
C(2)-N(2)-Pd(1)	125.0(3)
C(19)-N(2)-Pd(1)	117.8(2)
C(12)-O(1)-Pd(1)	124.2(3)
C(10)-O(2)-Pd(1)	125.5(3)

C(15)-O(3)-Pd(2)	124.7(3)
C(17)-O(4)-Pd(2)	124.6(3)
N(1')-Pd(1)-N(2)	91.55(12)
N(1')-Pd(1)-O(2)	179.03(12)
N(2)-Pd(1)-O(2)	87.78(12)
N(1')-Pd(1)-O(1)	90.89(12)
N(2)-Pd(1)-O(1)	174.35(12)
O(2)-Pd(1)-O(1)	89.84(11)
N(1)-Pd(2)-N(2')	90.46(12)
N(1)-Pd(2)-O(4)	89.86(11)
N(2')-Pd(2)-O(4)	174.54(12)
N(1)-Pd(2)-O(3)	179.41(12)
N(2')-Pd(2)-O(3)	89.74(11)
O(4)-Pd(2)-O(3)	89.99(11)

Table B-5 Bond lengths [Å], angles [deg] and atomic coordinates for **3.4**

Atom1-Atom2	Distance
C(1)-N(1)	1.370(4)
C(1)-C(1)#1	1.379(7)
C(1)-C(2)	1.454(5)
C(2)-N(2)#1	1.311(4)
C(2)-C(3)	1.454(5)
C(3)-C(4)	1.400(5)
C(3)-C(8)	1.411(5)
C(4)-C(5)	1.383(5)
C(4)-H(4)	0.9500
C(5)-C(6)	1.393(5)
C(5)-H(5)	0.9500
C(6)-C(7)	1.375(5)
C(6)-H(6)	0.9500
C(7)-C(8)	1.400(5)
C(7)-H(7)	0.9500
C(8)-N(1)	1.394(4)
C(9)-F(1)	1.300(5)
C(9)-F(3)	1.327(5)
C(9)-F(2)	1.332(5)
C(9)-C(10)	1.527(6)
C(10)-O(1)	1.258(4)
C(10)-C(11)	1.373(6)
C(11)-C(12)	1.376(6)
C(11)-H(11)	0.9500
C(12)-O(2)	1.254(5)
C(12)-C(13)	1.533(6)
C(13)-F(5B)	1.24(3)

C(13)-F(4B)	1.26(2)
C(13)-F(6)	1.272(14)
C(13)-F(4)	1.285(10)
C(13)-F(5)	1.307(13)
C(13)-F(6B)	1.30(3)
C(14)-C(19)	1.372(5)
C(14)-C(15)	1.384(5)
C(14)-N(2)	1.444(4)
C(15)-C(16)	1.381(5)
C(15)-H(15)	0.9500
C(16)-C(17)	1.376(6)
C(16)-H(16)	0.9500
C(17)-O(3)	1.365(4)
C(17)-C(18)	1.387(6)
C(18)-C(19)	1.385(5)
C(18)-H(18)	0.9500
C(19)-H(19)	0.9500
C(20)-O(3)	1.412(6)
C(20)-H(20A)	0.9800
C(20)-H(20B)	0.9800
C(20)-H(20C)	0.9800
N(1)-Pd(1)	1.990(3)
N(2)-C(2)#1	1.311(4)
N(2)-Pd(1)	1.989(3)
O(1)-Pd(1)	2.029(2)
O(2)-Pd(1)	2.043(3)

Atom1-Atom2-Atom3	Distance
N(1)-C(1)-C(1)#1	124.8(4)
N(1)-C(1)-C(2)	110.2(3)
C(1)#1-C(1)-C(2)	125.0(4)
N(2)#1-C(2)-C(3)	130.4(3)
N(2)#1-C(2)-C(1)	124.1(3)
C(3)-C(2)-C(1)	105.4(3)
C(4)-C(3)-C(8)	120.1(3)
C(4)-C(3)-C(2)	133.8(3)
C(8)-C(3)-C(2)	105.8(3)
C(5)-C(4)-C(3)	119.1(3)
C(5)-C(4)-H(4)	120.4
C(3)-C(4)-H(4)	120.4
C(4)-C(5)-C(6)	120.3(3)
C(4)-C(5)-H(5)	119.8
C(6)-C(5)-H(5)	119.8
C(7)-C(6)-C(5)	121.6(3)
C(7)-C(6)-H(6)	119.2
C(5)-C(6)-H(6)	119.2

C(6)-C(7)-C(8)	118.9(3)
C(6)-C(7)-H(7)	120.6
C(8)-C(7)-H(7)	120.6
N(1)-C(8)-C(7)	128.7(3)
N(1)-C(8)-C(3)	111.3(3)
C(7)-C(8)-C(3)	119.9(3)
F(1)-C(9)-F(3)	107.9(4)
F(1)-C(9)-F(2)	107.5(4)
F(3)-C(9)-F(2)	105.8(4)
F(1)-C(9)-C(10)	112.1(4)
F(3)-C(9)-C(10)	112.9(4)
F(2)-C(9)-C(10)	110.3(4)
O(1)-C(10)-C(11)	129.2(4)
O(1)-C(10)-C(9)	112.2(3)
C(11)-C(10)-C(9)	118.6(3)
C(10)-C(11)-C(12)	121.6(4)
C(10)-C(11)-H(11)	119.2
C(12)-C(11)-H(11)	119.2
O(2)-C(12)-C(11)	129.3(4)
O(2)-C(12)-C(13)	113.0(4)
C(11)-C(12)-C(13)	117.7(4)
F(5B)-C(13)-F(4B)	110(2)
F(5B)-C(13)-F(6)	128(3)
F(4B)-C(13)-F(6)	84(3)
F(5B)-C(13)-F(4)	84(3)
F(4B)-C(13)-F(4)	28(3)
F(6)-C(13)-F(4)	108.6(11)
F(5B)-C(13)-F(5)	27(4)
F(4B)-C(13)-F(5)	127(2)
F(6)-C(13)-F(5)	105.7(11)
F(4)-C(13)-F(5)	106.0(11)
F(5B)-C(13)-F(6B)	108(3)
F(4B)-C(13)-F(6B)	103(3)
F(6)-C(13)-F(6B)	24(2)
F(4)-C(13)-F(6B)	122.9(13)
F(5)-C(13)-F(6B)	83(2)
F(5B)-C(13)-C(12)	109.5(17)
F(4B)-C(13)-C(12)	112.9(16)
F(6)-C(13)-C(12)	110.1(8)
F(4)-C(13)-C(12)	114.1(7)
F(5)-C(13)-C(12)	111.9(7)
F(6B)-C(13)-C(12)	113.6(13)
C(19)-C(14)-C(15)	119.8(3)
C(19)-C(14)-N(2)	119.7(3)
C(15)-C(14)-N(2)	120.5(3)
C(16)-C(15)-C(14)	119.6(4)

C(16)-C(15)-H(15)	120.2
C(14)-C(15)-H(15)	120.2
C(17)-C(16)-C(15)	120.4(4)
C(17)-C(16)-H(16)	119.8
C(15)-C(16)-H(16)	119.8
O(3)-C(17)-C(16)	116.1(4)
O(3)-C(17)-C(18)	123.6(4)
C(16)-C(17)-C(18)	120.3(3)
C(19)-C(18)-C(17)	118.8(4)
C(19)-C(18)-H(18)	120.6
C(17)-C(18)-H(18)	120.6
C(14)-C(19)-C(18)	121.0(3)
C(14)-C(19)-H(19)	119.5
C(18)-C(19)-H(19)	119.5
O(3)-C(20)-H(20A)	109.5
O(3)-C(20)-H(20B)	109.5
H(20A)-C(20)-H(20B)	109.5
O(3)-C(20)-H(20C)	109.5
H(20A)-C(20)-H(20C)	109.5
H(20B)-C(20)-H(20C)	109.5
C(1)-N(1)-C(8)	107.2(3)
C(1)-N(1)-Pd(1)	123.6(2)
C(8)-N(1)-Pd(1)	126.6(2)
C(2)#1-N(2)-C(14)	117.5(3)
C(2)#1-N(2)-Pd(1)	125.9(2)
C(14)-N(2)-Pd(1)	116.4(2)
C(10)-O(1)-Pd(1)	125.8(2)
C(12)-O(2)-Pd(1)	125.4(3)
C(17)-O(3)-C(20)	117.5(4)
N(2)-Pd(1)-N(1)	91.14(11)
N(2)-Pd(1)-O(1)	172.63(11)
N(1)-Pd(1)-O(1)	91.87(11)
N(2)-Pd(1)-O(2)	89.12(11)
N(1)-Pd(1)-O(2)	176.24(12)
O(1)-Pd(1)-O(2)	88.31(10)

Table B-6 - Bond lengths [Å], angles [deg] and atomic coordinates for **3.6**

Atom1-Atom2	Distance
C(1)-N(1)	1.356(4)
C(1)-C(9)	1.387(4)
C(1)-C(2)	1.467(4)
C(2)-N(3)	1.309(4)
C(2)-C(3)	1.463(4)
C(3)-C(4)	1.392(5)
C(3)-C(8)	1.415(4)

C(4)-C(5)	1.378(5)
C(4)-H(4)	0.9500
C(5)-C(6)	1.392(5)
C(5)-H(5)	0.9500
C(6)-C(7)	1.387(5)
C(6)-H(6)	0.9500
C(7)-C(8)	1.385(4)
C(7)-H(7)	0.9500
C(8)-N(1)	1.402(4)
C(9)-N(2)	1.383(4)
C(9)-C(10)	1.440(4)
C(10)-N(4)	1.333(4)
C(10)-C(11)	1.435(4)
C(11)-C(12)	1.405(4)
C(11)-C(16)	1.429(4)
C(12)-C(13)	1.365(5)
C(12)-H(12)	0.9500
C(13)-C(14)	1.408(5)
C(13)-H(13)	0.9500
C(14)-C(15)	1.368(5)
C(14)-H(14)	0.9500
C(15)-C(16)	1.398(4)
C(15)-H(15)	0.9500
C(16)-N(2)	1.371(4)
C(17)-F(2)	1.306(4)
C(17)-F(1)	1.321(4)
C(17)-F(3)	1.330(4)
C(17)-C(18)	1.530(5)
C(18)-O(1)	1.258(4)
C(18)-C(19)	1.384(5)
C(19)-C(20)	1.382(5)
C(19)-H(19)	0.9500
C(20)-O(2)	1.263(4)
C(20)-C(21)	1.528(5)
C(21)-F(6)	1.321(4)
C(21)-F(4)	1.333(4)
C(21)-F(5)	1.334(4)
C(22)-C(23)	1.389(5)
C(22)-C(27)	1.404(5)
C(22)-N(3)	1.436(4)
C(23)-C(24)	1.390(5)
C(23)-C(28)	1.506(5)
C(24)-C(25)	1.380(5)
C(24)-H(24)	0.9500
C(25)-C(26)	1.369(5)
C(25)-C(29)	1.513(5)

C(26)-C(27)	1.390(5)
C(26)-H(26)	0.9500
C(27)-C(30)	1.500(5)
C(28)-H(28A)	0.9800
C(28)-H(28B)	0.9800
C(28)-H(28C)	0.9800
C(29)-H(29A)	0.9800
C(29)-H(29B)	0.9800
C(29)-H(29C)	0.9800
C(30)-H(30A)	0.9800
C(30)-H(30B)	0.9800
C(30)-H(30C)	0.9800
C(31)-C(32)	1.390(4)
C(31)-C(36)	1.393(5)
C(31)-N(4)	1.432(4)
C(32)-C(33)	1.389(5)
C(32)-C(37)	1.503(5)
C(33)-C(34)	1.388(5)
C(33)-H(33)	0.9500
C(34)-C(35)	1.379(5)
C(34)-C(38)	1.507(5)
C(37)-H(37A)	0.9800
C(37)-H(37B)	0.9800
C(37)-H(37C)	0.9800
C(38)-H(38A)	0.9800
C(38)-H(38B)	0.9800
C(38)-H(38C)	0.9800
C(39)-C(36)	1.503(5)
C(39)-H(39A)	0.9800
C(39)-H(39B)	0.9800
C(39)-H(39C)	0.9800
C(35)-C(36)	1.389(5)
C(35)-H(35)	0.9500
N(1)-Pd(1)	1.987(3)
N(2)-Pd(1)	1.991(2)
N(4)-H(4N)	0.88(4)
O(1)-Pd(1)	2.022(2)
O(2)-Pd(1)	2.021(2)
C(40)-O(3)	1.091(16)
C(40)-C(41)#1	1.453(11)
C(40)-C(41)	1.478(12)
C(41)-H(41A)	0.9800
C(41)-H(41B)	0.9800
C(41)-H(41C)	0.9800

Atom1-Atom2-Atom3	Angle

N(1)-C(1)-C(9)	116.1(3)
N(1)-C(1)-C(2)	110.2(3)
C(9)-C(1)-C(2)	133.7(3)
N(3)-C(2)-C(3)	132.4(3)
N(3)-C(2)-C(1)	122.8(3)
C(3)-C(2)-C(1)	104.8(3)
C(4)-C(3)-C(8)	119.9(3)
C(4)-C(3)-C(2)	133.9(3)
C(8)-C(3)-C(2)	106.2(3)
C(5)-C(4)-C(3)	119.2(3)
C(5)-C(4)-H(4)	120.4
C(3)-C(4)-H(4)	120.4
C(4)-C(5)-C(6)	120.4(3)
C(4)-C(5)-H(5)	119.8
C(6)-C(5)-H(5)	119.8
C(7)-C(6)-C(5)	121.9(3)
C(7)-C(6)-H(6)	119.1
C(5)-C(6)-H(6)	119.1
C(8)-C(7)-C(6)	117.8(3)
C(8)-C(7)-H(7)	121.1
C(6)-C(7)-H(7)	121.1
C(7)-C(8)-N(1)	128.5(3)
C(7)-C(8)-C(3)	121.0(3)
N(1)-C(8)-C(3)	110.5(3)
N(2)-C(9)-C(1)	115.6(3)
N(2)-C(9)-C(10)	110.4(3)
C(1)-C(9)-C(10)	133.9(3)
N(4)-C(10)-C(11)	131.3(3)
N(4)-C(10)-C(9)	123.5(3)
C(11)-C(10)-C(9)	105.1(3)
C(12)-C(11)-C(16)	119.7(3)
C(12)-C(11)-C(10)	133.6(3)
C(16)-C(11)-C(10)	106.6(3)
C(13)-C(12)-C(11)	119.1(3)
C(13)-C(12)-H(12)	120.4
C(11)-C(12)-H(12)	120.4
C(12)-C(13)-C(14)	120.6(3)
C(12)-C(13)-H(13)	119.7
C(14)-C(13)-H(13)	119.7
C(15)-C(14)-C(13)	122.1(3)
C(15)-C(14)-H(14)	119.0
C(13)-C(14)-H(14)	119.0
C(14)-C(15)-C(16)	118.3(3)
C(14)-C(15)-H(15)	120.9
C(16)-C(15)-H(15)	120.9
N(2)-C(16)-C(15)	129.4(3)

N(2)-C(16)-C(11)	110.4(3)
C(15)-C(16)-C(11)	120.2(3)
F(2)-C(17)-F(1)	107.9(3)
F(2)-C(17)-F(3)	107.4(3)
F(1)-C(17)-F(3)	105.8(3)
F(2)-C(17)-C(18)	110.5(3)
F(1)-C(17)-C(18)	112.7(3)
F(3)-C(17)-C(18)	112.3(3)
O(1)-C(18)-C(19)	128.7(3)
O(1)-C(18)-C(17)	113.8(3)
C(19)-C(18)-C(17)	117.5(3)
C(20)-C(19)-C(18)	123.6(3)
C(20)-C(19)-H(19)	118.2
C(18)-C(19)-H(19)	118.2
O(2)-C(20)-C(19)	129.2(3)
O(2)-C(20)-C(21)	113.3(3)
C(19)-C(20)-C(21)	117.3(3)
F(6)-C(21)-F(4)	107.8(3)
F(6)-C(21)-F(5)	107.5(3)
F(4)-C(21)-F(5)	106.7(3)
F(6)-C(21)-C(20)	112.8(3)
F(4)-C(21)-C(20)	111.8(3)
F(5)-C(21)-C(20)	110.0(3)
C(23)-C(22)-C(27)	121.1(3)
C(23)-C(22)-N(3)	119.7(3)
C(27)-C(22)-N(3)	119.2(3)
C(22)-C(23)-C(24)	118.3(3)
C(22)-C(23)-C(28)	121.2(3)
C(24)-C(23)-C(28)	120.5(3)
C(25)-C(24)-C(23)	122.0(4)
C(25)-C(24)-H(24)	119.0
C(23)-C(24)-H(24)	119.0
C(26)-C(25)-C(24)	118.3(3)
C(26)-C(25)-C(29)	120.7(4)
C(24)-C(25)-C(29)	121.0(4)
C(25)-C(26)-C(27)	122.6(3)
C(25)-C(26)-H(26)	118.7
C(27)-C(26)-H(26)	118.7
C(26)-C(27)-C(22)	117.7(3)
C(26)-C(27)-C(30)	120.6(3)
C(22)-C(27)-C(30)	121.8(3)
C(23)-C(28)-H(28A)	109.5
C(23)-C(28)-H(28B)	109.5
H(28A)-C(28)-H(28B)	109.5
C(23)-C(28)-H(28C)	109.5
H(28A)-C(28)-H(28C)	109.5

H(28B)-C(28)-H(28C)	109.5
C(25)-C(29)-H(29A)	109.5
C(25)-C(29)-H(29B)	109.5
H(29A)-C(29)-H(29B)	109.5
C(25)-C(29)-H(29C)	109.5
H(29A)-C(29)-H(29C)	109.5
H(29B)-C(29)-H(29C)	109.5
C(27)-C(30)-H(30A)	109.5
C(27)-C(30)-H(30B)	109.5
H(30A)-C(30)-H(30B)	109.5
C(27)-C(30)-H(30C)	109.5
H(30A)-C(30)-H(30C)	109.5
H(30B)-C(30)-H(30C)	109.5
C(32)-C(31)-C(36)	121.2(3)
C(32)-C(31)-N(4)	120.7(3)
C(36)-C(31)-N(4)	117.9(3)
C(33)-C(32)-C(31)	118.1(3)
C(33)-C(32)-C(37)	119.9(3)
C(31)-C(32)-C(37)	122.0(3)
C(34)-C(33)-C(32)	122.4(3)
C(34)-C(33)-H(33)	118.8
C(32)-C(33)-H(33)	118.8
C(35)-C(34)-C(33)	117.6(3)
C(35)-C(34)-C(38)	121.4(3)
C(33)-C(34)-C(38)	121.1(3)
C(32)-C(37)-H(37A)	109.5
C(32)-C(37)-H(37B)	109.5
H(37A)-C(37)-H(37B)	109.5
C(32)-C(37)-H(37C)	109.5
H(37A)-C(37)-H(37C)	109.5
H(37B)-C(37)-H(37C)	109.5
C(34)-C(38)-H(38A)	109.5
C(34)-C(38)-H(38B)	109.5
H(38A)-C(38)-H(38B)	109.5
C(34)-C(38)-H(38C)	109.5
H(38A)-C(38)-H(38C)	109.5
H(38B)-C(38)-H(38C)	109.5
C(36)-C(39)-H(39A)	109.5
C(36)-C(39)-H(39B)	109.5
H(39A)-C(39)-H(39B)	109.5
C(36)-C(39)-H(39C)	109.5
H(39A)-C(39)-H(39C)	109.5
H(39B)-C(39)-H(39C)	109.5
C(34)-C(35)-C(36)	122.3(3)
C(34)-C(35)-H(35)	118.8
C(36)-C(35)-H(35)	118.8

C(35)-C(36)-C(31)	118.4(3)
C(35)-C(36)-C(39)	120.6(3)
C(31)-C(36)-C(39)	121.0(3)
C(1)-N(1)-C(8)	108.2(3)
C(1)-N(1)-Pd(1)	113.7(2)
C(8)-N(1)-Pd(1)	137.7(2)
C(16)-N(2)-C(9)	107.4(2)
C(16)-N(2)-Pd(1)	138.2(2)
C(9)-N(2)-Pd(1)	112.69(19)
C(2)-N(3)-C(22)	118.0(3)
C(10)-N(4)-C(31)	125.6(3)
C(10)-N(4)-H(4N)	116(2)
C(31)-N(4)-H(4N)	118(2)
C(18)-O(1)-Pd(1)	123.3(2)
C(20)-O(2)-Pd(1)	122.7(2)
N(1)-Pd(1)-N(2)	80.88(10)
N(1)-Pd(1)-O(2)	174.01(10)
N(2)-Pd(1)-O(2)	93.76(10)
N(1)-Pd(1)-O(1)	93.08(10)
N(2)-Pd(1)-O(1)	173.31(10)
O(2)-Pd(1)-O(1)	92.13(9)
O(3)-C(40)-C(41)#1	108.4(12)
O(3)-C(40)-C(41)	134.0(14)
C(41)#1-C(40)-C(41)	117.6(14)

Appendix C: ^{1}H and ^{13}C NMR of ligands and complexes

The low solubility of many of the ligands and complexes has made it difficult to collect complete ^{13}C data, however all data that was obtained is shown below.

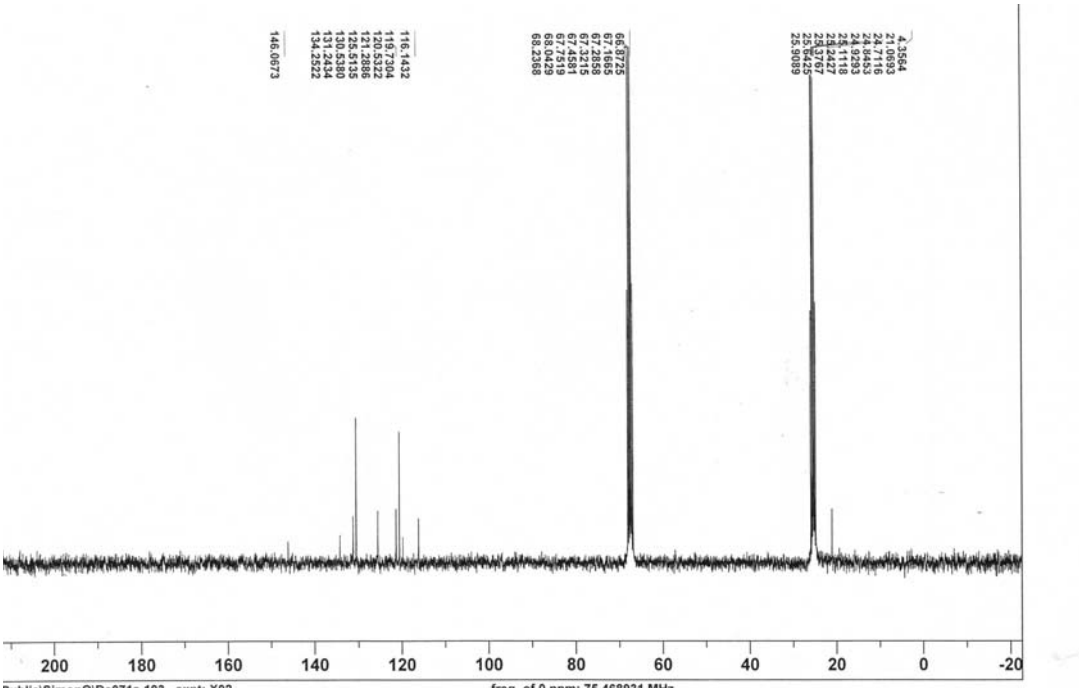

Appendix Figure 1: ^{13}C NMR of p-tolyl Nindigo 2.9

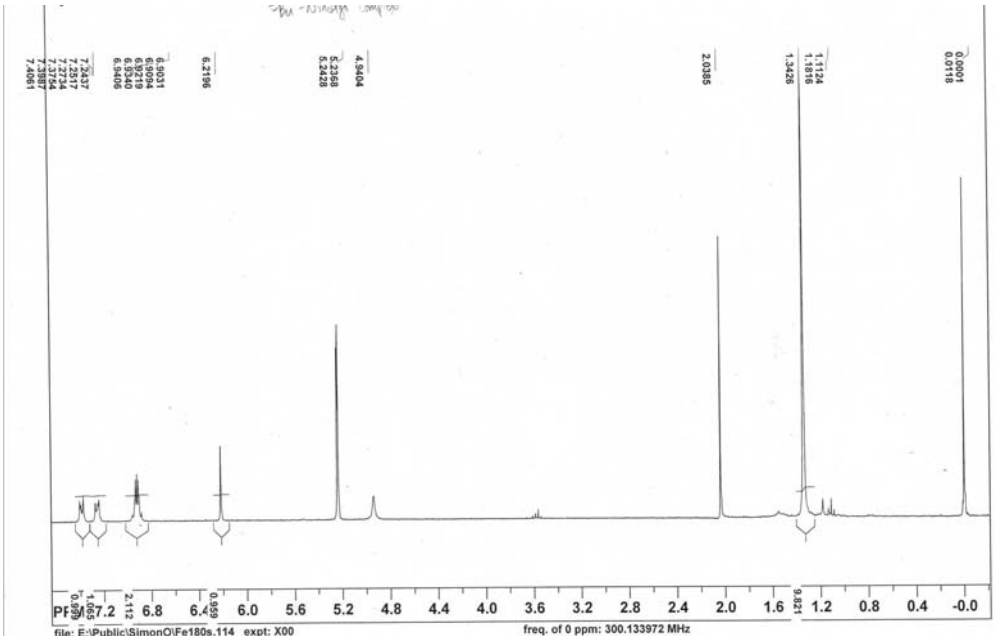

Appendix Figure 2: ^{1}H NMR of ^{t}Bu Nindigo 2.10

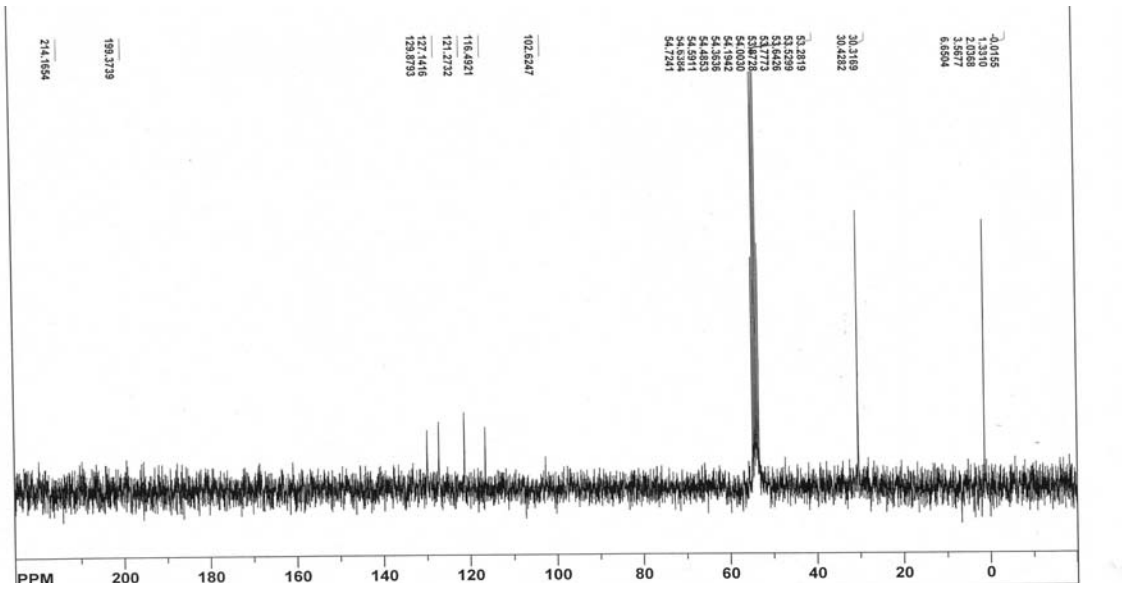

Appendix Figure 3: ^{13}C NMR of ^{t}Bu Nindigo 2.10

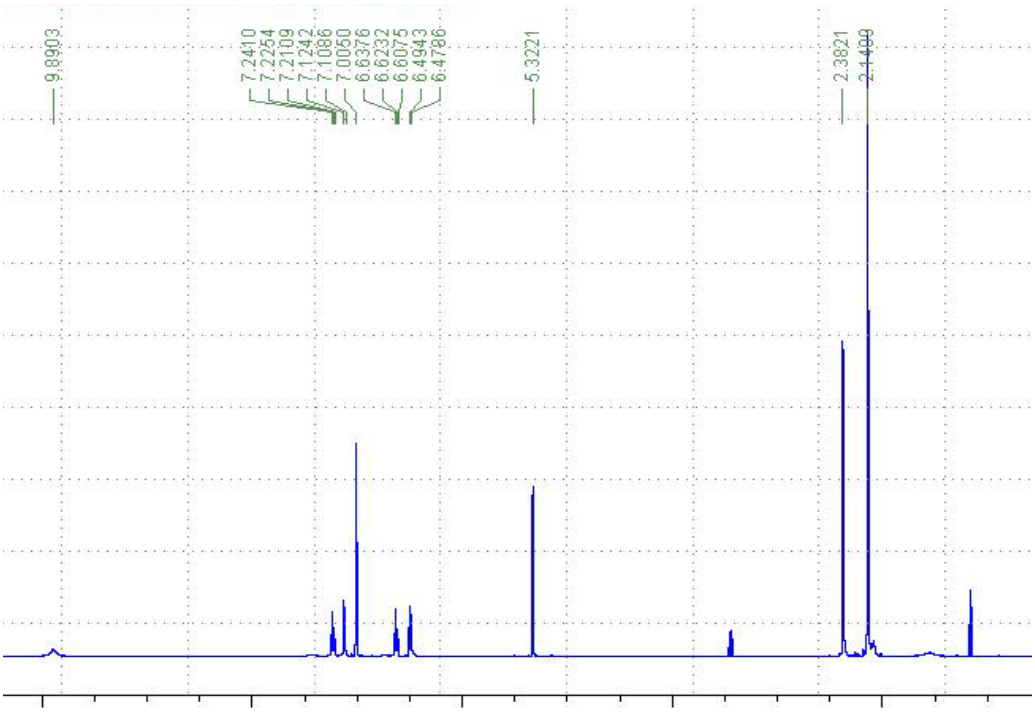

Appendix Figure 4: ^{1}H NMR of mesityl Nindigo 2.11

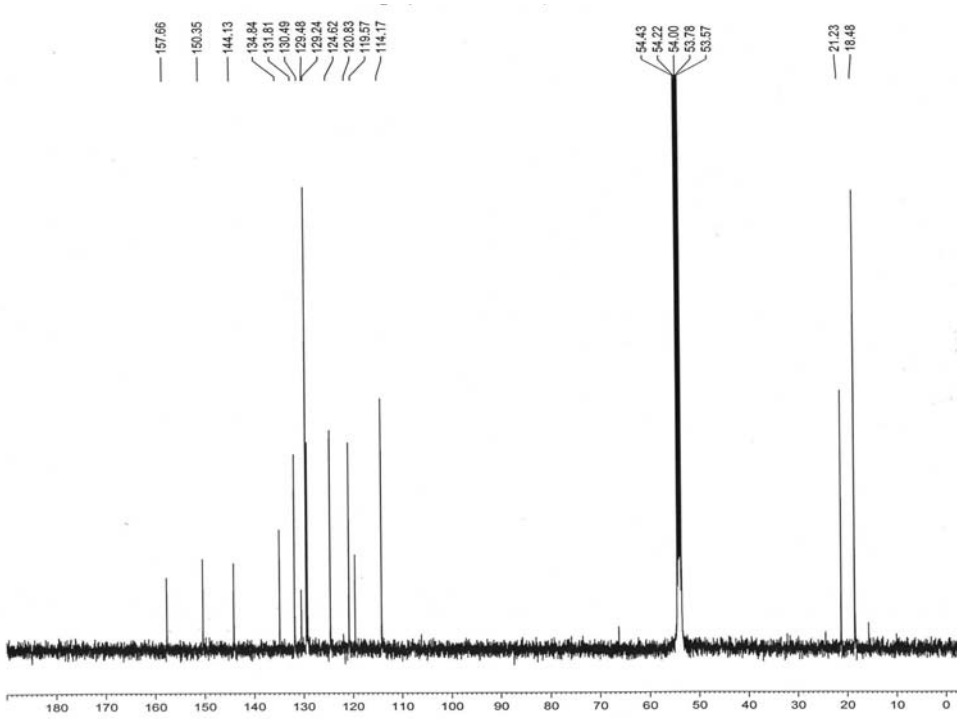

Appendix Figure 5: ^{13}C NMR of mesityl Nindigo 2.11

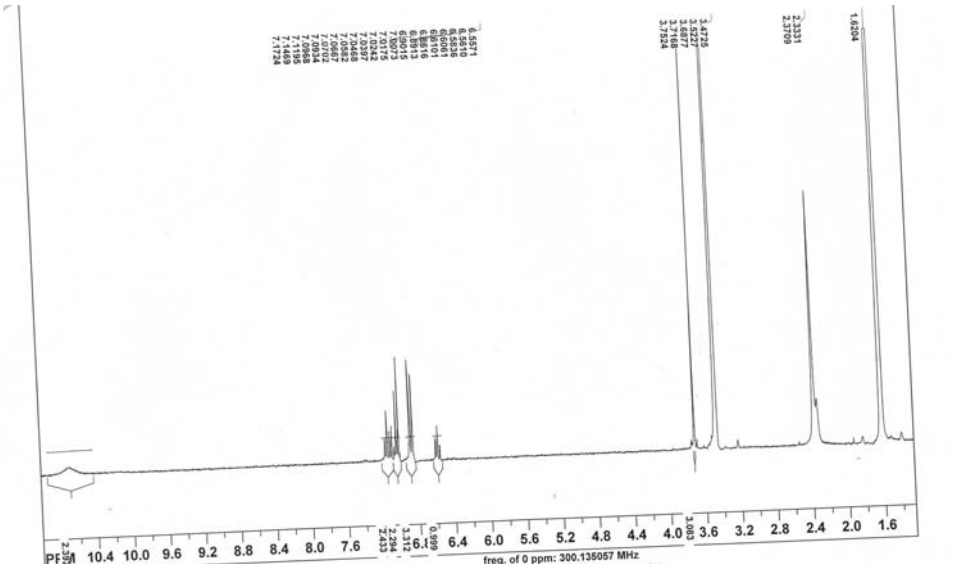

Appendix Figure 6: ^{1}H NMR of p-methoxyphenyl Nindigo 2.12

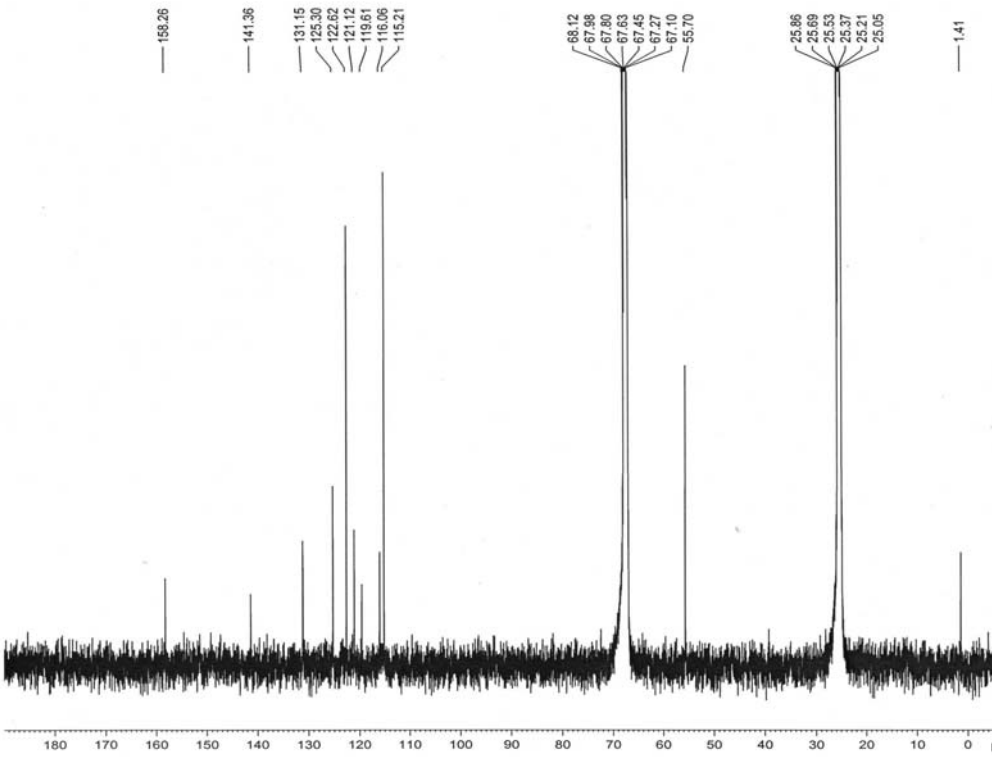

Appendix Figure 7: ^{13}C NMR of p-methoxyphenyl Nindigo 2.12

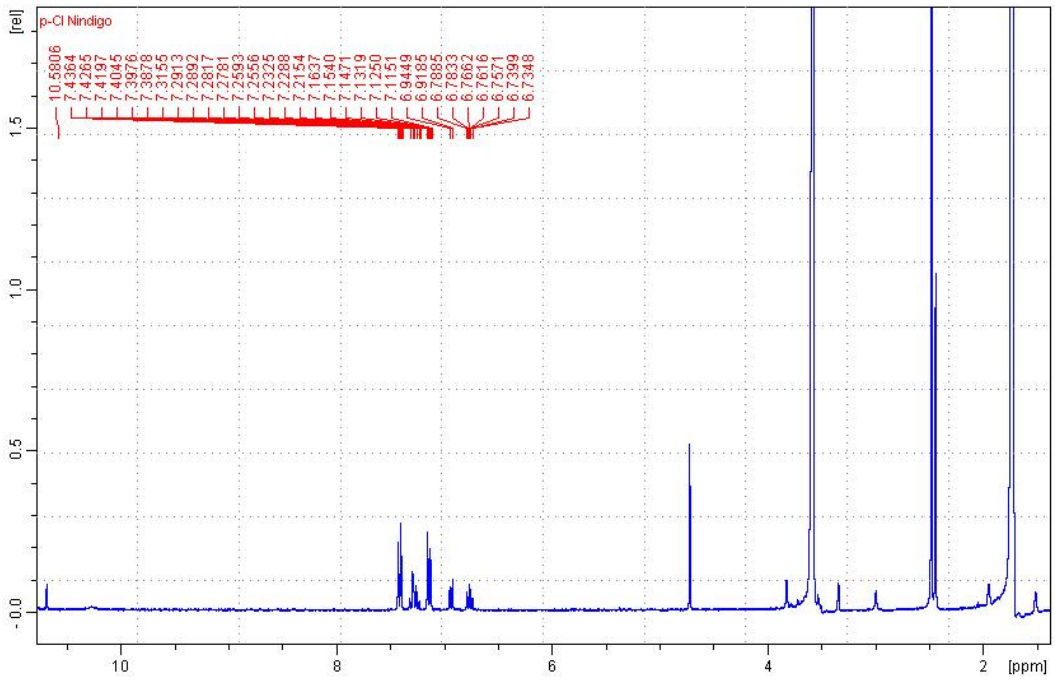

Appendix Figure 8: ^{1}H NMR of p-chlorophenyl Nindigo 2.13

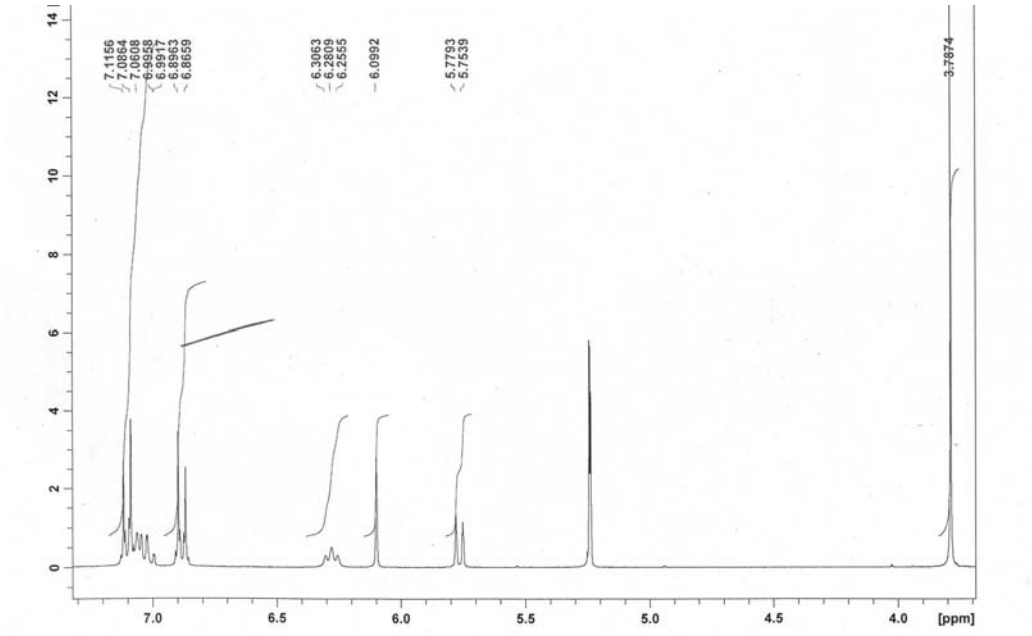

Appendix Figure 9: ^{1}H NMR of p-methoxyphenyl Nindigo complex 3.4

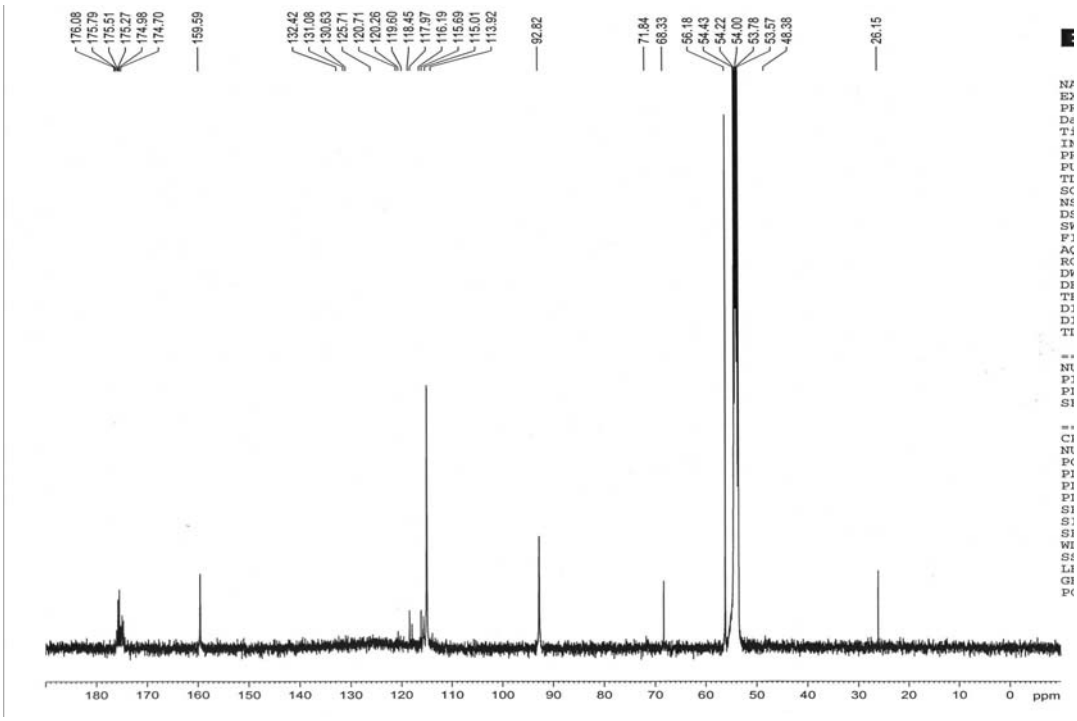

Appendix Figure 10: ^{13}C NMR of p-methyoxtphenyl Nindigo complex 3.4

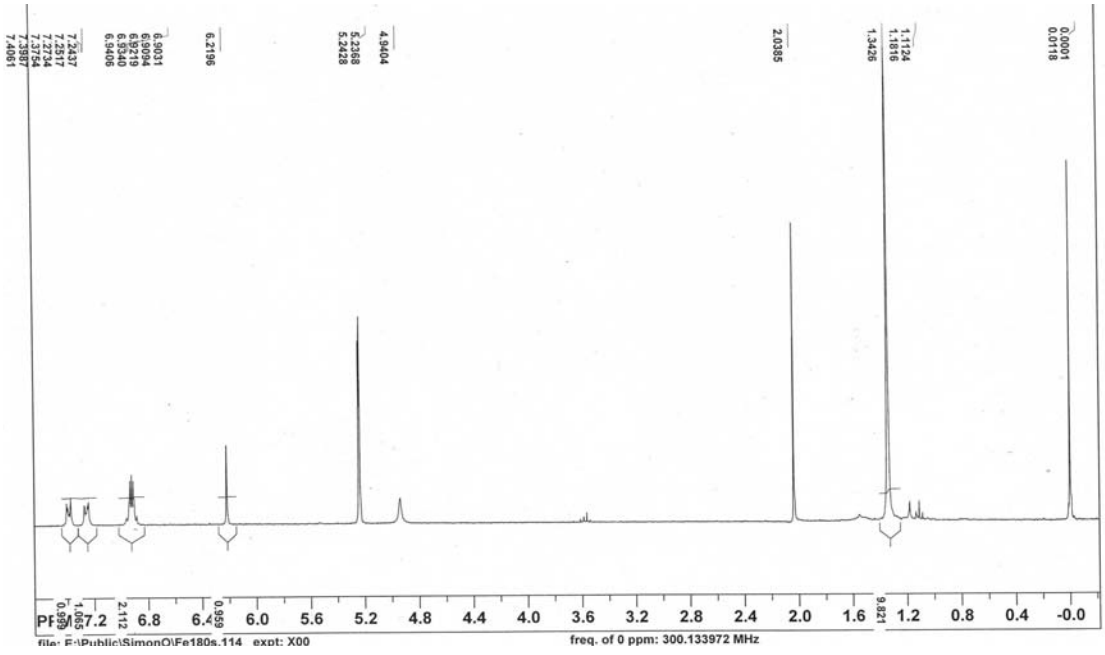

Appendix Figure 11: ^{1}H NMR of tBu Nindigo complex 3.5

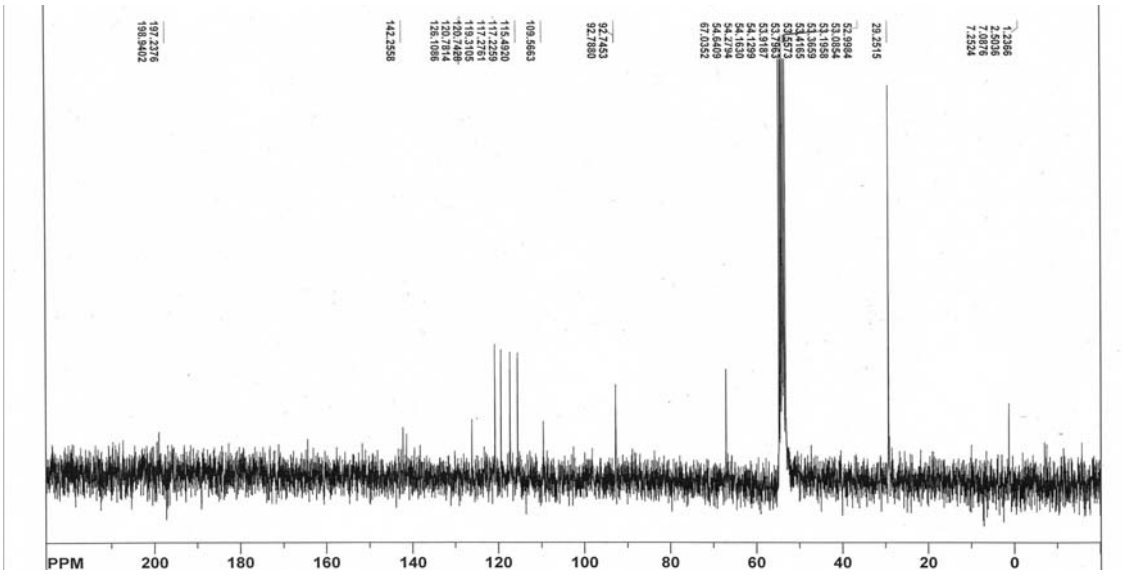

Appendix Figure 12: ^{13}C NMR of tBu Nindigo complex 3.5

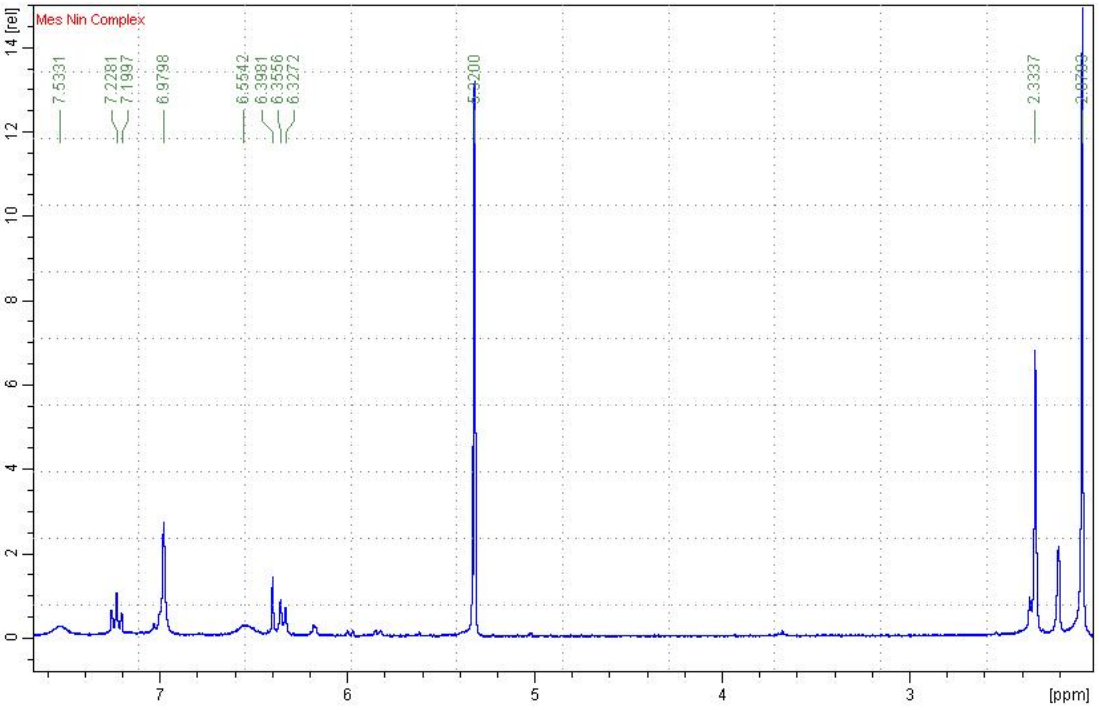

Appendix Figure 13: ^{1}H NMR of mesityl Nindigo complex 3.6

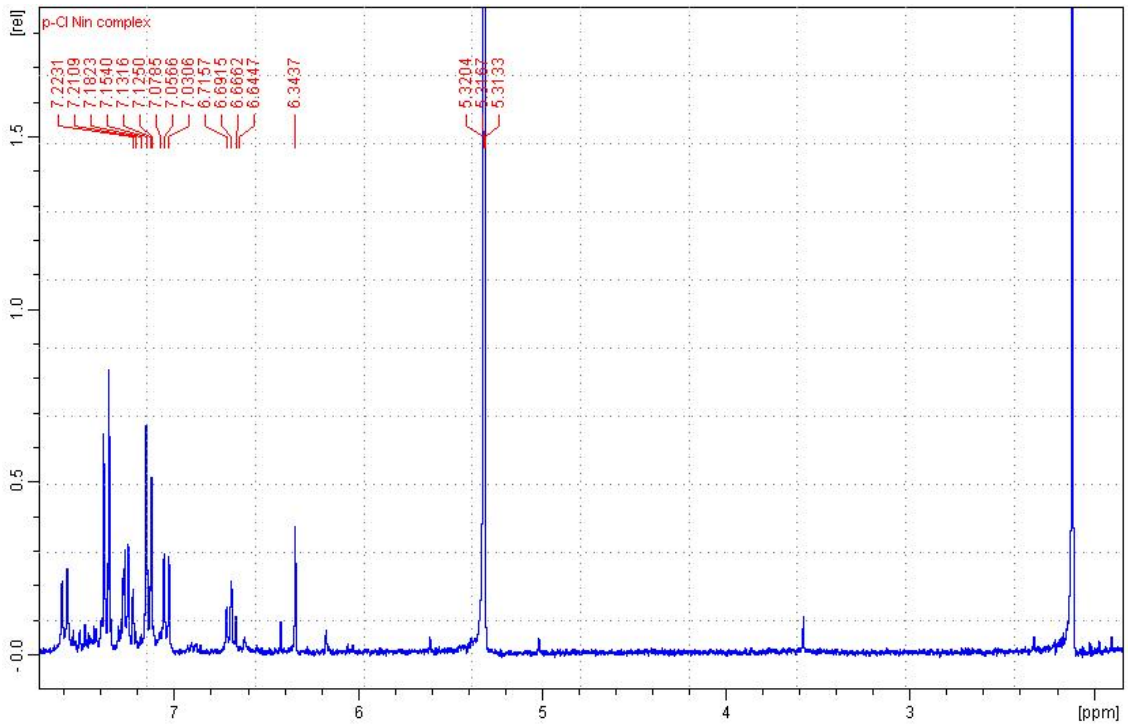

Appendix Figure 14: ^{1}H NMR of p-chlorophenyl Nindigo complex 3.7